UNIVERSITÀ DEGLI STUDI DI TRIESTE

UNIVERSITÀ DEGLI STUDI DI TRIESTE

XXXV CICLO DEL DOTTORATO DI RICERCA IN FISICA

VACUUM FLUCTUATIONS AND THEIR IMPLICATIONS FOR DARK MATTER, DYNAMICAL COLLAPSE MODELS AND DECOHERENCE

SETTORE SCIENTIFICO-DISCIPLINARE:
FIS/02 FISICA TEORICA MODELLI E METODI MATEMATICI

DOTTORANDO
ANIRUDH GUNDHI

COORDINATORE
PROF. FRANCESCO LONGO

Francesco Longo

SUPERVISORE DI TESI
PROF. ANGELO BASSI

Angelo Bassi

ANNO ACCADEMICO 2021/2022

Vacuum fluctuations and their implications for dark matter, dynamical collapse models and decoherence

Acknowledgements

I would like to thank Prof. Angelo Bassi for providing me the opportunity to pursue my PhD studies under his supervision. The discussions that I have had with him were all with a positive outlook, encouragement and the freedom to pursue research in a direction that I wanted to. It was a pleasure for me to work in such an environment.

I would like to thank Dr. Christian Friedrich Steinwachs, Dr. Matteo Carlesso, Prof. Sergey V. Ketov, with whom I collaborated for a major section of the thesis, and my friend and colleague, José Luis Gaona Reyes, to whom I could reach out without any hesitation and who was always present to help me with matters related to research or otherwise. I would also like to thank Davide Bason and Oliviero Angeli for the several fruitful discussions that I had with them during the last phase of the research.

I express my gratitude towards Prof. Lorenzo Di Pietro and Prof. Claus Kiefer for a critical reading of the thesis. The constructive feedback that they provided has been crucial and has resulted in an improved presentation of the research carried out for the thesis.

The financial and administrative support that I received from the University of Trieste, and the stimulating scientific environment that it provided, was essential for the work presented here. I thank all its staff members who have assisted me during the course of the PhD.

Life in Trieste would not have been the same without Michele Vischi, Giovanni Di Bartolomeo, Andrea Sangiovanni, Chiara Crinò, Francesca Gebbia, Ankur, Chia Ahmed and Nicola Battigello, to whom I thank for all the memories that I have with them.

While there are several others whose constant support I have benefited from, I would like to thank, in particular, Prof. Bikram Phookun, Rahul Mehra and Aditya Kela who have always encouraged and motivated me to pursue research and have helped me overcome the moments of self-doubt.

It goes without saying that the work presented here would not have been possible without the continuous support of my parents Mrs. Bhawna Gundhi and Mr. Praful Gundhi, and my sister Mrs. Divya Gupta. I thank you for keeping my spirits up during the most difficult times and celebrating all my minor achievements.

"To be able to count on success,
we should have either to approach the work from new angles
or to endeavour to penetrate further
by increased attention and deeper interest."

Translated from *Sigmund Freud,*
in *Jokes and Their Relations to the Unconscious,*
by *James Strachey*.

Contents

1 Introduction **3**

2 Stochastic calculus **6**
- 2.1 Markov processes . . . 6
- 2.2 Chapman-Kolmogorov equation . . . 7
- 2.3 The Wiener process . . . 8
- 2.4 Stochastic differential equations . . . 10
  - 2.4.1 Ito representation . . . 10
  - 2.4.2 Stratonovich representation . . . 12

3 Models of wavefunction collapse **14**
- 3.1 The modified dynamics . . . 14
- 3.2 The master equation . . . 16
- 3.3 Mass proportional collapse dynamics . . . 17
- 3.4 Discussion . . . 18

4 Inflation **20**
- 4.1 Background dynamics . . . 20
- 4.2 Perturbations . . . 22
- 4.3 Quantization . . . 24
- 4.4 The power spectrum . . . 26
- 4.5 Discussion . . . 28

5 Primordial black holes from inflationary dynamics **30**
- 5.1 The model . . . 30
  - 5.1.1 Inflation from modified gravity . . . 31
  - 5.1.2 Generalization of Starobinsky's model . . . 32
- 5.2 Covariant multi-field formalism . . . 33
  - 5.2.1 Background dynamics . . . 33
  - 5.2.2 Perturbations . . . 35
- 5.3 The two-field potential landscape . . . 36
- 5.4 The amplification mechanism . . . 39
- 5.5 The stochastic formalism . . . 40
- 5.6 Numerical treatment . . . 42
- 5.7 The power spectrum . . . 43

5.7.1 Starobinsky's model . . . 43
5.7.2 The two-field inflationary model . . . 44
5.8 PBH formation . . . 45
5.8.1 PBH abundance . . . 46
5.8.2 Primordial black holes as cold dark matter . . . 48
5.9 Results . . . 49
5.9.1 Mass windows $M^{I}_{\rm PBH}$ and $M^{II}_{\rm PBH}$ . . . 49
5.9.2 LIGO mass window $M^{III}_{\rm PBH}$ . . . 50
5.10 Identification with the Higgs field . . . 51
5.11 Constraining the parameters . . . 52
5.11.1 CMB constraint . . . 52
5.11.2 Constraint imposed by the PBH mass . . . 53
5.11.3 Constraint imposed by the peak amplitude . . . 54
5.12 Discussion . . . 57

6 Inflationary cosmology and its implications for dynamical collapse models 58
6.1 Mass proportional CSL model . . . 58
6.2 Interaction picture framework . . . 59
6.3 Choice of the collapse operator . . . 61
6.4 CSL corrections to the power spectrum . . . 62
6.4.1 Inflation . . . 62
6.4.2 Radiation dominated era . . . 65
6.5 Discussion . . . 68

7 The electromagnetic vacuum as the environment of an electron 69
7.1 The Lagrangian and the Hamiltonian formalism . . . 70
7.1.1 The Lagrangian . . . 70
7.1.2 The Hamiltonian . . . 71
7.2 The master equation . . . 72
7.3 The dissipation and the noise kernels . . . 77
7.4 Integrals involving the dissipation kernel . . . 78
7.5 The Abraham-Lorentz equation as a classical limit . . . 79
7.6 Decoherence . . . 82
7.7 Discussion . . . 84

8 Summary and outlook 85

Chapter 1

Introduction

The von Neumann collapse formulation gives an unsatisfactory and an inconsistent account of the quantum measurement problem. It assumes that if no measurement is made on a physical system, its state evolves in a linear and deterministic manner. If, however, a measurement is made, the system is asserted to jump randomly, instantaneously and non-linearly onto an eigenstate of the observable being measured. It thus supposes two unrelated dynamical laws, one of which must be applied depending on whether or not a measurement is being made, but without specifying what constitutes a measurement.

Hugh Everett III provided a logically consistent resolution to the problem by lifting the artificial divide between the measuring apparatus and the system being observed and postulating the existence of the universal system-apparatus wavefunction. At the time of the measurement, following the rules of standard linear quantum dynamics, the system and the apparatus become correlated to each other such that the universal wavefunction goes into a superposition of different states, each of which represents the apparatus being fully correlated to a given value of the system observable. Everett simply assumed that the universal wavefunction always evolves linearly, in accordance with standard quantum mechanics, and never undergoes a von Neumann like collapse. Nevertheless, in each of the configurations that it remains to be in a superposition of, the measuring apparatus records a definitive outcome.

While Everett may have been content with the fact that each of these branches of the wavefunction can consistently model the subjective experience of having a definitive outcome in an experiment, the desire to ask more from the quantum theory or to assign a specific physical meaning to each of these branches has resulted in the many worlds interpretation of quantum mechanics. The discontent with the simultaneous co-existence of several possible measurement records (that Everett's view predicts) while having access to only one, may lead one towards the direction of dynamical collapse models. In these models, a non-linear and stochastic time evolution of the wavefunction is considered as an alternative to the Schrödinger equation, such that the localization of the universal wavefunction, around a unique measurement record, is achieved continuously and asymptotically in time. Further, these models also lead to certain predictions that are different from those of standard quantum mechanics. It is then natural to ask whether or not collapse models are consistent with observations and for what values of the free parameters that they introduce. Besides several laboratory experiments, the possibility to constrain these models via the measurements of the cosmic microwave background (CMB) has been recently discussed in the

literature. Cosmological inflation, constraining the models of wavefunction collapse via the CMB observations and investigating the possibility of decoherence due to vacuum fluctuations (which has been previously argued in the literature to be a fundamental and an unavoidable source of decoherence), are the subjects of this thesis.

Cosmological inflation is widely regarded to be a part of standard cosmology. Not only does it solve several cosmological puzzles, the quantum fluctuations of the inflaton field are also believed to seed the formation of stars, galaxies and the temperature anisotropy of the CMB radiation. The same perturbations, when amplified on a certain length scale, can also trigger the formation of primordial black holes that may further account for the observed cold dark matter content in the universe. However, there is still no general consensus on the nature of the scalar field driving inflation. Two of the simplest candidates, Starobinsky inflation and non-minimal Higgs inflation, are also among the most successful ones. In the first part of the thesis, a combination of the two models is constructed which is not only consistent with the CMB observations but also offers the possibility to account for the observed cold dark matter content in the universe by triggering the formation of primordial black holes.

While the quantum perturbations offer to account for the structure in the universe, they also pose conceptual problems concerning its apparent classicality. Several works have sought a possible resolution by considering the continuous spontaneous localization (CSL) models. The non-linear evolution of the wavefunction that these models introduce, leads to a continuous localization of the wavefunction within the time intervals which scale inversely with the size (the total mass or the number of particles) of the system so that the quantum-to-classical transition is achieved continuously. In the second part of the thesis, working within the framework of standard cosmological perturbation theory, a possible generalization of the mass proportional CSL model to a cosmological setting is proposed which is found to be compatible with the CMB constraints.

The suppression of quantum superpositions does not necessarily require modifications to the Schrödinger equation. It can also be achieved within the framework of standard quantum mechanics due to decoherence. The phenomenon of decoherence or the suppression of the quantum superpositions is inevitable at the level of the system being *observed*, as soon as one realizes the practical impossibility of completely isolating the system from its environment. Nevertheless, one may still wonder what happens to macroscopic superpositions inside an ideal vacuum? Some works have even argued for the possibility that even the *environment* of the fundamentally unavoidable vacuum fluctuations can lead to decoherence. In order to address this question, in the third and final part of the thesis, the interaction of a non-relativistic electron with the electromagnetic vacuum is studied within the framework of open quantum systems. It is found that for an electron at rest, the vacuum fluctuations do not behave as an ordinary environment, such as that comprising of thermal photons or air molecules, and that it does not lead to irreversible loss of coherence. In addition, when the same mathematical formalism is applied to study the phenomenon of radiation emission by an accelerated non-relativistic electron, the resulting equation of motion appears to be free of the problems associated with the equation that is derived within classical electrodynamics: the run-away solution of the Abraham-Lorentz formula. While there has been a general expectation that these issues should not persist at a quantum mechanical level, it has not been shown clearly how they can be overcome. The discussion presented in the final part of the thesis offers to do so.

The thesis is organized as follows. Chapters 2, 3 and 4 provide a brief overview of stochastic calculus, models of wavefunction collapse and inflationary cosmology respectively, with a focus on the concepts that were central to the research. Then, in chapter 5, the work related to primor-

dial black holes is presented. Chapter 6 discusses a possible generalization of the CSL dynamics to inflationary cosmology. Chapter 7 concerns the interaction of a non-relativistic electron with the vacuum fluctuations and a possible resolution of the problems associated with the Abraham-Lorentz formula. The discussion concludes with chapter 8 in which the results obtained in the thesis are summarized.

The research presented in the thesis has resulted in the following publications:

1 **Publication I**. Anirudh Gundhi, Sergei V. Ketov, and Christian F. Steinwachs. Primordial black hole dark matter in dilaton-extended two-field Starobinsky inflation. *Phys. Rev. D, 103(8):083518, 2021*.

2 **Publication II**. Anirudh Gundhi and Christian F. Steinwachs. Scalaron–Higgs inflation reloaded: Higgs-dependent scalaron mass and primordial black hole dark matter. *Eur. Phys. J. C, 81(5):460, 2021*.

3 **Publication III**. Anirudh Gundhi, José Luis Gaona-Reyes, Matteo Carlesso, and Angelo Bassi. Impact of Dynamical Collapse Models on Inflationary Cosmology. *Phys. Rev. Lett., 127(9):091302, 2021*.

4 **Preprint**. Anirudh Gundhi, Angelo Bassi. On the motion of an electron through vacuum fluctuations. *arXiv:2301.11946*.

Chapter 2

Stochastic calculus

The goal of this chapter is to provide a brief introduction to the Fokker-Planck equation, the Wiener processes and Ito calculus. They are needed to formulate some of the concepts that are to follow in the subsequent chapters. The discussion is based on chapters three and four of the textbook by C.W. Gardiner [54].

2.1 Markov processes

Stochastic processes evolve probabilistically in time, as they involve a time dependent random variable $X(t)$. Let x_0, x_2, ..., x_N be N measurements of $X(t)$, at times t_0, t_2, ..., t_N respectively, in one particular run of an 'experiment'. The mathematical description of such a process requires the knowledge of all the joint probability densities $p(x_N, t_N; x_{N-1}, t_{N-1}; ...; x_0, t_0)$, or equivalently, the conditional probability distributions which can be defined in terms of the joint distributions

$$p(x_N, t_N; x_{N-1}, t_{N-1}; ...; x_0, t_0 | y_N, \tau_N; y_{N-1}, \tau_{N-1}; ...; y_0, \tau_0) := \frac{p(x_N, t_N; x_{N-1}, t_{N-1}; ...; y_0, \tau_0)}{p(y_N, \tau_N; y_{N-1}, \tau_{N-1}; ...; y_0, \tau_0)} . \tag{2.1}$$

Markov processes belong to a special class of stochastic processes which satisfy the Markovian assumption

$$p(x_N, t_N; x_{N-1}, t_{N-1}; ...; x_0, t_0 | y_N, \tau_N; y_{N-1}, \tau_{N-1}; ...; y_0, \tau_0) = p(x_N, t_N; x_{N-1}, t_{N-1}; ...; x_0, t_0 | y_N, \tau_N) . \tag{2.2}$$

Thus, for Markov processes, the conditional probability is determined completely by the latest condition. Using the property

$$p(x_N, t_N; x_{N-1}, t_{N-1}; ...; x_0, t_0) = p(x_N, t_N | x_{N-1}, t_{N-1}; ...; x_0, t_0) \times p(x_{N-1}, t_{N-1}; ...; x_0, t_0) \tag{2.3}$$

and applying the Markovian assumption iteratively, we get

$$\begin{aligned} &p(x_N, t_N; x_{N-1}, t_{N-1}; ...; x_0, t_0) = \\ &= p(x_N, t_N | x_{N-1}, t_{N-1}) \times p(x_{N-1}, t_{N-1} | x_{N-2}, t_{N-2}) \times ... \times p(x_1, t_1 | x_0, t_0) \times p(x_0, t_0) . \end{aligned} \tag{2.4}$$

From the properties of the joint probability distribution, we have $p(x_1,t_1) = \int dx_2 p(x_1,t_1;x_2,t_2)$. Also, since $p(x_1,t_1|x_3,t_3) = \int dx_2 p(x_1,t_1;x_2,t_2|x_3,t_3) = \int dx_2 p(x_1,t_1|x_2,t_2;x_3,t_3)p(x_2,t_2|x_3,t_3)$, using Markovianity we get the Chapman-Kolmogorov equation

$$p(x_1,t_1|x_3,t_3) = \int dx_2 p(x_1,t_1|x_2,t_2)p(x_2,t_2|x_3,t_3)\,. \tag{2.5}$$

In the next section the differential version of Eq. (2.5) will be derived, as both the Fokker-Planck equation and the Wiener process are nothing but a special case of the differential Chapman-Kolmogorov equation.

2.2 Chapman-Kolmogorov equation

A Markov sample path is a continuous function of time, if we have for ever ϵ with probability one

$$\lim_{\Delta t\to 0}\frac{1}{\Delta t}\int_{|x-z|>\epsilon} dx p(x,t+\Delta t|z,t) = 0\,. \tag{2.6}$$

We will include, for the time being, also the more general, non-continuous, *jump processes* in which the right hand side of Eq. (2.6) is non-zero. The following conditions are assumed to be true for all $\epsilon > 0$

$$\lim_{\Delta t\to 0}\frac{1}{\Delta t}p(x,t+\Delta t|z,t) = J(x|z,t)\,, \qquad |x-z|\geq\epsilon\,, \tag{2.7}$$

$$\lim_{\Delta t\to 0}\frac{1}{\Delta t}\int_{|x-z|<\epsilon} dx(x-z)p(x,t+\Delta t|z,t) = A(z,t)\,, \tag{2.8}$$

$$\lim_{\Delta t\to 0}\frac{1}{\Delta t}\int_{|x-z|<\epsilon} dx(x-z)^2 p(x,t+\Delta t|z,t) = B(z,t)\,. \tag{2.9}$$

Here, J is the jump coefficient, while A and B are the drift and the diffusion coefficients respectively. All the higher order coefficients of the form similar to Eqs. (2.8) and (2.9) can be shown to vanish [54].

The derivation begins by considering the time evolution of the expectation value of a generic function $f(x)$

$$\begin{aligned}\partial_t\langle f\rangle &= \frac{\int dx f(x)p(x,t+\Delta t|y,t') - \int dx f(x)p(x,t|y,t')}{\Delta t}\\ &= \frac{\int\int dxdz f(x)p(x,t+\Delta t|z,t)p(z,t|y,t') - \int dz f(z)p(z,t|y,t')}{\Delta t}\,,\end{aligned} \tag{2.10}$$

where the Chapman-Kolmogorov equation (2.5) is used in the second line. The spatial integral can be split into the two regions $|x-z|<\epsilon$ and $|x-z|\geq\epsilon$. Since the higher moments vanish, it is sufficient to expand $f(x)$ to second order $f(x) = f(z) + \frac{\partial f}{\partial z}(x-z) + \frac{1}{2}\frac{\partial^2 f}{\partial z^2}(x-z)^2$. The time evolution then becomes

$$\begin{aligned}\partial_t\langle f\rangle = &\frac{\int\int_{|x-z|<\epsilon} dzp(z,t|y,t')dx\left(f(z)+f'(z)(x-z)+f''(z)\frac{(x-z)^2}{2}\right)p(x,t+\Delta t|z,t)}{\Delta t} +\\ &+\frac{\int\int_{|x-z|\geq\epsilon} dxdz f(x)p(x,t+\Delta t|z,t)p(z,t|y,t') - \int\int dxdz f(z)p(x,t+\Delta t|z,t)p(z,t|y,t')}{\Delta t}\,.\end{aligned} \tag{2.11}$$

A few comments are in order here. The split into the two regions $|x-z| < \epsilon$ and $|x-z| \geq \epsilon$ is only made for the positive term in the second line of Eq. (2.10). Moreover, for the negative term, we just multiplied the original term with $1 = \int dx p(x, t+\Delta t|z,t)$. The Taylor expansion of $f(x)$ was only performed for the positive term and only in the region $|x-z| < \epsilon$. Grouping the various terms together, we get

$$\begin{aligned}\partial_t \langle f \rangle = &\int dz \left(f'(z) A(z,t) p(z,t|y,t') + \frac{1}{2} f''(z) B(z,t) p(z,t|y,t') \right) \\ &+ \frac{\int\int_{|x-z|<\epsilon} dx dz f(z) p(x,t+\Delta t|z,t) p(z,t|y,t') - \int\int dx dz f(z) p(x,t+\Delta t|z,t) p(z,t|y,t')}{\Delta t} \\ &+ \frac{\int\int_{|x-z|\geq\epsilon} dx dz f(x) p(x,t+\Delta t|z,t) p(z,t|y,t')}{\Delta t} \end{aligned} \tag{2.12}$$

The second line in Eq. (2.12) is just $-\frac{\int\int_{|x-z|\geq\epsilon} dx dz f(z) p(x,t+\Delta t|z,t) p(z,t|y,t')}{\Delta t}$. Using the definition of the jump coefficient we get

$$\begin{aligned}\partial_t \langle f \rangle &= \int dz \left(f'(z) A(z,t) p(z,t|y,t') + \frac{1}{2} f''(z) B(z,t) p(z,t|y,t') \right) \\ &\quad + \int\int_{|x-z|\geq\epsilon} dz dx f(z) \left(J(z|x,t) p(x,t|y,t') - J(x|z,t) p(z,t|y,t') \right) \\ &= \int dz f(z) \left(-\frac{\partial}{\partial z} \left(A(z,t) p(z,t|y,t') \right) + \frac{1}{2} \frac{\partial^2}{\partial z^2} \left(B(z,t) p(z,t|y,t') \right) \right. \\ &\quad \left. + \oint dx \left(J(z|x,t) p(x,t|y,t') - J(x|z,t) p(z,t|y,t') \right) \right) . \end{aligned} \tag{2.13}$$

Here, integration by parts has been performed for the terms involving the drift and the diffusion coefficients and the notation $\int_{|x-z|\geq\epsilon} dx g(x,z) := \oint dx g(x,z)$ has also been introduced. Recalling that $\int dz f(z) \partial_t p(z,t|y,t') := \partial_t \langle f \rangle$, the differential form of the Chapman-Kolmogorov equation is obtained to be

$$\begin{aligned}\partial_t p(z,t|y,t') = &-\frac{\partial}{\partial z} \left(A(z,t) p(z,t|y,t') \right) + \frac{1}{2} \frac{\partial^2}{\partial z^2} \left(B(z,t) p(z,t|y,t') \right) \\ &+ \oint dx \left(J(z|x,t) p(x,t|y,t') - J(x|z,t) p(z,t|y,t') \right) . \end{aligned} \tag{2.14}$$

2.3 The Wiener process

A particular case of interest is when the jump coefficient is zero, the drift coefficient is zero and the diffusion coefficient is set to one. This special case is that of the standard Wiener process whose probability distribution is obtained by solving

$$\partial_t p(w,t|w_0,t_0) = \frac{1}{2} \frac{\partial^2}{\partial w^2} p(w,t|w_0,t_0) . \tag{2.15}$$

In the Fourier space, $q(s,t) = \frac{1}{\sqrt{2\pi}} \int dw e^{iws} p(w,t|w_0,t_0)$, the solution is obtained to be

$$q(s,t) = \exp\left[-\frac{1}{2}s^2(t-t_0)\right] q(s,t_0)\,, \tag{2.16}$$

which is determined completely after assuming the initial condition

$$p(w,t_0|w_0,t_0) = \delta(w-w_0) \implies q(s,t_0) = \frac{1}{\sqrt{2\pi}} \exp(isw_0)\,. \tag{2.17}$$

The solution $p(w,t|w_0,t_0)$ is obtained by taking the inverse Fourier transform of $q(s,t)$ to be

$$p(w,t|w_0,t_0) = \frac{1}{\sqrt{(2\pi(t-t_0))}} \exp\left[-\frac{1}{2}\frac{(w-w_0)^2}{(t-t_0)}\right]\,. \tag{2.18}$$

An important property of the Wiener process is the statistical independence of the increment Δw_i. Since the Wiener process is Markovian (c.f. Eq. (2.4)), the joint probability density of a given realization of the process can be written as

$$p(w_n,t_n;w_{n-1},t_{n-1};...;w_0,t_0) = \prod_{i=0}^{n-1} p(w_{i+1},t_{i+1}|w_i,t_i) p(w_0,t_0)\,. \tag{2.19}$$

Using the probability distribution (2.18) we get

$$p(w_n,t_n;w_{n-1},t_{n-1};...;w_0,t_0) = \prod_{i=0}^{n-1} \exp\left[-\frac{1}{2}\frac{(w_{i+1}-w_i)^2}{(t_{i+1}-t_i)}\right] p(w_0,t_0)\,. \tag{2.20}$$

Defining $\Delta w_i := w_{i+1} - w_i$ and $\Delta t_i := t_{i+1} - t_i$, one obtains the factored product

$$p(\Delta w_n;\Delta w_{n-1};...;w_0) = \prod_{i=0}^{n-1} \exp\left[-\frac{1}{2}\frac{\Delta w_i^2}{\Delta t_i}\right] p(w_0,t_0)\,. \tag{2.21}$$

This shows that the increments Δw_i are statistically independent to each other and to w_0. Using this property, one can further deduce the auto-correlation functions of the Wiener process $W(t) = (w_n,t_n;w_{n-1},t_{n-1};...;w_0,t_0)$, defined as

$$\langle W(t)W(s)|[w_0,t_0]\rangle = \int dw_1 dw_2 w_1 w_2 p(w_1,t;w_2,s|w_0,t_0). \tag{2.22}$$

Without loss of generality one can assume $t > s$. Then

$$\langle W(t)W(s)|[w_0,t_0]\rangle = \langle [W(t)-W(s)]\, W(s)\rangle + \langle [W(s)]^2\rangle\,. \tag{2.23}$$

The first term on the RHS vanishes. This is because $W(t) - W(s)$ is statistically independent to $W(s)$. Therefore, their averages can be factored out which are zero. Computing the remaining second term we get

$$\langle W(t)W(s)|[w_0,t_0]\rangle = s - t_0 + w_0^2. \tag{2.24}$$

The result is obtained by remembering that the variance of the Gaussian (2.18) is the time difference $s - t_0$ and that at $t = t_0$ we were at w_0 with probability one. In the other case when $s > t$, we get $t - t_0 + w_0^2$. The two cases can be combined as

$$\langle W(t)W(s)|[w_0,t_0]\rangle = \min(t-t_0, s-t_0) + w_0^2\,. \tag{2.25}$$

This result will play a central role in the study of stochastic differential equations (SDE).

2.4 Stochastic differential equations

The goal is to study the Langevin equation for the variable $x(t)$ of the form

$$\frac{dx}{dt} = a(x,t) + b(x,t)\xi(t)\,. \tag{2.26}$$

Here, $a(x,t)$ and $b(x,t)$ are known functions and $\xi(t)$ is the stochastic term with

$$\langle \xi(t) \rangle = 0, \qquad \langle \xi(t)\xi(t') \rangle = \delta(t-t'). \tag{2.27}$$

Note that any non-zero mean of $\langle \xi(t) \rangle$ can be absorbed in the definition of $a(x,t)$. However, the infinite variance of this idealized noise raises technical difficulties. The integration of Eq. (2.26) implies the existence $u(t) = \int_0^t dt' \xi(t')$. It can be shown that $u(t') = \lim_{\epsilon \to 0} \left[\int_0^{t'-\epsilon} ds \xi(s) \right]$ and $u(t) - u(t') = \int_{t'}^t ds \xi(s)$ are statistically independent to each other. This implies that $u(t)$ must be Markovian. It can further be shown that the drift and the diffusion coefficients are obtained to be

$$\begin{aligned} A(u_0,t) &= \lim_{\Delta t \to 0} \frac{\langle u(t+\Delta t) - u_0 | [u_0,t] \rangle}{\Delta t} = 0\,, \\ B(u_0,t) &= \lim_{\Delta t \to 0} \frac{\langle (u(t+\Delta t) - u_0)^2 \, | [u_0,t] \rangle}{\Delta t} = 1\,. \end{aligned} \tag{2.28}$$

Thus, $u(t) = \int_0^t ds \xi(s) = W(t)$ is a Wiener process. But now we have a paradox. On one hand we know that the sample paths of the Wiener processes are non-differentiable. On the other hand, by definition, it is the differential of $u(t)$ that gives back $\xi(t)$. The solution to the paradox lies in realizing that, strictly speaking, the differential Langevin equation (2.26) does not exist. However, the corresponding integral equation

$$x(t) - x(0) = \int_0^t a[x(s),s]ds + \int_0^t b[x(s),s]dW(s) \tag{2.29}$$

does. The precise way of defining and evaluating the stochastic integral $\int_0^t b[x(s),s]dW(s)$ leads to two main representations of the Langevin equation. The Ito equation and the Stratonovich equation.

2.4.1 Ito representation

The stochastic integral $\int_{t_0}^t dt' G(t') dW(t')$ is first defined as a limit of sums

$$S_n = \sum_{i=1}^n G(\tau_i)[W(t_i) - W(t_{i-1})]. \tag{2.30}$$

In general, τ_i can lie anywhere within the interval $t_i - t_{i-1}$. The Ito integral is obtained by taking $\tau_i = t_{i-1}$. The stochastic integral of the function $G(t)$ is defined as the mean-squared limit

$$\int_{t_0}^t G(t')dW(t') = \text{mslim}_{n\to\infty} \left\{ \sum_{i=1}^n G(t_{i-1}) \left[W(t_i) - W(t_{i-1}) \right] \right\}, \tag{2.31}$$

where the sequence of a random variable X_m is said to converge to X in the mean squared limit when

$$\lim_{m\to\infty} \int d\omega p(\omega) \left[X_m(\omega) - X(\omega)\right]^2 = 0\,. \tag{2.32}$$

In what follows, we will assume the function $G(t)$ to be *nonanticipating*. That is, $\forall\ t$ and $\forall\ s$ with $t < s$, $G(t)$ is assumed to be statistically independent of $W(s) - W(t)$. Note that with the Ito prescription, this will always be the case inside the summation if $G(t)$ is some function $F(W(t))$ of the Wiener process.

Evaluating the stochastic integrals, with the Ito prescription, requires proving that effectively $dW(t)^2 = dt$ and $dW(t)^{2+N} = 0$. The equality is again understood in the sense of the mean-squared limit. For the first statement, we need to evaluate

$$I = \lim_{n\to\infty} \left\langle \left[\sum_i G_{i-1} \left(\Delta W_i^2 - \Delta t_i\right)\right]^2 \right\rangle . \tag{2.33}$$

Simply expanding the square of the sum, we get

$$I = \lim_{n\to\infty} \left\langle \sum_i G_{i-1}^2 \left(\Delta W_i^2 - \Delta t_i\right)^2 \right\rangle + \lim_{n\to\infty} \left\langle \sum_{i<j} 2G_{i-1}G_{j-1} \left(\Delta W_i^2 - \Delta t_i\right) \left(\Delta W_j^2 - \Delta t_j\right) \right\rangle . \tag{2.34}$$

In the first term, G is a non-anticipating function and therefore G_{i-1} is statistically independent to ΔW_i. Thus, their means can be factorized. In the second term for $i < j$, $G_{i-1}G_{j-1}\left(\Delta W_i^2 - \Delta t_i\right)$ is statistically independent to $\left(\Delta W_j^2 - \Delta t_j\right)$ and the means of these two terms can also be factorized. Due to the Gaussian nature of the Wiener process, we have $\langle \Delta W_i^2 \rangle = \Delta t_i$ and $\langle (\Delta W_i^2 - \Delta t_i)^2 \rangle = 2\Delta t_i^2$. The integral reduces to $I = 2\sum_i \langle G_{i-1}^2 \rangle \Delta t_i^2$ which is equal to zero for most functions G. Thus, for all practical purposes, ΔW_i^2 can be replaced with Δt_i for the evaluation of the Ito integrals. While the second statement $dW(t)^{2+N} = 0$ can also be proven formally, one can instead take an intuitive stance. Higher powers of dW will give higher powers of dt (for example $dW^3 \approx dt^{3/2}$) which are set to zero in ordinary calculus. Only the terms upto dW^2 must be retained in stochastic calculus in the same spirit as only the terms upto first order in dt are retained in ordinary calculus. With this intuition, the derivative of W^n can be calculated easily as

$$\begin{aligned} d[W(t)]^n &= [W(t) + dW(t)]^n - W(t)^n = \sum_{r=0}^{n} \frac{n!}{r!\,(n-r)!} W^{n-r} dW^r - W^n \\ &= W^n + n\,W^{n-1} dW + \frac{n(n-1)}{2} W^{n-2} dW^2 - W^n \\ &= n\,W^{n-1} dW + \frac{n(n-1)}{2} W^{n-2} dt\,. \end{aligned} \tag{2.35}$$

Using the relation above, the stochastic integral for an arbitrary polynomial of W can be evaluated as

$$\int W^n dW = \frac{W(t)^{n+1} - W(t_0)^{n+1}}{n+1} - \frac{n}{2} \int_{t_0}^{t} W(t')^{n-1} dt'\,. \tag{2.36}$$

Another useful expression, along the same line of reasoning, is obtained for a function of the stochastic variable W and time t

$$\begin{aligned} df[W(t),t] &= \frac{\partial f}{\partial t}dt + \frac{\partial f}{\partial W}dW + \frac{1}{2}\frac{\partial^2 f}{\partial W^2}dW^2 \\ &= \left(\frac{\partial f}{\partial t} + \frac{1}{2}\frac{\partial^2 f}{\partial W^2}\right)dt + \frac{\partial f}{\partial W}dW\,. \end{aligned} \tag{2.37}$$

Therefore, for a function $f[x(t)]$, with $x(t)$ satisfying the Langevin equation (2.26) we obtain

$$df[x(t)] = \left[a[x(t)]\frac{\partial f}{\partial x} + \frac{1}{2}b[x(t)]^2\frac{\partial^2 f}{\partial x^2}\right]dt + b[x(t)]\frac{\partial f}{\partial x}dW(t)\,. \tag{2.38}$$

The basic identities that have been presented provide a brief overview of how differentiation and integration can be performed for functions of stochastic variables. The Ito convention (2.30) is one of the two main conventions found in the literature. The discussion ends with the following section in which a transformation law is derived which allows one to express a given Ito SDE in the Stratonovich representation such that both the SDEs have the same solution.

2.4.2 Stratonovich representation

The Stratonovich integral is defined as

$$\mathrm{S}\int_{t_0}^{t} G[x(t'),t']dW(t') = \operatorname*{mslim}_{n\to\infty}\sum_{i=1}^{n} G\left\{\frac{x(t_i)+x(t_{i-1})}{2}, t_{i-1}\right\}[W(t_i)-W(t_{i-1})]\,. \tag{2.39}$$

Because of the differences between the Ito and the Stratonovich prescriptions of computing integrals, the same solution $x(t)$ obeys different looking SDEs in the two representations. In the Stratonovich representation, let

$$x(t) = x(t_0) + \int_{t_0}^{t} dt'\alpha[x(t'),t'] + S\int_{t_0}^{t} dW(t')\beta[x(t'),t'] \tag{2.40}$$

be the same solution as that for the Ito SDE

$$dx(t) = a[x(t),t]dt + b[x(t),t]dW(t)\,. \tag{2.41}$$

The relationship between $\alpha[x(t)]$ and $a[x(t)]$ (and $\beta[x(t)]$ and $b[x(t)]$) remains to be determined.

$$\mathrm{S}\int_{t_0}^{t} \beta[x(t'),t']dW(t') = \sum_{i=1}\beta\left[\frac{x(t_i)+x(t_{i-1})}{2}, t_{i-1}\right][W(t_i)-W(t_{i-1})]\,. \tag{2.42}$$

Since $x(t_i) = x(t_{i-1}) + \Delta x$, using Eq. (2.41)

$$x(t_i) - x(t_{i-1}) = \Delta x(t_i) = a[t_{i-1}]\Delta t_i + b[t_{i-1}]\Delta W(t_i)\,, \tag{2.43}$$

we get

$$\begin{aligned} \beta\left[x(t_{i-1}) + \frac{\Delta x}{2}, t_{i-1}\right] &= \beta[t_{i-1}] + \left(\frac{\Delta t_i}{2}a[t_{i-1}]\partial_x\beta[t_{i-1}] + \frac{\Delta t_i}{4}\frac{1}{2}b^2[t_{i-1}]\partial_x^2\beta[t_{i-1}]\right) \\ &\quad + b[t_{i-1}]\partial_x\beta[t_{i-1}]\frac{(W(t_i)-W(t_{i-1}))}{2}\,. \end{aligned} \tag{2.44}$$

Plugging this back in the Stratonovich sum (2.42) and retaining terms only upto order $dW^2 = dt$ we get

$$\mathrm{S}\int_{t_0}^{t} \beta dW = \int_{t_0}^{t} \beta dW + \frac{1}{2}\int_{t_0}^{t} b\partial_x \beta dt' \,. \tag{2.45}$$

In Eq. (2.45) the Stratonovich sum (LHS) has been expressed in terms of the Ito sum (RHS). Using this result in Eq. (2.40), identifying $b = \beta$, we get $\alpha = a - \frac{1}{2} b\partial_x b$. Thus the solution to the differential equation

$$dx = adt + bdW \,, \tag{2.46}$$

in which the solution is obtained by performing integration following the Ito prescription, is same as the solution to the differential equation

$$dx = \left(a - \frac{1}{2} b\partial_x b\right) dt + bdW \,, \tag{2.47}$$

in which the integral is performed following the Stratonovich prescription.

Chapter 3

Models of wavefunction collapse

If a system is prepared to be in a superposition of two different states, standard quantum mechanics governed by the Schrödinger equation predicts that it remains to be in such a configuration indefinitely. The difficulty then arises in explaining why in the double-slit experiment do we see the photon at a definite location on the screen. Moreover, all systems, irrespective of their sizes, are predicted to sustain this superposition on all length scales at all times. This seems to be in conflict with the observation that macroscopic objects are never perceived to be in such de-localized states. While the phenomenon of decoherence [114] addresses the question at a practical level, one may find such an explanation unsatisfactory as it still does not establish a clear relationship between the wavefunction, which is at the heart of the Schrödinger equation, and the observed outcome in an experiment. Such a connection is offered by the models of wavefunction collapse [9]. Dynamical reduction models introduce non-linearity and stochasticity into the Schrödinger equation such that if the wavefunction is initially prepared to be in a superposition, it randomly localizes around one of the possible outcomes. The wavepacket reduction typically occurs on time scales which are inversely proportional to the size of the system. In this way, macroscopic objects are guaranteed a definite position in space and the quantum-to-classical transition is achieved continuously. This chapter provides a brief overview of how this modified dynamics is constructed. A comprehensive review of the subject can be found in [9].

3.1 The modified dynamics

In dynamical collapse models, the wavefunction is assumed to satisfy the Ito stochastic differential equation

$$d\left|\psi\right\rangle = \left[\hat{A}dt + \hat{B}dW\right]\left|\psi\right\rangle \,, \tag{3.1}$$

where, $W(t)$ is a real Wiener process and $\hat{A}$ and $\hat{B}$ are generic operators. For simplicity, it will be assumed in this chapter that

$$\hat{B}^{\dagger} = \hat{B} \tag{3.2}$$

$$\mathbb{E}(dW) = 0\,, \qquad \mathbb{E}(dW^2) = \gamma dt\,. \tag{3.3}$$

The stochastic element that enters the modified equation is introduced in order to respect the statistical nature of quantum dynamics. Collapse models associate the detection of the particle at a definite location on the screen to the localization of the initial wavefunction around that spatial location. Nevertheless, such a localization must occur stochastically and must be consistent with the Born rule. Because of this reason, between the time interval $t_0 + dt$ and t_0, the Wiener process is assumed to be realized with the probability

$$P_{\text{cooked}}(dW') = P_{\text{raw}}(dW) \cdot \langle \psi(t_0 + dt) | \psi(t_0 + dt) \rangle \ . \tag{3.4}$$

Here, P_{raw} is the original normalized probability distribution of the Wiener process that appears in the raw process (3.1) and P_{cooked} is the assumed physical probability distribution with which it would be realized in a physical process. If the wavefunction is initially normalised at time t_0, then we get

$$P_{\text{cooked}}(dW') = P_{\text{raw}}(dW) \cdot (1 + d\left(\langle \psi | \psi \rangle\right)) \, . \tag{3.5}$$

Using Eq. (3.5), normalization of the cooked probability gives the constraint $\mathbb{E}(d\left\langle \psi | \psi \right\rangle) = 0$. The raw process (3.1) does not preserve the norm such that $d\left(\langle \psi | \psi \rangle\right)$ is in general non-zero and from Eq. (3.1) is obtained to be

$$d\left\langle \psi | \psi \right\rangle = \langle d\psi | \psi \rangle + \langle \psi | d\psi \rangle + \langle d\psi | d\psi \rangle = dt \left\langle \psi \right| \left(\hat{A} + \hat{A}^\dagger\right) \left| \psi \right\rangle + 2dW \left\langle \psi \right| \hat{B} \left| \psi \right\rangle + \left\langle \psi \right| \hat{B}^2 \left| \psi \right\rangle dW^2 \, . \tag{3.6}$$

The normalization constraint on P_{cooked} thus yields a constraint on the operators $\hat{A}$ and $\hat{B}$ given by

$$\hat{A} + \hat{A}^\dagger = -\gamma \hat{B}^2 \, . \tag{3.7}$$

Writing $\hat{A}$ as the sum of the purely Hermitian part $(-\gamma \hat{B}^2/2)$ and a purely non-Hermitian part $(:= -i\hat{H})$, Eq. (3.1) becomes

$$d\left| \psi \right\rangle = \left[-i\hat{H}dt - \frac{\gamma dt}{2} \hat{B}^2 + \hat{B} dW \right] \left| \psi \right\rangle \ . \tag{3.8}$$

For $|\psi\rangle$ to represent the physical statevector, it must be normalized. However, for all practical purposes we can still work with the raw process (3.8). We can simply solve the differential equation (3.8) and compute the physical probabilities by using the normalized wavevector and remembering that the physical stochastic process (dW') is realized with the cooked probability and not P_{raw}.

Alternatively, we can also write down the equation for the physical process which preserves the norm and in which the stochastic process is realized with P_{raw} without resorting to the cooked prescription. The non-linear stochastic differential equation (SDE) governing the dynamics of the normalized physical statevector is given by [9]

$$d\left| \phi(t) \right\rangle = \left[-i\hat{H}dt - \frac{\gamma dt}{2} \left(\hat{B} - \langle \hat{B} \rangle \mathbb{1}\right)^2 + \left(\hat{B} - \langle \hat{B} \rangle \mathbb{1}\right) dW \right] \left| \phi \right\rangle \ . \tag{3.9}$$

where $\langle \cdot \rangle := \langle \phi | \cdot | \phi \rangle$.

3.2 The master equation

The differences in predictions arising due to the modified dynamics can be calculated from the time evolution of the density matrix. Since the functional form of the linear SDE is similar to the non-linear one, one can work with Eq. (3.8) and substitute $\hat{B} \to \hat{B} - \langle \hat{B} \rangle \mathbb{1}$ at the end. After taking an additional average over the different realizations of the raw Wiener process, the master equation is obtained from Eq. (3.8) to be

$$d\hat{\rho} = \mathbb{E}\left[(d\,|\psi\rangle)\,\langle\psi| + |\psi\rangle\, d\,\langle\psi| + (d\,|\psi\rangle)d\,\langle\psi|\right] = -i\left[\hat{H},\hat{\rho}\right] - \frac{\gamma dt}{2}\left\{\hat{B}^2,\hat{\rho}\right\} + \gamma dt\hat{B}\hat{\rho}\hat{B}\,. \tag{3.10}$$

The last two terms involving the operator $\hat{B}$ can be written as a double commutator such that

$$d\hat{\rho} = -i\left[\hat{H},\hat{\rho}\right]dt - \frac{\gamma dt}{2}\left[\hat{B},\left[\hat{B},\hat{\rho}\right]\right]\,. \tag{3.11}$$

First, we notice that the equation remains unchanged for the physical density matrix corresponding to the statevector $|\phi\rangle$ in the physical process (3.9). This is because $\langle \hat{B} \rangle \mathbb{1}$ does not contribute to the double commutator. More directly, in going from the raw process (3.8) to a physical one, the extra factor of $\langle\psi|\psi\rangle$ that would appear in the expression for the normalized physical density matrix in the denominator would be cancelled by the same factor that would appear in the numerator when the stochastic averages are computed using the cooked prescription.

Second, and more importantly, we notice that the same master equation (3.11) would be obtained if we consider the Schrödinger equation to be governed by a stochastic Hamiltonian [1]. If we identify the full Hamiltonian with [1]

$$H_{\text{full}} = \hat{H} + \hat{B}\xi(t)\,, \tag{3.12}$$

where $\xi(t) = dW/dt$, then

$$|\psi(t,W)\rangle = \exp\left\{-i\left(\int \hat{H}dt + \int \hat{B}dW\right)\right\}|\psi(t_0)\rangle\,. \tag{3.13}$$

The density matrix $\hat{\rho}$ becomes a function t and the stochastic process W. In Eq. (2.37) of chapter (2), for a generic function of the stochastic variable W and the time t, the following identity was derived

$$\langle df[W(t),t]\rangle = \left(\frac{\partial f}{\partial t} + \frac{\gamma}{2}\frac{\partial^2 f}{\partial W^2}\right)dt\,. \tag{3.14}$$

The additional factor of γ appearing in Eq. (3.14) is a due to the modified normalization of the Wiener process compared to the one in chapter 2.

We know from standard quantum mechanics that a single derivative of the density matrix yields a single commutator with the Hamiltonian, and a double derivative would give a double commutator term. Identifying f in Eq. (3.14) with $\hat{\rho}$, the double commutator in Eq. (3.11) would come from the stochastic Hamiltonian (due to the double partial derivative with respect to W in

[1] Note that the stochastic differential equation corresponding to the solution (3.13) does not look like the Schrödinger in the Ito representation. It does so in the Stratonovich representation. Thus, when we consider a stochastic Hamiltonian what we have in mind is the formal solution (3.13).

Eq. (3.14)) and the single commutator from the original Hamiltonian as in the standard dynamics. Therefore, the modified predictions for the non-linear SDE (3.9) can be computed using standard perturbation theory by identifying the stochastic perturbation $\hat{H}_{\text{st}}$

$$\hat{H}_{\text{st}} = \hat{B}\xi(t)\,. \tag{3.15}$$

It is also easy to see how the collapse operator leads to decoherence. Projecting the master equation (3.11) in the position basis, ignoring the standard Liouville-von Neuman term and choosing $\hat{B}$ to be the position operator $\hat{x}$ [46] we get

$$d\rho(x', x, t) = -\frac{\gamma dt}{2}(x' - x)^2 \rho(x', x, t)\,. \tag{3.16}$$

We see that a suitable choice of the collapse operator indeed leads to decoherence. An important point to notice is that the suppression of the off-diagonal elements does not guarantee the reduction of the statevector. As it has already been argued, one would arrive at the same master equation (3.11) simply due to the presence of a stochastic term in the full Hamiltonian. However, if this was actually the source of the decoherence term, the evolution of the statevector would remain linear. Identifying the stochastic perturbation is only for the practical ease of performing calculations. Within the framework of collapse models, one always has Eq. (3.9) in mind such that the observed definitive outcomes are associated to the localization of the wavefunction.

3.3 Mass proportional collapse dynamics

In the mass proportional Continuous Spontaneous Localization (CSL) model, the collapse operator is chosen to be the smoothed mass density operator such that the rate of the collapse increases with the number of particles in the system [58, 57]. In this section, the amplification of the collapse mechanism for a macroscopic system is first illustrated by simpler considerations. It will then be used as a motivation to write down the equation defining the mass proportional CSL model.

To begin, the physical space is considered to be divided into cells of size $\propto r_{\text{c}}^3$. We can imagine that a set of collapse operators $\{\hat{B}^i\}$ and a set of Wiener processes $\{W^i\}$ with $\mathbb{E}(dW^i dW^j) = \gamma dt \delta_{ij}/r_{\text{c}}^3$, corresponding to the different spatial cells, govern the stochastic evolution of the statevector. That is,

$$d\,|\psi\rangle = \left[\hat{A}dt + r_{\text{c}}^3 \sum_i \hat{B}_i dW^i\right] |\psi\rangle\ . \tag{3.17}$$

The same reasoning starting from Eq. (3.1) upto Eq. (3.9) leads to the following master equation corresponding to the raw process in Eq. (3.17) :

$$d\hat{\rho} = \sum_i r_{\text{c}}^3 \left(-\frac{\gamma dt}{2}\left\{\hat{B}_i^2, \hat{\rho}\right\} + \gamma dt \hat{B}_i \hat{\rho} \hat{B}_i\right) = -\sum_i \frac{\gamma r_{\text{c}}^3 dt}{2}\left[\hat{B}_i, \left[\hat{B}_i, \hat{\rho}\right]\right]\ , \tag{3.18}$$

where the Liouville-von Neuman term has been omitted for simplicity. Next, we take the set of collapse operators to be the number density operators $\{\hat{N}_i\}/r_{\text{c}}^3$, where $\hat{N}_i$ counts the number of particles in the i^{th} cell. Then, projecting the master equation equation onto the basis states $|n_1, n_2, ..., n_N\rangle$ and $|m_1, m_2, ..., m_N\rangle$, where $|n_i\rangle$ and $|m_i\rangle$ denote two possible states of the system

in which there are n_i and m_i particles in the i^{th} cell respectively, the off-diagonal elements of the density matrix decay as

$$d\rho_{mn} = -\sum_i \frac{\gamma dt (n_i - m_i)^2}{2r_C^3}\rho_{mn}\,. \tag{3.19}$$

It can now be seen how a definitive outcome is achieved on time scales that is governed by the parameter $\lambda \propto \gamma/r_C^3$ and the number of particles in the system. For a given value of λ, the rate of collapse is greatly enhanced as the number of particles increase, thereby leading to the quantum-to-classical transition.

The mass proportional CSL model can be regarded as a generalization of the toy model considered above. It is defined through the following stochastic differential equation

$$\mathrm{d}\,|\phi\rangle = \Bigg[-i\hat{H}\mathrm{d}t + \frac{\sqrt{\gamma}}{m_0}\int \mathrm{d}\mathbf{x}\left[\hat{M}(\mathbf{x}) - \langle\hat{M}(\mathbf{x})\rangle\right]\mathrm{d}W_t(\mathbf{x}) \tag{3.20}$$

$$-\frac{\gamma}{2m_0^2}\int \mathrm{d}\mathbf{x}\mathrm{d}\mathbf{y}\left[\hat{M}(\mathbf{x}) - \langle\hat{M}(\mathbf{x})\rangle\right]G(\mathbf{x}-\mathbf{y})\left[\hat{M}(\mathbf{y}) - \langle\hat{M}(\mathbf{y})\rangle\right]\mathrm{d}t\Bigg]\,|\phi\rangle\,, \tag{3.21}$$

where $\hat{H}$ is the Hamiltonian of the system, γ is a phenomenological parameter of the model encoding the strength of the collapse process, m_0 is the reference mass taken to be that of a proton and $\langle\cdot\rangle$ denotes the expectation value on the physical state $|\phi\rangle$. The noise $W_t(\mathbf{x})$ defined at each point in space is characterized through the correlation

$$\mathbb{E}\left[\xi_t(\mathbf{x})\xi_{t'}(\mathbf{y})\right] = G(\mathbf{x}-\mathbf{y})\delta(t-t'), \qquad \text{where} \qquad G(\mathbf{x}-\mathbf{y}) = \frac{1}{(4\pi r_C^2)^{3/2}}e^{-\frac{(\mathbf{x}-\mathbf{y})^2}{4r_C^2}}\,, \tag{3.22}$$

with $\xi_t(\mathbf{x}) = \mathrm{d}W_t(\mathbf{x})/\mathrm{d}t$ and r_C denoting the second phenomenological parameter of the model. Finally, the operator $\hat{M}(\mathbf{x})$ in Eq. (3.21) is the mass density operator, given by

$$\hat{M}(\mathbf{x}) = \sum_j m_j \hat{a}_j^\dagger(\mathbf{x})\hat{a}_j(\mathbf{x}), \tag{3.23}$$

where the operators $\hat{a}_j^\dagger(\mathbf{x})$ and $\hat{a}_j(\mathbf{x})$ are the creation and annihilation operators of a particle of type j in the space point $\mathbf{x}$.

3.4 Discussion

CSL models can be regarded as phenomenological models which solve the measurement problem in quantum mechanics. In particular, the models are agnostic to the physical origin of the stochastic noise. The modified dynamics also introduces new parameters into the statevector evolution which draw the line between the microscopic and the macroscopic world. Nevertheless, the modifications induced by these models can be experimentally falsified as shown in Fig. 3.1. The parameter λ in Fig. 3.1 is related to γ as $\lambda = \gamma/\left(4\pi r_C^2\right)^{3/2}$ with r_C being the same as in Eq. (3.22). The different colored regions depict the disallowed region of the r_C-λ parameter space by different laboratory experiments. The white and the light grey areas are not probed by experiments. Still, the light grey area is excluded since in this region the collapse dynamics would be too weak and would not suppress macroscopic superpositions: a central motivation behind the collapse models. Further details related to Fig. 3.1 can be found in [26].

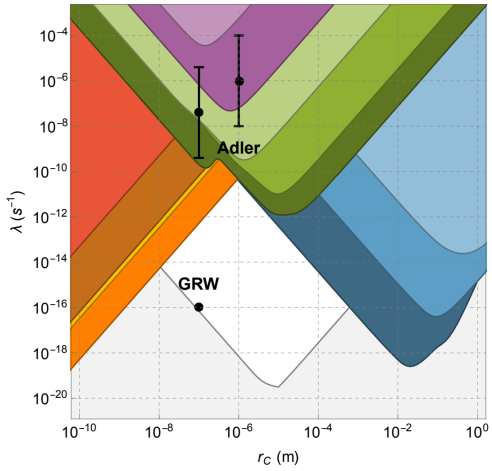

Figure 3.1: Figure taken from [26] depicting the various experimental bounds on the free parameters of the CSL model.

Chapter 4

Inflation

The Cosmic Microwave Background radiation exhibits a blackbody spectrum at a temperature of 2.725K [89, 90] which is observed to be the same for light coming from different directions with a deviation on the order of 10^{-5}K [117]. Most of the different spatial points from which this light was emitted in the remote past and has only reached us now, would paradoxically seem to remain causally disconnected to each other, even up until the time at which this light was emitted, and yet lead to the observed blackbody spectrum, unless the early universe went through a phase of accelerated expansion (c.f. [103] for a discussion on the horizon problem). Cosmological inflation refers to this phase of the early universe preceding the radiation dominated era. Inflationary models not only explain the accelerated expansion of the background spacetime, but also predict the existence of the small temperature anisotropy in the CMB radiation due to the quantum fluctuations of the scalar field that drove inflation. A brief overview of the key concepts involved is provided in this chapter, while a more pedagogical discussion can be found in [103, 109].

4.1 Background dynamics

The action governing the inflationary dynamics is given by

$$S = \int \mathrm{d}^4x\sqrt{-g}\left[\frac{M_\mathrm{P}^2}{2}R - \frac{1}{2}g^{\mu\nu}\partial_\mu\varphi\partial_\nu\varphi - V(\varphi)\right], \tag{4.1}$$

where R denotes the Ricci scalar corresponding to a background spacetime metric $g_{\mu\nu}$, g denotes the metric determinant and φ denotes an arbitrary scalar field with the scalar potential $V(\varphi)$. The action is written within the reduced Planck units where $\hbar = c = 1$ and $M_\mathrm{P} := 1/\sqrt{8\pi G}$ where G denotes the Newton's constant.

The dynamics is studied by writing the metric and the scalar field as the sum of the homogeneous background and the inhomogeneous perturbations such that

$$g_{\mu\nu}(\eta, \mathbf{x}) = g_{\mu\nu}(\eta) + \delta g_{\mu\nu}(\eta, \mathbf{x}), \qquad \varphi(\eta, \mathbf{x}) = \varphi(\eta) + \delta\varphi(\eta, \mathbf{x}). \tag{4.2}$$

We first focus on the background dynamics which, generally, can be determined independently of the perturbations. The background metric is taken to be the flat Friedmann-Lemaître-Robertson-

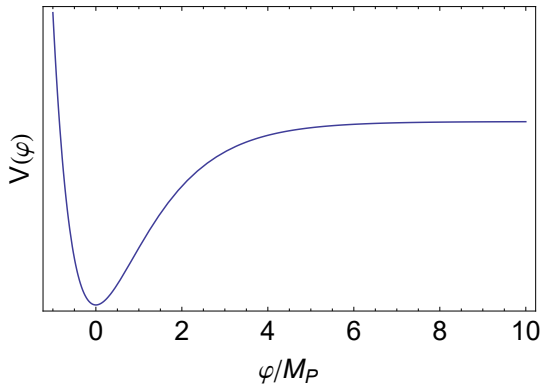

Figure 4.1: Inflationary potential featuring a flat plateau for large values of φ.

Walker metric [1]

$$ds^2 = a^2(\eta)(-d\eta^2 + d\mathbf{x}^2)\,, \tag{4.3}$$

where $a(\eta)$ is the scale factor and η is the conformal time. The time evolution of the background quantities is obtained by solving for the equation of motion for the background scalar field $\varphi(\eta)$

$$\ddot{\varphi} + 2h\dot{\varphi} + a^2 V_{,\varphi} = 0\,, \tag{4.4}$$

together with the two Friedmann equations

$$3M_{\rm P}^2 h^2 = \frac{\dot{\varphi}^2}{2} + a^2 V(\varphi)\,, \tag{4.5}$$

$$h^2 - \dot{h} = \frac{\dot{\varphi}^2}{2M_{\rm P}^2}\,. \tag{4.6}$$

In Eqs. (4.4)-(4.6) the overdot denotes the derivative with respect to the conformal time and $h := \dot{a}/a$. In this chapter we reserve the overdot for the derivative taken with respect to the conformal time η and not for the cosmic time t. Note that the parameter h is not the same as the Hubble parameter H, which is instead defined in terms of the cosmic time $dt = a(\eta)d\eta$ as

$$H := \frac{1}{a}\frac{da}{dt}. \tag{4.7}$$

Thus, H and h are related by $h = aH$. For the ease of comparison with the discussion presented in

[1] Even if one starts from a more general metric including a non-zero uniform spatial curvature, the additional contribution coming from the curvature term to the dynamics is subdominant with respect to the contribution from the scalar field and can therfore be neglected [103].

chapter 5, Eqs. (4.4)-(4.6) are also presented in terms of the cosmic time t below

$$\frac{d^2}{dt^2}\varphi = -3H\dot{\varphi} + V_{,\varphi}\ , \tag{4.8}$$

$$3M_{\rm P}^2H^2 = \frac{1}{2}\left(\frac{d\varphi}{dt}\right)^2 + V\left(\varphi\right)\ , \tag{4.9}$$

$$\frac{dH}{dt} = -\frac{M_{\rm P}^{-2}}{2}\left(\frac{d\varphi}{dt}\right)^2\ . \tag{4.10}$$

Once the inflationary potential has been specified, the time evolution of the background quantities $(a(\eta), \varphi(\eta))$ can be determined completely subject to initial conditions. For a given inflationary potential, such as the one depicted in Fig. 4.1, the background dynamics is actually fully determined by Eqs. (4.4) and (4.5). For instance, using Eq. (4.9), one can express H completely in terms of the field φ and its time derivative. Doing that in Eq. (4.8), we get a closed equation for φ which can then be solved exactly (at least numerically). The initial conditions determine the amount of inflation that the universe goes through [103, 109, 10]. By choosing a certain amount which is large enough to solve the horizon problem, one can fix the initial conditions and obtain the background dynamics.

Due to the presence of the friction term in Eq. (4.4) and the flat plateau of the inflationary potential where $(V_{,\varphi})^2 \ll V^2(\varphi)/M_{\rm P}^2$, any initial field velocities would converge to smaller values such that $\dot{\varphi}^2 \ll a^2V(\varphi)$. In such a situation, $3M_P^2H^2 \approx V(\varphi)$. Since the inflationary dynamics predominantly occurs along the flat plateau of the scalar potential, the Hubble parameter assumes an almost constant value. From Eq. (4.7) this implies $a(t) \approx a(t_0)\exp\{H(t-t_0)\}$ thereby resulting in an exponential expansion of the universe.

However, this phase of rapid expansion does not last forever. This is because the value of the Hubble parameter keeps on decreasing slowly during inflation due to the small but a non-zero slope of the potential. This decrease is parameterized by the slow-roll parameter $\varepsilon_{\rm H}$ which is defined as

$$\varepsilon_{\rm H} := -\frac{1}{H}\frac{d\ln H}{dt}. \tag{4.11}$$

The slow-roll parameter takes small positive values during inflation such that $\varepsilon_{\rm H} \ll 1$. Its value typically increases monotonically during inflation as the scalar field rolls down towards the minimum of the potential. From Eqs. (4.7) and (4.11) we see that $\varepsilon_{\rm H} = 1$ when $d^2a/dt^2 = 0$. The condition $\varepsilon_{\rm H} = 1$ thus marks the end of inflation. After the end of inflation, the inflaton oscillates along the minimum of the scalar potential at $\varphi = 0$ and the energy content of the inflaton field is transferred to radiation by a process called reheating. A discussion on reheating can be found in [103, 109] and the references therein.

Having reviewed how the inflationary background dynamics governed by a scalar field leads to a finite period of exponential expansion of the universe, we now study the evolution of perturbations.

4.2 Perturbations

In addition to the accelerated expansion of the homogeneous background spacetime $(\varphi(\eta), a(\eta))$, inflation also predicts the existence of inhomogeneous perturbations $(\delta\varphi\left(\eta, \mathbf{x}\right), \delta g_{\mu\nu}\left(\eta, \mathbf{x}\right))$ which

are of quantum mechanical origin. To take them into account, one needs to go beyond the FLRW metric which makes the computation slightly more involved. However, a simplification occurs owing to the fact that to first order in perturbations, $\delta\varphi(\eta, \mathbf{x})$ only couples to the scalar perturbations of the metric $\delta g_{\mu\nu}(\eta, \mathbf{x})$ [91, 103, 109]. The discussion here will be restricted to the dynamics of the scalar perturbations only, as it is the most relevant for the work presented in the thesis. The general metric including all the scalar degrees of freedom is given by

$$\mathrm{d}s^2 = a^2(\eta)\left[-(1+2A)\,\mathrm{d}\eta^2 + 2B_{,i}\,\mathrm{d}x^i\mathrm{d}\eta + \left((1+2\psi)\delta_{ij} + 2E_{,ij}\right)\mathrm{d}x^i\mathrm{d}x^j\right]. \tag{4.12}$$

The metric in Eq. (4.12) is thus parameterized by only four scalar functions (A, B, ψ, E). For instance, any vector B^i can be written as the gradient of a scalar and the curl of a vector. Thus, we see that only the gradient term ($B_{,i} := \partial_{x^i} B$) is retained in the g_{0i} components, where B is a general scalar function.

To obtain the equation governing the dynamics of $\delta\varphi$, we write down the Klein-Gordon equation for the full scalar field $\varphi^{\mathrm{t}}(\eta, \mathbf{x}) = \varphi(\eta) + \delta\varphi\,(\eta, \mathbf{x})$, which is given by

$$\partial_\mu\left[\sqrt{-g}g^{\mu\nu}\partial_\nu\varphi^{\mathrm{t}}\right] - \sqrt{-g}V_{,\varphi^{\mathrm{t}}} = 0\,. \tag{4.13}$$

Having already determined the evolution of the background, the dynamics of the perturbation $\delta\varphi$ can then be filtered out as [2]

$$\partial_\mu\left[\left(\delta\sqrt{-g}\right)g^{\mu\nu}\partial_\nu\varphi + \sqrt{-g}\left(\delta g^{\mu\nu}\right)\partial_\nu\varphi + \sqrt{-g}g^{\mu\nu}\partial_\nu\left(\delta\varphi\right)\right] - \left(\delta\sqrt{-g}\right)V_{,\varphi} - \sqrt{-g}V_{,\varphi\varphi}\,\delta\varphi = 0\,. \tag{4.14}$$

We see that the dynamics of $\delta\varphi$ is coupled to that of $\delta g_{\mu\nu}$. To simplify the calculations, we fix a specific gauge such that two out of the four scalar functions are eliminated from the perturbed metric. This is due to the fact that by choosing appropriately δx^0 and $\delta x^i = \partial^i f$ in an infinitesimal coordinate transformation $x^\mu \to x^\mu + \delta x^\mu$, one can induce perturbations in the metric which cancel out two of the four scalar functions (A, B, ψ, E) in Eq. (4.12). We choose the gauge in which $\psi = B = 0$ [97], as the calculations are easier to perform. In this gauge, the Fourier modes $\delta g_{\mu\nu}(\eta, \mathbf{k})$ become

$$\delta g_{\mu\nu}(\eta, \mathbf{k}) = \begin{pmatrix} -2A_{\mathbf{k}}a^2(\eta) & 0 \\ 0 & \left(-2k_ik_jE_{\mathbf{k}}\right)a^2(\eta) \end{pmatrix}. \tag{4.15}$$

Making use of the background equations of motion, Eq. (4.14) can be expressed in the Fourier space as

$$\ddot{\delta\varphi}_{\mathbf{k}} + 2h\dot{\delta\varphi}_{\mathbf{k}} + (k^2 + a^2V_{,\varphi\varphi})\delta\varphi_{\mathbf{k}} + 2A_{\mathbf{k}}a^2V_{,\varphi} - \dot{\varphi}(\dot{A}_{\mathbf{k}} + k^2\dot{E}_{\mathbf{k}}) = 0\,, \tag{4.16}$$

where $k^2 := \mathbf{k}\cdot\mathbf{k}$. Further, using the Einstein's equations for the perturbations $\delta G_{\mu\nu} = \delta T_{\mu\nu}/M_{\mathrm{P}}^2$ which are given by [97]

$$2A_{\mathbf{k}} = \frac{\dot{\bar{\varphi}}\delta\varphi_{\mathbf{k}}}{M_{\mathrm{P}}^2 h}\,, \tag{4.17}$$

$$\dot{A}_{\mathbf{k}} + k^2\dot{E}_{\mathbf{k}} = \frac{\delta\varphi_{\mathbf{k}}}{M_{\mathrm{P}}^2}\frac{d}{d\eta}\left(\frac{\dot{\bar{\varphi}}}{h}\right), \tag{4.18}$$

[2] The entities appearing without a δ are understood to be the ones corresponding to the homogeneous background.

the metric perturbations $A_{\mathbf{k}}$ and $E_{\mathbf{k}}$ can be expressed in terms of $\delta\varphi_{\mathbf{k}}$. This yields a closed equation for $\delta\varphi_{\mathbf{k}}$

$$\delta\ddot{\varphi}_{\mathbf{k}} + 2h\delta\dot{\varphi}_{\mathbf{k}} + \left[k^2 + a^2 V_{,\varphi\varphi} - \frac{1}{M_{\rm P}^2 a^2}\frac{d}{d\eta}\left(\frac{a^2\dot{\varphi}^2}{h}\right)\right]\delta\varphi_{\mathbf{k}} = 0\,. \tag{4.19}$$

To be able to compare more explicitly with the discussion presented in chapter 5, Eq. (4.19) is also expressed in terms of the cosmic time t below

$$\frac{d^2}{dt^2}\delta\varphi_{\mathbf{k}} + 3H\frac{d}{dt}\delta\varphi_{\mathbf{k}} + \left[k^2 + V_{,\varphi\varphi} - \frac{1}{M_{\rm P}^2 a^3}\frac{d}{dt}\left(\frac{a^3(d\varphi/dt)^2}{H}\right)\right]\delta\varphi_{\mathbf{k}} = 0\,. \tag{4.20}$$

In terms of $u(\eta,\mathbf{x})$ and $z(\eta)$ defined as

$$u(\eta,\mathbf{x}) := a\delta\varphi(\eta,\mathbf{x})\,, \qquad z := aM_{\rm P}\sqrt{2\varepsilon_{\rm H}}\,, \tag{4.21}$$

Eq. (4.19) takes the compact form

$$\ddot{u}_{\mathbf{k}}(\eta) + \left(k^2 - \frac{\ddot{z}}{z}\right)u_{\mathbf{k}}(\eta) = 0\,. \tag{4.22}$$

We note that Eq. (4.22) can also be obtained from the action

$$\delta S^{(2)} = \frac{1}{2}\int d\eta \int d^3x \left[\dot{u}^2 - \delta^{ij}\partial_i u\partial_j u + \frac{\ddot{z}}{z}u^2\right]\,. \tag{4.23}$$

We see from the discussion presented in this section that the dynamics of all the scalar degrees of freedom, and hence any physical quantity of interest that is a function of the scalar perturbations only, can be determined by $\delta\varphi$. However, one needs to be careful as the calculations were performed in a specific gauge. While it makes the calculations simpler, working within a specific gauge has the disadvantage of including unphysical gauge artifacts. To eliminate this possibility, one can instead construct and work with quantities which remain invariant under infinitesimal coordinate transformations. One such quantity is the Mukhanov-Sasaki variable [111, 93]

$$\delta\varphi_g := \delta\varphi - \dot{\varphi}\frac{\psi}{h}. \tag{4.24}$$

Working with the gauge-invariant variables from the very beginning instead of choosing a specific gauge, one arrives at the gauge-invariant version of the action (4.23) in which $u \to u_g := a\delta\varphi_g$ [111, 93, 92]. From now onwards it will be implicitly assumed that the perturbations correspond to their gauge-invariant versions as defined in Eq. (4.24), but without explicitly retaining the index g in the subscript.

4.3 Quantization

From the action (4.23), the Lagrangian in the Fourier space can be identified as

$$L = \int d^3k\mathcal{L}(\mathbf{k}) = \frac{1}{2}\int d^3k\left(|\dot{u}_{\mathbf{k}}(\eta)|^2 - \omega_k^2(\eta)|u_{\mathbf{k}}(\eta)|^2\right)\,, \qquad \omega_k^2(\eta) := \mathbf{k}\cdot\mathbf{k} - \frac{\ddot{z}}{z}\,. \tag{4.25}$$

Identifying the conjugate momentum

$$\pi_{\mathbf{k}}(\eta) = \frac{\partial \mathcal{L}(\mathbf{k})}{\partial \dot{u}^*_{\mathbf{k}}(\eta)} \tag{4.26}$$

for the complex field $u_{\mathbf{k}}(\eta)$, the Hamiltonian is obtained to be

$$H = \frac{1}{2}\int d^3k \left(\pi_{\mathbf{k}}(\eta)\pi^*_{\mathbf{k}}(\eta) + \omega_k^2(\eta) u_{\mathbf{k}}(\eta) u^*_{\mathbf{k}}(\eta)\right) . \tag{4.27}$$

Its clear that the real ($u^R_{\mathbf{k}}(\eta)$) and the imaginary ($u^I_{\mathbf{k}}(\eta)$) parts form independent degrees of freedom. Quantization is performed by imposing the commutation relations

$$\left[\hat{u}^R_{\mathbf{k}_1}(\eta), \hat{\pi}^R_{\mathbf{k}_2}(\eta)\right] = \left[\hat{u}^I_{\mathbf{k}_1}(\eta), \hat{\pi}^I_{\mathbf{k}_2}(\eta)\right] = i\hbar\delta(\mathbf{k}_1 - \mathbf{k}_2) . \tag{4.28}$$

The probability for the perturbations to have a configuration $u(\eta, \mathbf{x})$ is given by the wavefunctional $\Psi[u(\eta, \mathbf{x})]$, which can be written as [88]

$$\Psi[\eta, u(\mathbf{x})] = \prod_{\mathbf{k}} \Psi^R_{\mathbf{k}}\left[\eta, u^R_{\mathbf{k}}\right] \Psi^I_{\mathbf{k}}\left[\eta, u^I_{\mathbf{k}}\right] . \tag{4.29}$$

The individual elements of the product on the right hand side satisfy the Schrödinger equation

$$i\frac{\partial}{\partial\eta}\Psi^{R,I}_{\mathbf{k}}\left[\eta, u^{R,I}_{\mathbf{k}}\right] = \frac{1}{2}\left[\left(\frac{-i\delta}{\delta u^{R,I}_{\mathbf{k}}}\right)^2 + \left(\omega_k(\eta) u^{R,I}_{\mathbf{k}}\right)^2\right] \Psi^{R,I}_{\mathbf{k}}\left[\eta, u^{R,I}_{\mathbf{k}}\right] . \tag{4.30}$$

Eq. (4.30) can be solved with the Gaussian ansatz

$$\Psi^{R,I}_{\mathbf{k}}\left[\eta, u^{R,I}_{\mathbf{k}}\right] = N_{\mathbf{k}}(\eta) e^{-\Omega_{\mathbf{k}}(\eta)\left(u^{R,I}_{\mathbf{k}}\right)^2} , \tag{4.31}$$

with the constraints

$$\frac{\dot{N}_{\mathbf{k}}}{N_{\mathbf{k}}} = -i\Omega_{\mathbf{k}}(\eta) , \qquad \dot{\Omega}_{\mathbf{k}} = -2i\Omega^2_{\mathbf{k}}(\eta) + \frac{i}{2}\omega_k^2(\eta) , \tag{4.32}$$

imposed by the Schrödinger equation. It is clear that only the real part of $\Omega_{\mathbf{k}}$ influences the probability distribution $P[u_{\mathbf{k}}]$, whose normalization gives an additional constraint

$$P\left[u^R_{\mathbf{k}}\right] = |N_{\mathbf{k}}(\eta)|^2 e^{-2\sigma(\eta)\left(u^R_{\mathbf{k}}\right)^2} , \qquad \sigma := \mathrm{Re}\{\Omega_{\mathbf{k}}\} , \qquad |N_{\mathbf{k}}| = \left(\frac{2\sigma}{\pi}\right)^{1/4} . \tag{4.33}$$

The solution to the second equation in (4.32) reads [88]

$$\Omega_{\mathbf{k}}(\eta) = -\frac{i}{2}\frac{\dot{f}_{\mathbf{k}}(\eta)}{f_{\mathbf{k}}(\eta)} , \tag{4.34}$$

where $f_{\mathbf{k}}(\eta)$ is the solution to the differential equation (4.22). Using the first equality in Eq. (4.32) we get $N_{\mathbf{k}} = 1/\sqrt{f_{\mathbf{k}}}$ such that

$$P\left[u^R_{\mathbf{k}}\right] = \frac{1}{|f_{\mathbf{k}}(\eta)|}\exp\left\{-\frac{\pi (u^R_{\mathbf{k}})^2}{|f_{\mathbf{k}}(\eta)|^2}\right\}, \qquad P\left[u^R_{\mathbf{k}}, u^I_{\mathbf{k}}\right] = P\left[u^R_{\mathbf{k}}\right] P\left[u^I_{\mathbf{k}}\right] = \frac{1}{|f_{\mathbf{k}}(\eta)|^2}\exp\left\{-\frac{\pi |u_{\mathbf{k}}|^2}{|f_{\mathbf{k}}(\eta)|^2}\right\}. \tag{4.35}$$

Since the perturbations in the real space are a linear combination of the different modes $\delta\varphi_{\mathbf{k}}$, we infer that the underlying probability distribution for the perturbations in the real space must also be a Gaussian. This remains true as long as we are interested in the regime where the perturbations predominantly evolve linearly [103] [3]. Nevertheless, within this regime, to determine the statistical properties of the perturbations, it is sufficient to calculate the two-point correlation. This is parametrized by the power spectrum of the inflationary perturbations which is then constrained by observations.

4.4 The power spectrum

Upon quantization (back in the Heisenberg picture), the status of the classical perturbation $u(\eta, \mathbf{x})$ is raised to that of a field operator $\hat{u}(\eta, \mathbf{x})$ such that

$$\hat{u}(\eta, \mathbf{x}) = \int \frac{d^3k}{(2\pi)^{3/2}} \exp(i\mathbf{k}\cdot\mathbf{x})\hat{u}_{\mathbf{k}}(\eta)\,. \tag{4.36}$$

Further, the operator $\hat{u}_{\mathbf{k}}(\eta)$ can be written in terms of the creation and annihilation operators as

$$\hat{u}_{\mathbf{k}}(\eta) = v_k(\eta)\hat{a}_{\mathbf{k}} + v^*_k(\eta)\hat{a}^\dagger_{-\mathbf{k}}. \tag{4.37}$$

The power spectrum $\mathcal{P}_u$ (to be defined later) of the operator $\hat{u}(\eta, \mathbf{x})$ is related to the two-point correlation function $\mathcal{C}_u(\mathbf{x}, \mathbf{x}')$ [103, 109, 10] which is given by

$$\mathcal{C}_u(\mathbf{x}, \mathbf{x}', \eta) = \langle 0|\, \hat{u}(\eta, \mathbf{x}')\hat{u}(\eta, \mathbf{x})\, |0\rangle\,. \tag{4.38}$$

Using Eqs. (4.36) and (4.37) we get

$$\mathcal{C}_u(\mathbf{x}, \mathbf{x}', \eta) = \int \frac{d^3k d^3k'}{(2\pi)^3}\, \langle 0|\, \hat{a}_{\mathbf{k}}\hat{a}^\dagger_{-\mathbf{k}'}\, |0\rangle\, v_k(\eta)v^*_{k'}(\eta)e^{i(\mathbf{k}\cdot x + \mathbf{k}'\cdot\mathbf{x}')}\,. \tag{4.39}$$

From the standard commutation relations of the creation and annihilation operators and integrating over $\mathbf{k}'$, Eq. (4.39) becomes

$$\mathcal{C}_u(\mathbf{x}, \mathbf{x}', \eta) = \int \frac{d^3k}{(2\pi)^3}|v_k(\eta)|^2 e^{i\mathbf{k}\cdot(\mathbf{x}-\mathbf{x}')}\,. \tag{4.40}$$

Next we complete the angular integrals in the reciprocal space to obtain

$$\mathcal{C}_u(\mathbf{x}, \mathbf{x}', \eta) = \int_0^\infty \frac{dkk^2}{2\pi^2}|v_k(\eta)|^2 \frac{\sin(kr)}{kr}\,, \qquad r := |\mathbf{x} - \mathbf{x}'|\,. \tag{4.41}$$

[3] A discussion on non-Gaussianity can be found in [7].

We see that the Copernican principle holds at a statistical level because the correlation depends only on r, making it invariant under both translations and rotations [103]. The power spectrum can be defined in terms of the starting two-point correlation such that

$$\mathcal{C}_u(\mathbf{x}, \mathbf{x}', \eta) := \int_0^\infty d\ln(k) \mathcal{P}_u(k, \eta) \frac{\sin(kr)}{kr}\,, \tag{4.42}$$

which implies

$$\mathcal{P}_u(k, \eta) = \frac{k^3}{2\pi^2} |v_k(\eta)|^2. \tag{4.43}$$

From the discussion in Sec. 4.3, we see that for a given inflationary model, the power spectrum encodes the predictions for the observed statistical properties of the cosmological perturbations. One such quantity of interest which is observationally constrained is the comoving curvature perturbation $\hat{\mathcal{R}}$. It is related to $\hat{u}$ as

$$\hat{\mathcal{R}} := \hat{u}/z = \frac{\delta\varphi_g}{\sqrt{2\varepsilon_{\rm H}} M_{\rm P}} = \frac{1}{\sqrt{2\varepsilon_{\rm H}} M_{\rm P}} \left(\delta\varphi - \frac{d\varphi}{dt}\frac{\psi}{H}\right)\,. \tag{4.44}$$

In the last equation, while it was implicit, the subscript g has been re-introduced to emphasize that $\mathcal{R}$ is the gauge-invariant version of the metric perturbation ψ, which is related to the intrinsic spatial curvature on hypersurfaces of constant conformal time η. It is thus called the comoving curvature perturbation as the comoving gauge is defined by the condition $\delta\varphi = 0$ [109].

The power spectrum $\mathcal{P}_\mathcal{R}$ of $\hat{\mathcal{R}}$ can be obtained from the power spectrum of $\mathcal{P}_u$ as $\mathcal{P}_\mathcal{R} = \mathcal{P}_u/z^2$. The modes $v_k(\eta)$, that enter the expression of the power spectrum, are the solutions to differential equation (4.22). In the perfect de Sitter limit, in which one ignores the contributions coming from the slow-roll parameter (Eq. (4.11)), the Hubble parameter can be treated as a constant and we have the relations

$$a(\eta) \approx -1/(H\eta)\,, \qquad \frac{\ddot{z}}{z} \approx \frac{\ddot{a}}{a} \approx \frac{2}{\eta^2}. \tag{4.45}$$

In this limit, the solution to Eq. (4.22) for the modes $v_k(\eta)$ gives

$$v_k(\eta) = \frac{A(-\frac{\cos(k\eta)}{k\eta} - \sin(k\eta))}{\sqrt{2k}} + \frac{B\left(-\cos(k\eta) + \frac{\sin(k\eta)}{k\eta}\right)}{\sqrt{2k}}. \tag{4.46}$$

To fix the free parameters A and B, one imposes the Bunch-Davies vacuum condition [103, 109, 10]. Such a condition demands the system to be in the ground state $|0\rangle$ of the Hamiltonian corresponding to the action functional for u [cf. Eq. (4.23)] at $\eta \to -\infty$. The differential equation satisfied by the modes in this limit is identical to that of a simple harmonic oscillator. For the simple harmonic oscillator, the time evolution of the creation and annihilation operators in the Heisenberg picture yields the following constraint for $\hat{u}$ in Eq. (4.37)

$$v_k(\eta)|_{\eta\to-\infty} = \frac{\exp(-ik\eta)}{\sqrt{2k}}. \tag{4.47}$$

This gives $B = -1$ and $A = i$. In the perfect de Sitter limit, the full solution $v_k(\eta)$ then reads [103]

$$v_k(\eta) = \frac{e^{-i\eta k}\left(1 - \frac{i}{\eta k}\right)}{\sqrt{2k}}. \tag{4.48}$$

In the superhorizon limit $k\eta \ll 1$, that is, when we consider a cosmological perturbation of wavelength a/k much larger than the length scale $1/H$, the expression for the modes in Eq. (4.48) simplifies to [103]

$$v_k(\eta) \overset{k\eta \ll 1}{\approx} -\frac{i}{\sqrt{2}}\frac{1}{\eta k^{3/2}}. \tag{4.49}$$

Using this result, we obtain the power spectrum $\mathcal{P}_\mathcal{R}$ in the superhorizon limit to be

$$\mathcal{P}_\mathcal{R} = \frac{\mathcal{P}_u(k,\eta)}{2a^2\varepsilon_{\rm H}M_{\rm P}^2} \approx \frac{1}{2\varepsilon_{\rm H}M_{\rm P}^2}\left(\frac{H}{2\pi}\right)^2. \tag{4.50}$$

We see that for a perfect de Sitter solution of the modes (c.f. Eq. (4.48)), the power spectrum is independent of both the conformal time η and the scale k. In a more general treatment in which the slow-roll dependence is taken into account, the power spectrum acquires a mild scale dependence. The power spectrum is then parametrized as [109, 103]

$$\mathcal{P}_\mathcal{R} = A^*_\mathcal{R}\left(\frac{k}{k_*}\right)^{n^*_\mathcal{R}-1}. \tag{4.51}$$

In the power law parameterization of the power spectrum in Eq. (4.51), the amplitude $A_\mathcal{R}$ denotes the strength of the power spectrum at a certain wavenumber, while the parameter $n_\mathcal{R}$ is the measure of the deviation of the power spectrum from perfect scale invariance. The closer $n_\mathcal{R}$ is to unity, the weaker is the scale dependence.

4.5 Discussion

The *Planck* CMB anisotropy measurements constrain the values of $A^*_\mathcal{R}$ and $n^*_\mathcal{R}$, at the pivot scale $k_* = 0.05\,\mathrm{Mpc}^{-1}$, to be

$$A^*_\mathcal{R} = (2.099 \pm 0.014) \times 10^{-9} \quad \text{and} \quad n^*_\mathcal{R} = 0.9649 \pm 0.0042\,, \tag{4.52}$$

at the 68% confidence level. In the following chapters the inflationary dynamics is studied in two different contexts. In chapter 5, a model of inflation is considered that leads to the production of small Primordial Black Holes (PBHs) after the end of inflation. If the number of PBHs produced are just right, the model would then offer a possible explanation for the observed cold dark matter content in the universe. PBHs sourced by the inflationary perturbations require the amplitude of the perturbations to be significantly higher on certain length scales which are much smaller compared to the ones probed by the CMB measurements. The model constructed must be such that it respects the constraints mentioned in Eq. (4.52), while at the same time, leads to an amplification of the power spectrum on a smaller length scale, say $k_{\rm PBH}$. An increased value of the power spectrum at $k_{\rm PBH}$ essentially implies a larger variance of the underlying Gaussian probability density

corresponding to the same length scale. This makes it more likely to generate a large amplitude perturbation and thus more primordial black holes with a mass that is related to the value of $k_{\rm PBH}$.

Then, in chapter 6, we investigate if the models of wavefunction collapse, as presented in chapter 3, can be generalized to a cosmological setting such that they are consistent with the CMB constraints. The derivation of the power spectrum here was presented within the standard quantization scheme. When the Schrödinger equation is modified as in collapse models, there will be corrections induced to the power spectrum whose numerical value would depend upon the free parameters of the models of wavefunction collapse. Via the power spectrum, the CMB observations therefore offer the possibility to constrain the parameters of the collapse models, apart from the constrains that are already imposed from the standard laboratory experiments.

Chapter 5

Primordial black holes from inflationary dynamics

Primordial Black Holes (PBHs) may provide an explanation of the origin of Cold Dark Matter (CDM) without assuming new particles. Their formation can be triggered by the large density fluctuations generated during inflation. In addition to the relevance of PBHs in explaining the observed CDM, they also provide constraints on inflationary models complementary to those coming from the observations of the Cosmic Microwave Background (CMB). Therefore, they offer the possibility to break the degeneracy between a number of different inflationary models which are all compatible with the CMB observations. A review of the topic and the various cosmological and astrophysical constraints that have been put on PBHs can be found in [30, 80, 27, 28] and the references therein. As mentioned in chapter 4, PBH generation requires the amplification of the power spectrum on a certain length scale. The inflationary power spectrum is in turn completely determined by the potential of the scalar field driving inflaton. The challenge then becomes to come up with a suitable model of inflation that results in such an amplification of the power spectrum, while being compatible with all the observational constraints. In the next section, inspired from Starobinsky's quadratic model of $f(R)$ gravity [118], such a two-field model of inflation is constructed. The model is found to be compatible with the CMB observations and offers the possibility to account for the observed CDM content. The discussion presented here is based on publication I [68] and publication II [70].

5.1 The model

We begin with Starobinsky's model which is defined by the action [118]

$$S_{\rm Star}[g] = \frac{M_{\rm P}^2}{2}\int {\rm d}^4x\sqrt{-g}\left(R + \frac{1}{6m_0^2}R^2\right) . \tag{5.1}$$

It contains two dimensionful parameters: the reduced Planck mass $M_{\rm P} = 1/\sqrt{8\pi G_{\rm N}}$ and the scalaron mass m_0. As in chapter 4, we adopt the reduced Planck units.

For large curvatures $R/m_0^2 \gg 1$, the R^2 term in Eq. (5.1) dominates. In this regime, the action is rendered invariant under the global scale transformations $\tilde{g}_{\mu\nu} = \alpha^{-2} g_{\mu\nu}$, where α is a constant. This is because, under these transformations, the Ricci scalar transforms as $\tilde{R} = \alpha^2 R$ and therefore $\sqrt{-g}R^2 = \sqrt{-\tilde{g}}\tilde{R}^2$. At high curvatures/energies, action (5.1) is thus asymptotically scale invariant. This symmetry is desirable to have for the realization of the (almost) scale invariant inflationary power spectrum. Indeed, the predictions of the Starobinsky model are found to be in perfect agreement with the recent *Planck* data [3].

However, it might still not be apparent how action (5.1) is related to the discussion presented in chapter 4, in which inflation was driven by a scalar field with a corresponding scalar potential. We shall see in the next section that the modified gravity terms, such as the R^2 term, contain an additional scalar propagating degree of freedom, the scalaron [120, 118], which plays the role of the inflaton driving inflation.

5.1.1 Inflation from modified gravity

Action (5.1) belongs to the more general class of models for which the action reads

$$S[g, \varphi] = \int \mathrm{d}^4x \sqrt{-g} \left\{ f(R, \varphi) - \frac{1}{2} g^{\mu\nu} \partial_\mu \varphi \partial_\nu \varphi \right\}. \tag{5.2}$$

Eq. (5.2), in addition to action (5.1), includes a scalar field φ with a generic scalar potential $V(\varphi)$ and a generic coupling to gravity. To extract the additional scalar degree of freedom, we see that Eq. (5.2) can be equivalently written as

$$S[g, \varphi, \psi] = \int \mathrm{d}^4x \sqrt{-g} \Big[f(\psi, \varphi) + (R - \psi) f_{,\psi}(\psi, \varphi) - \frac{1}{2} \partial_\mu \varphi \partial^\mu \varphi \Big]. \tag{5.3}$$

In Eq. (5.3), an additional scalar field ψ has been introduced which functionally replaces R in the function f. The equation of motion for ψ is given by

$$f_{,\psi\psi}(R - \psi) = 0. \tag{5.4}$$

Since we are interested in a modified gravity action such that $f(R, \varphi)$ contains also second or higher powers of R, we have $f_{,\psi\psi} \neq 0$. The EOM (5.4) then implies $\psi = R$. Therefore, on-shell, we see that action (5.3) is equivalent to the original action (5.2). Next, we define the scalaron χ by

$$\chi^2 := f_{,\psi}(\psi, \varphi). \tag{5.5}$$

The explicit functional form of $f(\psi, \varphi)$ (or equivalently $f(R, \varphi)$), together with the condition $f_{,\psi\psi} \neq 0$, allows one to invert Eq. (5.5) and to express $\psi = \psi(\chi, \varphi)$ as a function of χ and φ. In particular, we can write action (5.3) in terms of the scalaron χ as

$$S[g, \varphi, \chi] = \int \mathrm{d}^4x \sqrt{-g} \left[\chi^2 R - \frac{1}{2} \partial_\mu \varphi \partial^\mu \varphi - W(\chi, \varphi) \right]. \tag{5.6}$$

Here, the two-field scalar potential has been identified to be

$$W(\chi, \varphi) = \chi^2 \psi(\chi, \varphi) - f(\psi(\chi, \varphi), \varphi). \tag{5.7}$$

The action in Eq. (5.2) has now been brought into a more familiar form. In chapter 4 the inflationary dynamics was considered to be driven by a single scalar field φ, minimally coupled to gravity[1].

[1] Minimal coupling implies that the only coupling between the gravity sector and the scalar field is through the presence of $\sqrt{-g}$.

Instead, when one considers $f(R,\varphi)$ models of gravity, the additional scalar degree of freedom which is extracted from the modified gravity sector, turns out to be non-minimally coupled to gravity. With a conformal transformation, however, even this non-minimal coupling can be made to disappear. As presented in more detail in [69], under the conformal transformation

$$g_{\mu\nu} = \Omega \hat{g}_{\mu\nu}, \qquad \Omega := \frac{1}{2}\frac{M_{\rm P}^2}{\chi^2}\,, \tag{5.8}$$

action (5.6) becomes

$$S[\hat{g},\varphi,\hat{\chi}] = \int \mathrm{d}^4x\sqrt{-\hat{g}}\left[\frac{M_{\rm P}^2}{2}\hat{R} - \frac{1}{2}e^{-\sqrt{\frac{2}{3}}\frac{\hat{\chi}}{M_{\rm P}}}\partial_\mu\varphi\partial^\mu\varphi - \frac{1}{2}\partial_\mu\hat{\chi}\partial^\mu\hat{\chi} - \hat{W}(\hat{\chi},\varphi)\right], \tag{5.9}$$

with,

$$\hat{\chi} = \sqrt{6}M_{\rm P}\ln\left(\frac{\sqrt{2}\chi}{M_{\rm P}}\right), \qquad \hat{W}(\varphi,\hat{\chi}) := \left.\frac{M_{\rm P}^4}{4\chi^4}W(\varphi,\chi)\right|_{\chi=\hat{\chi}} = e^{-2\sqrt{\frac{2}{3}}\frac{\hat{\chi}}{M_{\rm P}}}W(\hat{\chi},\varphi)\,. \tag{5.10}$$

We see that starting from a generic $f(R,\varphi)$ model, an inflationary potential can be algorithmically extracted. For Starobinsky's model (5.1), in which $\varphi = 0$, one gets the single-field potential

$$\hat{W}_{\rm Star}(\hat{\chi}) := \hat{W}(\hat{\chi},\varphi)|_{\varphi=0} = \frac{3}{4}m_0^2M_{\rm P}^2\left(1-\exp\left(-\sqrt{\frac{2}{3}}\frac{\hat{\chi}}{M_{\rm P}}\right)\right)^2. \tag{5.11}$$

The potential features the desirable constant plateau for large values of $\hat{\chi}$. In fact, Fig. 4.1 depicting the typical inflationary potential in chapter 4 was obtained for the Starobinsky potential itself.

5.1.2 Generalization of Starobinsky's model

In the new model that is proposed in the thesis, Starobinsky's model is considered in the presence of a scalar field. In addition, the dimensionful constants $(M_{\rm P}^2, m_0^2)$ in Eq. (5.1) are replaced with general functions of φ such that

$$f(R,\varphi) = \frac{U(\varphi)}{2}\left(R + \frac{1}{6\,M^2(\varphi)}R^2\right) - V(\varphi). \tag{5.12}$$

Following the same algorithm as before, the scalar two-field potential extracted from Eq. (5.12) reads

$$\hat{W}(\varphi,\hat{\chi}) = \frac{V(\varphi)}{F^2(\hat{\chi})} + \frac{3}{4}m^2(\varphi)\,M_{\rm P}^2\left(1-\frac{U(\varphi)}{M_{\rm P}^2F(\hat{\chi})}\right)^2, \qquad F(\hat{\chi}) := \exp\left(\sqrt{\frac{2}{3}}\frac{\hat{\chi}}{M_{\rm P}}\right), \tag{5.13}$$

where $m^2(\varphi)$ is defined to be

$$m^2(\varphi) := M^2(\varphi)\frac{M_{\rm P}^2}{U(\varphi)}\,. \tag{5.14}$$

In order to specify the model completely, the following assumptions are made

$$U(\varphi) = M_{\rm P}^2 + \xi\varphi^2, \tag{5.15}$$

$$m^2(\varphi) = m_0^2 + \zeta\varphi^2, \tag{5.16}$$

$$V(\varphi) = \frac{\lambda}{4}\varphi^4. \tag{5.17}$$

For (5.15)-(5.17), the two-field potential $\hat{W}(\varphi, \hat{\chi})$ in Eq. (5.13) reduces to

$$\hat{W}(\hat{\chi}, \varphi) = \frac{\lambda\varphi^4 + 3M_{\rm P}^2\left(m_0^2 + \zeta\varphi^2\right)\left(1 + \xi\frac{\varphi^2}{M_{\rm P}^2} - F\right)^2}{4F^2}. \tag{5.18}$$

We see that in addition to the two mass parameters $M_{\rm P}$ and m_0 present in Starobinsky's model (5.1), the new two-field potential depends also on the three dimensionless parameters ξ, ζ, and λ.

The assumptions (5.15)-(5.17) are motivated by the following considerations. The First motivation is that Starobinsky's model (5.1) is recovered in the limit $\varphi \to 0$ so that its compatibility with the CMB constraints can be inherited. Then, an additional $\varphi \to -\varphi$ symmetry is assumed leaving only φ-even terms. Finally, higher powers of φ in Eqs. (5.15) and (5.16) are also assumed to be un-important for inflationary dynamics. A term of the form $m_{\rm D}^2\,\varphi^2$ in (5.17), in the view of the EF potential (5.18), is also neglected since it would be irrelevant as long as $m_{\rm D}^2 \ll \zeta M_{\rm P}^2$ or $m_{\rm D}^2 \ll \xi m_0^2$. Moreover, as we shall see later, since a significant PBH production requires $\xi \gg 1$, the term $m_{\rm D}^2\,\varphi^2$ can be neglected as long as $m_{\rm D}^2 \lesssim m_0^2$. It would be interesting to study the impact of a large mass $m_{\rm D}^2 \gtrsim m_0^2$, which, however, goes beyond the scope of the work presented here.

5.2 Covariant multi-field formalism

5.2.1 Background dynamics

In the new model we have two scalar fields. The field φ and the scalaron $\hat{\chi}$ extracted from the modified gravity sector. To compare the dynamics with single-field inflation, this extra dimensionality of the field-space is most elegantly captured by recasting Eq. (5.9) in the form

$$S[\hat{g}, \Phi] = \int {\rm d}^4x\sqrt{-\hat{g}}\left[\frac{M_{\rm P}^2}{2}\hat{R} - \frac{\hat{g}^{\mu\nu}}{2}G_{IJ}\Phi^I_{,\mu}\Phi^J_{,\nu} - \hat{W}\right]. \tag{5.19}$$

Here, the scalars $\Phi^I(x)$ are regarded as local coordinates of the scalar field-space with the metric G_{IJ}, such that

$$\Phi^I = \begin{pmatrix} \hat{\chi} \\ \varphi \end{pmatrix}, \qquad G_{IJ}(\Phi) = \begin{pmatrix} 1 & 0 \\ 0 & F^{-1}(\hat{\chi}) \end{pmatrix}. \tag{5.20}$$

We see that the field-space metric G_{IJ} is not flat. That is, there does not exist a transformation $(\hat{\chi}, \varphi) \to (\hat{\chi}', \varphi')$ for which $G'_{IJ} = {\rm diag}(1, 1)$. Alternatively, one can also compute the Ricci scalar

for the metric G_{IJ} and see that it is non-zero. This observation calls for the introduction of the covariant time derivative D_t

$$D_t V^I := \dot{V}^I + \dot{\Phi}^J \Gamma^I_{JK}(\Phi) V^K \,, \tag{5.21}$$

where the Christoffel connection Γ^I_{JK} is defined with respect to the field-space metric (5.20). In terms of D_t, the background Friedmann equations and the Klein-Gordon equations for the homogeneous scalar fields $\Phi^I(t)$ read

$$H^2 = \frac{M_{\rm P}^{-2}}{3}\left[\frac{1}{2}G_{IJ}\dot{\Phi}^I\dot{\Phi}^J + \hat{W}(\Phi)\right], \tag{5.22}$$

$$\dot{H} = -\frac{M_{\rm P}^{-2}}{2}G_{IJ}\dot{\Phi}^I\dot{\Phi}^J, \tag{5.23}$$

$$D_t\dot{\Phi}^I = -3H\dot{\Phi}^I - G^{IJ}\hat{W}_{,J}\,. \tag{5.24}$$

As in chapter 4, the homogeneous and the isotropic background dynamics of the metric is determined by the flat Friedmann-Lemaître-Robertson-Walker (FLRW) line element

$$\mathrm{d}s^2 = -\mathrm{d}t^2 + a^2\delta_{ij}\mathrm{d}x^i\mathrm{d}x^j\,, \qquad H = \frac{\dot{a}}{a}\,. \tag{5.25}$$

Here, t is the cosmic Friedmann time, $a(t)$ is the scale factor, the indices (i, j) denote spatial indices and take values from 1 to 3 and $\delta_{ij} = \mathrm{diag}(1, 1, 1)$. The calculations in this chapter make no reference to the conformal time η. The overdot in this chapter represents a derivative taken with respect to the cosmic time t and not the conformal time as in chapter 4.

Coming back to the background dynamics, further simplification occurs in introducing the unit vector $\hat{\sigma}^I$ which is tangential to the inflationary trajectory such that

$$\hat{\sigma}^I := \frac{\dot{\Phi}^I}{\dot{\sigma}}, \qquad G_{IJ}\hat{\sigma}^I\hat{\sigma}^J = 1, \qquad \dot{\sigma} := \sqrt{G_{IJ}\dot{\Phi}^I\dot{\Phi}^J}. \tag{5.26}$$

Since the field-space is two dimensional, the two-field background dynamics is decomposed into a direction along $\hat{\sigma}^I$ and a direction along the unit vector $\hat{s}^I$ orthogonal to $\hat{\sigma}^I$,

$$G_{IJ}\hat{s}^I\hat{s}^J = 1\,, \qquad G_{IJ}\hat{s}^I\hat{\sigma}^J = 0. \tag{5.27}$$

The two conditions in Eq. (5.27) completely determine the two components of $\hat{s}^I$ upto a sign. For that, we adopt the convention in which $\hat{s}^I$ is proportional to the acceleration vector ω^I

$$\omega^I = D_t\hat{\sigma}^I\,, \qquad \hat{s}^I := \frac{\omega^I}{\omega}\,, \qquad \omega := \sqrt{G_{IJ}\omega^I\omega^J}. \tag{5.28}$$

Since the field-space $(\hat{\chi}, \varphi)$ is two dimensional, it is completely spanned by the unit vectors $(\hat{\sigma}^I, \hat{s}^I)$.

Projecting (5.22)-(5.24) along $\hat{\sigma}^I$ and $\hat{s}^I$ yields

$$H^2 = \frac{M_{\rm P}^{-2}}{3}\left(\frac{1}{2}\dot{\sigma}^2 + \hat{W}\right), \tag{5.29}$$

$$\dot{H} = -\frac{M_{\rm P}^{-2}}{2}\dot{\sigma}^2, \tag{5.30}$$

$$\ddot{\sigma} = -3H\dot{\sigma} - \hat{W}_{,\sigma}, \tag{5.31}$$

$$\omega = -\frac{\hat{W}_{,s}}{\dot{\sigma}}, \tag{5.32}$$

where, the derivatives of $\hat{W}$ along $\hat{\sigma}^I$ and $\hat{s}^I$ are defined by

$$\hat{W}_{,\sigma} := \frac{\partial \hat{W}}{\partial \Phi^I}\hat{\sigma}^I, \qquad \hat{W}_{,s} := \frac{\partial \hat{W}}{\partial \Phi^I}\hat{s}^I. \tag{5.33}$$

We see that Eqs. (5.29)-(5.31) resemble closely the background equations (4.8)-(4.10), obtained for single-field inflation in chapter (4). The same resemblance also holds at the level of perturbations. The additional parameter ω in Eq. (5.32), which is absent in single-field inflation, plays a crucial role in the amplification of $\mathcal{P}_{\mathcal{R}}$ as we shall see next.

5.2.2 Perturbations

As we have seen in chapter 4, the perturbed FLRW line element (including only the scalar degrees of freedom) reads

$$\mathrm{d}s^2 = -(1+2A)\,\mathrm{d}t^2 + 2aB_{,i}\mathrm{d}x^i\mathrm{d}t + a^2\left(\delta_{ij} + 2E_{ij}\right)\mathrm{d}x^i\mathrm{d}x^j. \tag{5.34}$$

Here $E_{ij} := \psi\delta_{ij} + E_{,ij}$. The only difference is that instead of a single matter-field perturbation $\delta\phi$, we have a two dimensional column vector of perturbations

$$\delta\Phi^I = \begin{pmatrix} \delta\hat{\chi} \\ \delta\varphi \end{pmatrix}. \tag{5.35}$$

Like in single-field inflation, the gauge-invariant multi-field Mukhanov-Sasaki variables can be constructed as [63]

$$\delta\Phi^I_{\rm g} := \delta\Phi^I + \frac{\dot{\Phi}^I}{H}\psi. \tag{5.36}$$

Projecting Eq. (5.36) along $\hat{\sigma}^I$ and $\hat{s}^I$ we get

$$Q_\sigma = \hat{\sigma}^J G_{IJ}\delta\Phi^I_{\rm g}, \qquad Q_{\rm s} = \hat{s}^J G_{IJ}\delta\Phi^I_{\rm g}. \tag{5.37}$$

The comoving curvature perturbation $\mathcal{R}$ is related to Q_σ as [103]

$$\mathcal{R}(t,\mathbf{k}) = \frac{H}{\dot{\sigma}}Q_\sigma(t,\mathbf{k}), \tag{5.38}$$

which is identical to its relationship with $\delta\varphi$ in single-field models of inflation (c.f. Eq. (4.44)).

There is, however, a crucial difference. While $\mathcal{R}$ depends explicitly only on Q_σ, the time evolution of Q_σ is coupled to that of Q_s. In single-field inflationary models there is no additional matter scalar field that can influence the dynamics of $\delta\phi$. This coupling between Q_σ and Q_s is essentially what would lead to the amplification of $\mathcal{R}$ as we desire for the production of PBHs. To see this, we look at the equations of motion for Q_σ and Q_s. Eq. (4.20) in chapter 4 governs the time evolution of $\delta\varphi$ in single-field models of inflation. In two-field models of inflation one derives the EOM for the column vector of perturbations $\delta\Phi^I_{\rm g}$ [112, 97, 63]. Projecting it along $\hat{\sigma}^I$ and $\hat{s}^I$ yields the coupled EOMs for Q_σ and Q_s. They are given by

$$\ddot{Q}_\sigma(t,\mathbf{k}) + 3H\dot{Q}_\sigma(t,\mathbf{k}) + \Omega_{\sigma\sigma}(t,\mathbf{k})Q_\sigma(t,\mathbf{k}) = f(\mathrm{d}/\mathrm{d}t)(\omega Q_{\rm s}), \tag{5.39}$$

$$\ddot{Q}_{\rm s}(t,\mathbf{k}) + 3H\dot{Q}_{\rm s}(t,\mathbf{k}) + m_{\rm s}^2(t,\mathbf{k})Q_{\rm s}(t,\mathbf{k}) = 0\,. \tag{5.40}$$

Following the conventions in [69] the following quantities are defined

$$\Omega^I{}_J := M^I{}_J - M_{\rm P}^{-2}a^{-3}D_t\left(\frac{a^3}{H}\dot{\Phi}^I\dot{\Phi}_J\right), \qquad \Omega_{\sigma\sigma} = \hat{\sigma}^I\hat{\sigma}^J\Omega_{IJ} - \omega^2\,, \tag{5.41}$$

$$M_{IJ} := \frac{k^2}{a^2} + \nabla_I\nabla_J\hat{W} + R_{IKJL}\dot{\Phi}^K\dot{\Phi}^L\,, \qquad m_{\rm s}^2 = \hat{s}^I\hat{s}^J M_{IJ} + 3\omega^2\,, \tag{5.42}$$

while the source term appearing on the right hand side of Eq. (5.39) is given by

$$f(\mathrm{d}/\mathrm{d}t) := 2\left[\frac{\mathrm{d}}{\mathrm{d}t} - \left(\frac{W_{,\sigma}}{\dot{\sigma}} + \frac{\dot{H}}{H}\right)\right]. \tag{5.43}$$

Eq. (5.39) shows that the adiabatic modes $Q_\sigma(t,\mathbf{k})$ are sourced by the product $\omega Q_{\rm s}(t,\mathbf{k})$. We see that the two additional quantities which have no analogue in single-field dynamics: the turnrate ω in Eq. (5.28) at the level of the background dynamics and the isocurvature perturbation Q_s in Eq. (5.37) at the level of the perturbations, combine together to allow for an amplification of the power spectrum. Only when the combination of ω and $Q_{\rm s}$ is sufficiently large, are the modes $Q_\sigma(t,\mathbf{k})$ amplified, leading to the amplification of the comoving curvature power spectrum. In the next section, by elaborating more on the properties of the two-field potential $\hat{W}$, we shall see why the model allows for the isocurvature pumping mechanism to work.

5.3 The two-field potential landscape

As shown in Fig. 5.1, the landscape of the two-field potential (5.18) is dominated by three valleys separated by two hills symmetrically located around $\varphi = 0$. The background trajectory, with arbitrary starting point, is expected to *fall* into one of these valleys whose solution is determined by solving the valley equation

$$\hat{W}_{,\varphi}(\hat{\chi},\varphi) = 0\,. \tag{5.44}$$

That the background trajectory must satisfy the condition (5.44) follows from the background dynamics (of φ in particular)

$$\hat{\chi}'' + (\varepsilon_{\rm H} - 3)\left(\hat{\chi}' - M_{\rm P}^2 \frac{\hat{W}_{,\hat{\chi}}}{\hat{W}}\right) + \frac{1}{2}F_{,\hat{\chi}}\left(\frac{\varphi'}{F}\right)^2 = 0\,, \tag{5.45}$$

$$\varphi'' + (\varepsilon_{\rm H} - 3)\,F\left(\frac{\varphi'}{F} - M_{\rm P}^2 \frac{\hat{W}_{,\varphi}}{\hat{W}}\right) - F_{,\hat{\chi}}\hat{\chi}'\frac{\varphi'}{F} = 0\,. \tag{5.46}$$

Here, the prime denotes the derivative with respect to the dimensionless time parameter N, defined by $dN = -Hdt$. Physically, $\Delta N = -1$ means that the scale factor has multipled by a factor of e, such that $a(N) = a(N_i)e^{N_i - N}$. N is therefore referred to as the number of e-folds or the e-folding number. For conventional reasons, N is counted backwards with $N = 0$ at the end of inflation.

For a fixed $\hat{\chi}$, we see that a necessary condition to reach a stationary point in the phase space (φ, φ') (which is to have $\varphi' = \varphi'' = 0$) is $\hat{W}_{,\varphi}\,|_{\hat{\chi}} = 0$. Thus, as $\hat{\chi}$ takes different values during the background evolution, the classical trajectory is obtained by solving (5.44) for $\varphi(\hat{\chi})$. For the two-field potential $\hat{W}$ in Eq. (5.18), Eq. (5.44) gives five solutions

$$\varphi_0(\hat{\chi}) = 0, \qquad \varphi_{\rm v}^{\pm}(\hat{\chi}), \qquad \varphi_{\rm h}^{\pm}(\hat{\chi}). \tag{5.47}$$

The solutions (5.47) correspond to the central valley at φ_0, the two outer valleys at $\varphi_{\rm v}^{\pm}$, and the two hills at $\varphi_{\rm h}^{\pm}$. The solutions $\varphi_{\rm v}^{\pm}(\hat{\chi})$ and $\varphi_{\rm h}^{\pm}(\hat{\chi})$ are only presented symbolically. It does not add to the discussion to present their lengthy expressions in terms of $\hat{\chi}$ explicitly.

At the onset of the inflationary dynamics, the initial value $\hat{\chi}_{\rm i}$ must be sufficiently large $\hat{\chi}_{\rm i}/M_{\rm P} \gg 1$ in order to guarantee that inflation lasts for at least $N \approx 60$ efolds. As the dynamics proceeds, the two outer valleys $\varphi_{\rm v}^{\pm}$ merge with φ_0 at some $\hat{\chi}$. After the valleys merge with φ_0, the potential landscape only features one central valley at $\varphi_0 = 0$. This can be seen more clearly in Fig. 5.2.

Therefore, the inflationary background trajectories, irrespective of their starting points, eventually end up running along the φ_0 valley. However, there is a field value $\hat{\chi}_{\rm c}$ at which the local φ_0 minimum turns into an unstable maximum (the right plot in Fig. 5.1). The critical point $\hat{\chi}_{\rm c}$ is determined by the condition

$$\hat{W}_{,\varphi\varphi}(\hat{\chi}, \varphi)\big|_{\varphi=0} = 0. \tag{5.48}$$

The solution of (5.48) only depends on $m_0/M_{\rm P}$ and ξ/ζ and is given by

$$\hat{\chi}_{\rm c} = M_{\rm P}\sqrt{\frac{3}{2}}\ln\left[1 + 2\frac{\xi}{\zeta}\left(\frac{m_0}{M_{\rm P}}\right)^2\right]. \tag{5.49}$$

At $\hat{\chi} = \hat{\chi}_{\rm c}$, when the second derivative $\hat{W}_{,\varphi\varphi}$ turns negative, the local minimum along the φ direction turns into an unstable local maximum and the two valleys symmetrically located around φ_0 emerge again (c.f. Fig. 5.2).

The inflationary trajectory which was previously running along φ_0 would now be pushed into one of the adjacent valleys that appear for $\hat{\chi} < \hat{\chi}_{\rm c}$. It is this instability and the fall of the inflationary trajectory that ultimately leads to the amplification of the power spectrum as we shall see next.

Before proceeding, it is important to mention that the reduction of the two-field potential into a global attractor along $\varphi = 0$ only happens if a certain parameter combination is realized. The

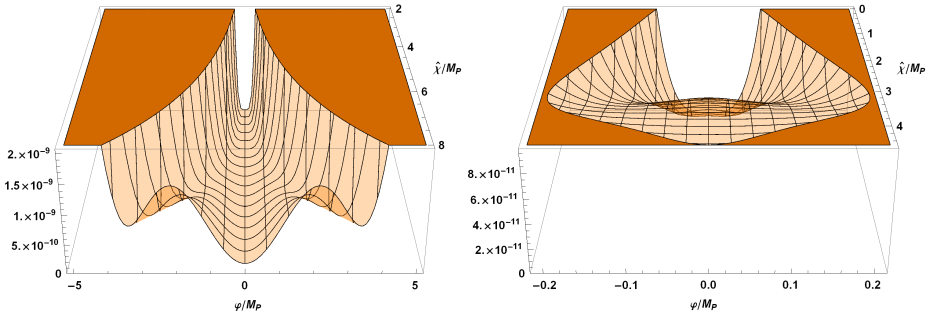

Figure 5.1: The landscape of the two-field potential (5.18) (left) and the vicinity of $\hat{\chi}_c$ (right).

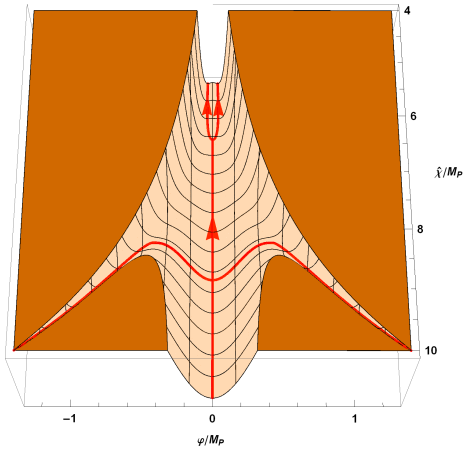

Figure 5.2: Overview of the two-field potential (5.18). The red lines sketch the inflationary trajectories running along the valleys in the direction of the arrows. φ_0 is a global attractor as the two valleys $\varphi_v^{\pm}$ merge with φ_0. After the valleys merge with φ_0, the potential landscape only features one central valley at $\varphi_0 = 0$. However, when we reach the critical point $\hat{\chi} = \hat{\chi}_c$, we see that φ_0 turns into a hill such that two valleys bifurcate adjacent to $\varphi_0 = 0$ for $\hat{\chi} < \hat{\chi}_c$.

necessary condition for that to occur is

$$x = \frac{6\xi^2 m_0^2}{\lambda M_P^2} < 1\,. \tag{5.50}$$

When $x \geq 1$, the potential landscape never reduces to a single global attractor. This is shown in Fig. 5.3. In such a scenario, if the initial conditions are such that the dynamics starts off inside one of the valleys $\varphi_v^{\pm}$, the trajectory stays in the valley forever, and does not go through the richer dynamics in which it is first brought along $\varphi = 0$ and is then pushed outwards due to the instability that occurs around $\hat{\chi}_c$. In such a scenario the predictions of the model would be dependent upon the initial conditions. If we start along $\varphi = 0$ in scenario two, as in the previous situation, the trajectory is pushed off the $\varphi = 0$ attractor for $\hat{\chi} < \hat{\chi}_c$ allowing for the amplification mechanism to work. If we start inside $\varphi_v^{\pm}$, nothing dramatic happens and we get no amplification of the power

spectrum. Thus, the request for the predictions of the model to be independent of the initial values of the fields leads us to only consider scenario one in which the inequality (5.50) is satisfied.

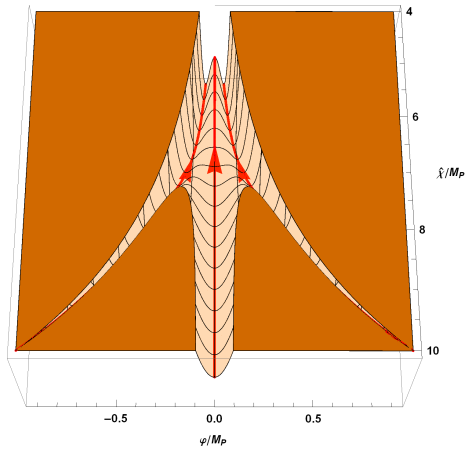

Figure 5.3: Figure depicting how in scenario two the valleys φ_0 and $\varphi_v^{\pm}$ never merge for any $\hat{\chi}$.

5.4 The amplification mechanism

We have seen in Sec. 5.3 that irrespective of where the inflationary trajectory starts on the potential landscape, it always ends up in the central valley $\varphi_0 = 0$. Therefore, the inflationary dynamics predominantly occurs along the $\hat{\chi}$ direction in the field-space such that $\hat{\sigma} = \hat{\chi}$ (c.f. Eq. (5.26)). The amplification of Q_σ in Eq. (5.39) requires as a necessary condition that Q_s in Eq. (5.40) be non-zero. Having identified the inflaton direction $\hat{\sigma}$ with $\hat{\chi}$, we see that $Q_\sigma \propto \delta\hat{\chi}$ and $Q_s \propto \delta\varphi$. The growth of Q_s in Eq. (5.40) is dictated by the effective mass m_s^2, which in our situation is proportional to $\hat{W}_{,\varphi\varphi}$.

When the inflationary trajectory runs along $\varphi = 0$, well before reaching the critical point $\hat{\chi}_c$, the potential along the φ direction is concave, i.e., $\hat{W}_{,\varphi\varphi} \gg 0$. This suppresses any possible growth of Q_s. However, as the trajectory reaches the critical point $\hat{\chi}_c$, $\hat{W}_{,\varphi\varphi}$ approaches zero and turns negative beyond the critical point $\hat{\chi}_c$. The inflationary trajectory which was earlier in a stable equilibrium along $\varphi = 0$, is now in an unstable equilibrium. During the small time the inflationary trajectory spends on this convex hill, and due to the negative effective mass $m_s^2 \propto \hat{W}_{,\varphi\varphi}$ that $Q_s \propto \delta\varphi$ experiences along the hill, Q_s grows exponentially. Shortly after going beyond $\hat{\chi}_c$, being in an unstable equilibrium, the trajectory slips down to one of the valleys adjacent to the hill along $\varphi = 0$. We see that the time at which the inflationary trajectory slips, which leads to the change in the inflaton direction $\hat{\sigma}$ and hence the growth of the turn rate ω defined in Eq. (5.28), is inevitably correlated to the time at which Q_s starts growing. Thus, the general conditions that are required for the sourcing of Q_σ (and hence $\mathcal{R}$), which to have the increase in the product ωQ_s, are naturally realized within the model.

5.5 The stochastic formalism

In general, the properties of $\mathcal{P}_{\mathcal{R}}$ for single-field inflationary models can be determined analytically. The same is more difficult to achieve for multifield models, especially when the background dynamics is as complicated as described above. In such a situation the power spectrum is computed by solving Eqs. (5.22)-(5.24) and Eqs. (5.39)-(5.40) numerically. While the time evolution of the perturbations is dependent upon the background, typically, the converse is not true. Therefore, one first solves the background equations (5.22)-(5.24) and then, using those solutions, solve for the perturbations $Q_s(t, \mathbf{k})$ and $Q_\sigma(t, \mathbf{k})$. This strategy works in most of the multi-field models of inflation but not for the two-field model under consideration. The reason is that if one doesn't take into account the feedback of the quantum fluctuations onto the background, the inflationary trajectory would roll forever in an unstable equilibrium along $\varphi_0 = 0$, even after crossing the critical point $\hat{\chi}_c$. However, physically, what is expected to happen is that the inevitable quantum fluctuations would eventually provide the required kick such that the trajectory falls into one of the adjacent valleys at some $\hat{\chi} < \hat{\chi}_c$.

In the vicinity of the critical point $\hat{\chi}_c$, the restoring classical force which keeps the trajectory focused to the φ_0 attractor, is no longer sufficiently strong to counteract the diffusive force that originates from the unavoidable quantum zero-point fluctuations which the trajectory experiences in the φ direction. For $\hat{\chi} < \hat{\chi}_c$, m_s^2 turns negative and the solution φ_0 becomes unstable. At the same time, the perturbation $\delta\varphi$ starts to grow and even dominates over the classical solution φ_0. In situations where the quantum diffusive force dominates the classical background drift, the standard formalism in which the background dynamics of the scalar fields is considered independently of the time evolution of the quantum fluctuations, breaks down.

Instead, the application of the stochastic formalism [119], which properly takes into account the back reaction of quantum fluctuations on the coarse grained classical background dynamics, is required. In the stochastic formalism, the dynamics of φ during the transition stage around $\hat{\chi}_c$ is determined by a probability density function $P(\varphi, N)$ that specifies the probability of the field having the value φ at a time N. The time evolution of $P(\varphi, N)$ is described by the Fokker-Planck equation (c.f. [127] and Eq. (2.14) in chapter 2),

$$\frac{\partial P}{\partial N} = -\frac{\partial}{\partial \varphi}\left[\mathcal{D}P\right] + \frac{1}{2}\frac{\partial^2}{\partial \varphi^2}\left[\mathcal{F}P\right]. \tag{5.51}$$

The right-hand-side of the Fokker-Planck equation (5.51) is characterized by two terms: a classical drift term with the coefficient $\mathcal{D}(\varphi, N)$ and a quantum diffusion term with the coefficient $\mathcal{F}(\varphi, N)$. For the decomposition $\varphi(N, \mathbf{x}) = \bar{\varphi}(N) + \delta\varphi(N, \mathbf{x})$ into a homogeneous background $\bar{\varphi}(N)$ and a Gaussian random fluctuation $\delta\varphi(N, \mathbf{x})$ with $\langle\delta\varphi\rangle = 0$, the coefficients are obtained as

$$\mathcal{D} = \frac{\mathrm{d}\langle\varphi\rangle}{\mathrm{d}N}, \qquad \mathcal{F} = \frac{\mathrm{d}\langle\delta\varphi^2\rangle}{\mathrm{d}N}. \tag{5.52}$$

In the following we omit the bar over a background quantity. Assuming slow-roll in the $\hat{\chi}$ and φ directions[2], the equation of motion (5.46) reduces to the single-field dynamics of φ depending only parametrically on $\hat{\chi}(N)$,

$$\varphi' \approx \frac{F(\hat{\chi})\hat{W}_{,\varphi}(\hat{\chi}, \varphi)}{3H^2}. \tag{5.53}$$

[2]Within the slow-roll approximation $\varphi'' \approx 0$, $\varepsilon_H \ll 1$ and the term proportional to $F_{,\hat{\chi}}\hat{\chi}'\varphi'/F$ can can also be neglected in (5.46)

Since we are interested in the dynamics around $\varphi = 0$, Taylor expansion of $\hat{W}_{,\varphi}$ yields the linearized equation which determines the drift coefficient

$$\mathcal{D}(\varphi, N) = \varphi' \approx \frac{m_\varphi^2}{3H^2}\varphi\,, \qquad m_\varphi^2(N) := F\hat{W}_{,\varphi\varphi}\,|_{\varphi=0}. \tag{5.54}$$

The variance $\langle \delta\varphi^2 \rangle$ after coarse graining over $k \gtrsim aH$ is given in terms of the power spectrum $\mathcal{P}_\varphi(k)$ of the scalar perturbation $\delta\varphi$ (c.f. Eq. (4.42) in chapter 4),

$$\left\langle \delta\varphi^2 \right\rangle = \int_0^{k\lesssim aH} \mathcal{P}_\varphi(k) d\ln k. \tag{5.55}$$

Within the time interval $-\Delta N$ (remembering that the number of efolds decrease as inflation proceeds), as the scale factor increases, some of the modes which were earlier averaged over now influence the background dynamics as they cross the horizon scale satisfying $k = aH = a_* e^{(N-N_*)}H$. They effectively provide an extra kick to the background dynamics by giving an extra contribution to the integral (5.55) by increasing its upper bound. Treating H as a constant, we obtain $d\ln k \approx -dN$ such that $\mathcal{F}$ in Eq. (5.52) becomes (c.f. Eq. (4.50))

$$\mathcal{F}(N) = -\,\mathcal{P}_\varphi(k)\big|_{k\lesssim aH} \approx -\left(\frac{H}{2\pi}\right)^2. \tag{5.56}$$

From Eq. (5.56) we also see that the precise choice of the coarse graining length scale is not important. Even if the dynamics was coarse grained over a different length scale $k \approx \varepsilon aH$, we see that the coefficient $\mathcal{F}$ would still be the same as the relationship between $d\ln k$ and dN is unchanged for a constant ε. Nevertheless, $1/H$ serves a natural length scale for the inflationary background dynamics such that the effective dynamics is obtained by averaging over the modes with physical wavelengths $a/k \lesssim 1/H$. Inserting (5.54) and (5.56) into (5.51), $P(\varphi, N)$ satisfies the Fokker-Planck equation

$$\frac{\partial P}{\partial N} = -\frac{m_\varphi^2}{3H^2}\frac{\partial(\varphi P)}{\partial\varphi} - \frac{H^2}{8\pi^2}\frac{\partial^2 P}{\partial\varphi^2}. \tag{5.57}$$

The Fokker-Planck equation (5.57) is solved by a Gaussian ansatz with a time dependent variance $S(N) = \langle\varphi^2\rangle(N)$,

$$P(\varphi, N) = \frac{1}{\sqrt{2\pi S(N)}}\exp\left(-\frac{\varphi^2}{2S(N)}\right). \tag{5.58}$$

Inserting (5.58) into (5.57) yields an equation for S,

$$\frac{dS}{dN} = \frac{2}{3}\frac{m_\varphi^2}{H^2}S - \frac{H^2}{4\pi^2}. \tag{5.59}$$

Eq. (5.59) for the variance S is interpreted as determining the time evolution of effective amplitude of the scalar field by identifying [108],

$$\varphi(N) \equiv \sqrt{S(N)}. \tag{5.60}$$

The stochastic formalism is applied for a period in which the quantum diffusive term $H^2/4\pi^2$ dominates the classical term $2m_\varphi^2 S/(3H^2)$ in Eq. (5.59). The stochastic stage starts at some point $\hat{\chi} > \hat{\chi}_c$ at which m_φ^2 falls from large positive values towards zero, and ends when it takes large negative values for some $\hat{\chi} < \hat{\chi}_c$. The onset of the stochastic stage can be determined by the condition $2m_\varphi^2/3H^2 < 1$. This ensures that for any inevitable initial increment of $S(N) \sim H^2/4\pi^2$ the diffusive term dominates the classical one. Similarly, the end of stochastic phase can be roughly estimated by the condition $2m_\varphi^2/3H^2 \approx -1$.

To estimate the duration ΔN of Stage 2, the time taken by $2m_\varphi^2/3H^2$ to change from 1 to -1 must be computed. For the potential (5.18), the ratio $2m_\varphi^2/3H^2$ around $\varphi = 0$ is given by

$$\frac{2m_\varphi^2}{3H^2} = 4\zeta F \frac{M_{\rm P}^2}{m_0^2} - 8\xi \frac{F}{F-1} \tag{5.61}$$

that, in turn, provides the estimate

$$\Delta F(\hat{\chi}) \approx \frac{1}{\zeta}\frac{m_0^2}{M_{\rm P}^2}. \tag{5.62}$$

Along φ_0, the difference ΔF can be estimated from Starobinsky inflation $\Delta F \approx \Delta N$ (c.f. Eq. (98) in [69]), leading to

$$\Delta N \approx \frac{1}{\zeta}\frac{m_0^2}{M_{\rm P}^2}\,, \tag{5.63}$$

which gives a direct relationship between the duration of the stochastic stage and the free parameters of the model.

5.6 Numerical treatment

The background evolution can be divided into three stages. The dynamics during Stage 1 where $\hat{\chi} \gg \hat{\chi}_c$ and Stage 3 where $\hat{\chi} \ll \hat{\chi}_c$ can be determined via the standard techniques, in which one ignores the feedback of the quantum fluctuations onto the background dynamics. Instead, the background dynamics during Stage 2 where $\hat{\chi} \approx \hat{\chi}_c$ is obtained by applying the stochastic formalism. This is because it is only during this phase that the changes in the field φ are dominated by the diffusive kicks due to the quantum modes $\delta\varphi_{\rm k}$ rather than the gradients of the background potential. The entire background dynamics is obtained by patching the numerical solutions of the equations in the individual stages in a way such that the preceding stage provides the initial conditions for the subsequent one.

During Stage 1 and Stage 3, the exact equations of motion (5.45) and (5.46) are solved numerically for both the scalar fields. During Stage 2, for which the stochastic formalism is used to describe the φ dynamics, the following equations are solved numerically

$$\frac{dS}{dN} = \frac{2}{3}\frac{m_\varphi^2}{H^2}S - \frac{H^2}{4\pi^2}, \tag{5.64}$$

$$\frac{d^2\hat{\chi}}{dN^2} = (3-\varepsilon_{\rm H})\left(\frac{d\hat{\chi}}{dN} - \frac{\hat{W}_{,\hat{\chi}}}{\hat{W}}M_{\rm P}^2\right). \tag{5.65}$$

In order to patch the numerical solutions obtained in the different stages, one needs to find the transition moments between them. During the first phase along φ_0, the steep positive curvature of the potential along the φ direction provides a strong restoring force which immediately erases the effect of the continuous quantum kicks trying to drive φ away from $\varphi = 0$. The moment N_1 of the transition between Stage 1 and Stage 2 is taken to be the moment at which for the first time the effect of a quantum kick will not be erased. This will be true when the drift term in (5.64) becomes comparable to the diffusive term for $S(N_1) = H^2(N_1)/(4\pi^2)$. The resulting condition is solved numerically for N_1 as

$$m_\varphi^2(N_1) = \frac{3}{2} H^2(N_1). \tag{5.66}$$

Since $S = \varphi^2$ is effectively zero before N_1, the complete set of initial conditions which result from patching Stage 1 and Stage 2 read

$$S(N_1) = 0, \tag{5.67}$$

$$\hat{\chi}|_{N_1}^{\mathrm{s2}} = \hat{\chi}|_{N_1}^{\mathrm{s1}}, \qquad \left.\frac{\mathrm{d}\hat{\chi}}{\mathrm{d}N}\right|_{N_1}^{\mathrm{s2}} = \left.\frac{\mathrm{d}\hat{\chi}}{\mathrm{d}N}\right|_{N_1}^{\mathrm{s1}}. \tag{5.68}$$

Stage 2 lasts until the curvature of the potential becomes dominant again (but this time with a negative sign). The time N_2, at which Stage 2 ends, is determined numerically from the condition

$$-\frac{2}{3}\frac{m_\varphi^2(N_2)}{H^2(N_2)} S(N_2) = \frac{H^2(N_2)}{4\pi^2}. \tag{5.69}$$

The initial conditions for Stage 3 are

$$\varphi|_{N_2}^{\mathrm{s3}} = S^{1/2}(N_2) \qquad \left.\frac{\mathrm{d}\varphi}{\mathrm{d}N}\right|_{N_2}^{\mathrm{s3}} = \frac{1}{2\sqrt{S}} \left.\frac{\mathrm{d}S}{\mathrm{d}N}\right|_{N_2}, \tag{5.70}$$

$$\hat{\chi}|_{N_2}^{\mathrm{s3}} = \hat{\chi}|_{N_2}^{\mathrm{s2}} \qquad \left.\frac{\mathrm{d}\hat{\chi}}{\mathrm{d}N}\right|_{N_2}^{\mathrm{s3}} = \left.\frac{\mathrm{d}\hat{\chi}}{\mathrm{d}N}\right|_{N_2}^{\mathrm{s2}}. \tag{5.71}$$

It should be emphasized that the second stage typically lasts for less than one efold ($|\Delta N| \lesssim 1$) and that the values acquired by φ at the beginning of Stage 3 are very small. This a posteriori justifies the assumptions of slow-roll along φ in (5.53), the Taylor expansion of the potential in (5.54), and the Gaussian solution (5.58) to the Fokker-Planck equation (5.57).

The numerical solutions for $\varphi(N)$, $\hat{\chi}(N)$ and $a(N)$ are then used in the equations for the perturbations (5.39) and (5.40), which are solved numerically with Bunch-Davis initial conditions imposed in the deep subhorizon regime. Finally, the power spectrum $\mathcal{P}_\mathcal{R}$ is then computed numerically by considering that the pivot scale $k_* = 0.002\,\mathrm{Mpc}^{-1}$ crosses the horizon at $N = 60$ [3, 103]. The numerical results are presented in the next section.

5.7 The power spectrum

5.7.1 Starobinsky's model

Since the new model proposed in the thesis is a generalization of Starobinsky's model, it is instructive to begin by looking at the predictions of the latter. The power spectrum of the comoving

curvature perturbation for Starobinsky's model (5.11) is shown in Fig. 5.4. Since it is a single-field model of inflation, Q_σ is the only perturbation that we have with $Q_s = 0$. As described in the previous sections, Fig. 5.4 is obtained by numerically determining the time evolution of $Q_\sigma(t, \mathbf{k})$ until the end of inflation which then yields the dependence of the comoving curvature perturbation $\mathcal{R}(\mathbf{k}, t_{\rm end})$ on $\mathbf{k}$, at the end of inflation $t_{\rm end}$ (c.f. Eq. (5.38)).

As mentioned in chapter 4, the power spectrum $\mathcal{P}_\mathcal{R}(\mathbf{k})$ is typically parametrized as a power law

$$\mathcal{P}_\mathcal{R}(k, t_{\rm end}) = \frac{k^3}{2\pi^2}|\mathcal{R}(\mathbf{k}, t_{\rm end})|^2 = A^*_\mathcal{R}\left(\frac{k}{k_*}\right)^{n^*_\mathcal{R}-1}, \tag{5.72}$$

with the values of $A^*_\mathcal{R}$ and $n^*_\mathcal{R}$, for the reference scale $k_* = 0.05\,\mathrm{Mpc}^{-1}$, experimentally constrained to be [3]

$$A^*_\mathcal{R} = (2.099 \pm 0.014) \times 10^{-9} \quad \text{and} \quad n^*_\mathcal{R} = 0.9649 \pm 0.0042\,. \tag{5.73}$$

In Fig. 5.4, the parameters $A^*_\mathcal{R}$ and $n^*_\mathcal{R}$ are obtained by making a straight line fit to the (numerically obtained) $\log_{10}\left(\mathcal{P}_\mathcal{R}(k, t_{\rm end})\right)$ vs $\log_{10}(k/k_*)$ plot. The precise value of $A^*_\mathcal{R}$ depends upon the free parameter m_0 in Starobinsky's model which is adjusted to fit the observational bounds. The value of the spectral index $n^*_\mathcal{R}$, however, does not depend explicitly upon the free parameter m_0 of the model. It can be seen that the predictions of Starobinsky's model are in perfect agreement with observations.

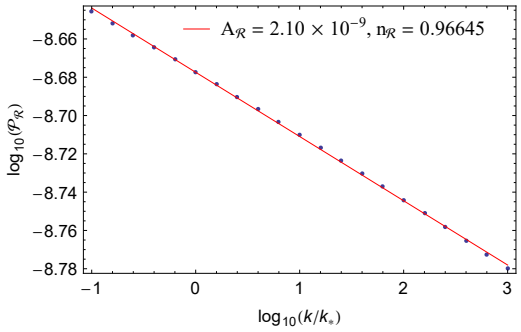

Figure 5.4: The log-log plot of the power spectra $\mathcal{P}_\mathcal{R}$ for Starobinsky's model plotted for the wavenumbers $2 \times 10^{-4}\mathrm{Mpc}^{-1} \lesssim k_{\rm CMB} \lesssim 2\,\mathrm{Mpc}^{-1}$ accessible to *Planck* [3].

5.7.2 The two-field inflationary model

In Sec. 5.4 it was argued that the two-field generalization of Starobinsky's model (5.18) might lead to the amplification of the power spectrum on a certain length scale. Having taken into account the subtleties of the model described in Sec. 5.4 and Sec. 5.5, $\mathcal{R}(\mathbf{k}, t_{\rm end})$ can again be determined numerically by solving the coupled Eqs. (5.39) and (5.40). The formation of a peak in the power spectrum $\mathcal{P}_\mathcal{R}$ of the comoving curvature perturbation is shown in Fig. 5.5.
Fig. 5.5 shows the weak logarithmic k dependence of the power spectrum $\mathcal{P}_\mathcal{R}$ for large wavelengths (small k) during the first slow-roll phase along φ_0 in Stage 1 with the amplitude $\mathcal{P}_\mathcal{R} \approx 10^{-9}$

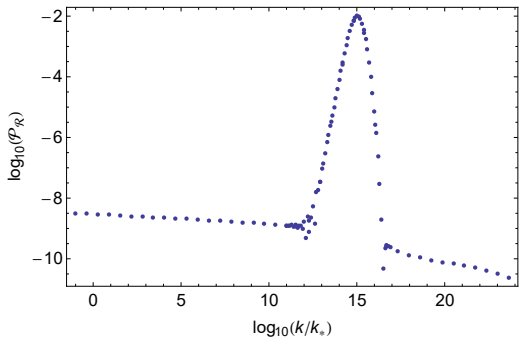

Figure 5.5: The log-log plot of the power spectra $\mathcal{P}_\mathcal{R}$ evaluated at the end of inflation $N = 0$ as a function of the wave number k.

required for the consistency with CMB measurements. At smaller wavelengths (larger k), $\mathcal{P}_\mathcal{R}$ experiences a strong amplification leading to a peak centered around $k_\mathrm{p}/k_* \approx 10^{15}$ with the amplitude $\mathcal{P}_\mathcal{R} \approx 10^{-2}$. This peak corresponds to the modes which cross the horizon during the turn/fall of the inflationary trajectory. For modes that cross the horizon during the slow-roll phase in Stage 3, the amplitude of $\mathcal{P}_\mathrm{R} \approx 10^{-10}$ is slightly smaller than that for the modes that cross the horizon during Stage 1.

As argued before, different modes start seeing the potential and its gradients at different times. This is because the k^2/a^2 term becomes subdominant with respect to the curvature of the potential at different times for different modes. Simply speaking, smaller wavelength (larger k) modes require the scale factor to be bigger in order for the k^2 term to be subdominant (c.f. Eq. (5.42)). For the large wavelength modes (for instance k_CMB), which begin to see the potential during Stage 1 itself, the perturbation Q_s is suppressed due to the large positive effective mass m_s^2 during Stage 1. For these modes Q_σ never gets amplified. The modes which begin to see the potential when $\hat{\chi}$ reaches the critical point $\hat{\chi}_\mathrm{c}$, Q_σ gets amplified because the perturbation $Q_s \propto \delta\varphi$ for these modes exits the horizon (i.e when $k = aH$) at a finite value. Unlike the k_CMB modes Q_s is therefore non-zero at $\hat{\chi} = \hat{\chi}_\mathrm{c}$, which is the time at which the amplification mechanism begins. The modes corresponding to even smaller wavelengths begin to see the inflationary potential only after the trajectory has already fallen into the adjacent valleys, near the end of inflation. They never get amplified since they exit the horizon after the amplification mechanism is over.

This provides a qualitative explanation of Fig. 5.5 in which we see that the power spectrum is amplified only for only a small window of length scales. In particular, the mechanism renders the predictions of the model the same as Starobinsky's model for the length scales probed by *Planck*.

5.8 PBH formation

Primordial black holes can form during the radiation dominated era, after the end of inflation, by the collapse triggered by large density perturbations imprinted during inflation. As mentioned in chapter 4, the probability of generating such a perturbation with a large amplitude is enhanced by the peaks in the inflationary power spectrum of the curvature perturbation [116, 75, 62, 22]. A

PBH forms whenever the overdensity

$$\delta(t,\mathbf{x}) := \frac{\rho(t,\mathbf{x}) - \bar{\rho}(t)}{\bar{\rho}(t)} \tag{5.74}$$

exceeds a critical value δ_c in a given (spherical) Hubble volume $V_H(t) := 4\pi r_H^3(t)/3$. The Hubble radius is defined as $r_H(t) := 1/H(t)$ and the background density in a flat FLRW universe is given by $\bar{\rho}(t) = 3H^2(t)/(8\pi G_N)$. With the help of numerical simulations, one arrives at the following relationship between the mass of the PBH M_{PBH}, the horizon mass $M_H = \bar{\rho}(t_f)V_H(t_f)$ at the time of formation t_f and the amplitude of the perturbation δ

$$M_{PBH}(\delta, t_f) = K\, M_H(t_f)(\delta - \delta_c)^\gamma\,. \tag{5.75}$$

The parameters K, δ_c and γ in Eq. (5.75) are determined numerically [76, 115, 94, 49].

5.8.1 PBH abundance

In order to calculate the PBH abundance, it is useful to define the fraction of the mass in the universe which collapsed into PBHs at the time of formation. This fraction β is defined as

$$\beta(t_f) := \frac{\rho_{PBH}(t_f)}{\bar{\rho}(t_f)}. \tag{5.76}$$

In the Press-Schechter formalism β is calculated as [106]

$$\beta(t_f) = 2\int_{\delta_c}^{\infty} \mathrm{d}\delta\, \frac{M_{PBH}(\delta, t_f)}{M_H(t_f)} P(\delta, t_f). \tag{5.77}$$

Here, $P(\delta, t_f)$ is the probability density function of generating an overdensity with amplitude δ at the moment of formation t_f. Assuming that the perturbations δ are independent random variables, they follow Gaussian statistics.[3] The lower integration bound in (5.77) is determined by the critical collapse density δ_c. The probability density of having an overdensity with amplitude δ is given by

$$P(\delta, t_f) = \frac{1}{\sqrt{2\pi\sigma^2(t_f)}} \exp\left\{\left(-\frac{1}{2}\frac{\delta^2}{\sigma^2(t_f)}\right)\right\}. \tag{5.78}$$

Hence, the perturbations forming PBHs are very rare and lie near the tail of the Gaussian PDF (5.78). Calculating β from (5.77) requires calculating the variance $\sigma^2(t_f) = \langle\delta^2(t_f)\rangle$ in (5.78). The Fourier transform of the density contrast $\delta(t,\mathbf{x})$ is given by

$$\delta(t,\mathbf{x}) = \int \frac{\mathrm{d}^3\mathbf{k}}{(2\pi)^{3/2}}\, e^{i\mathbf{k}\mathbf{x}}\delta_{\mathbf{k}}(t). \tag{5.79}$$

As described in chapter 4, $\sigma^2(t)$ is completely determined by the power spectrum $\mathcal{P}_\delta(t,k)$ via the two-point correlation function such that

$$\sigma^2(t) = \int_0^\infty \mathrm{d}(\ln k)\, \mathcal{P}_\delta(t,k), \tag{5.80}$$

$$\langle\delta_{\mathbf{k}}(t)\delta^*_{\mathbf{k}'}(t)\rangle = \frac{2\pi^2}{k^3}\mathcal{P}_\delta(t,k)\delta^3(\mathbf{k}-\mathbf{k}'). \tag{5.81}$$

[3] For a discussion on non-Gaussian effects, see e.g. [23, 132, 52, 134].

Since the perturbations $\delta_{\mathbf{k}}(t)$ arise from the comoving curvature perturbations $\mathcal{R}_{\mathbf{k}}(t)$ amplified during inflation, $\mathcal{P}_\delta(t,k)$ is related to the inflationary power spectrum $\mathcal{P}_\mathcal{R}(t,k)$. The linear relation between δ_k in the radiation dominated era and $\mathcal{R}_{\mathbf{k}}$ is given by [4]

$$\delta_{\mathbf{k}}(t) = \frac{4}{9}\left(\frac{k}{aH}\right)^2 T(t,k)\mathcal{R}_{\mathbf{k}}(t). \tag{5.82}$$

The transfer function $T(t,k)$ describes the sub-horizon dynamics $k > aH$ of $\delta_{\mathbf{k}}(t)$ after horizon re-entry, while $T(t,k) = 1$ for superhorizon scales $k < aH$. Thus, the variance (5.80) is obtained as

$$\sigma^2(t) = \int_0^\infty \mathrm{d}(\ln k)\,\frac{16}{81}\left(\frac{k}{a(t)H(t)}\right)^4 T^2(t,k)\,\mathcal{P}_\mathcal{R}(t,k). \tag{5.83}$$

The integral (5.83) diverges at the upper integration bound for small wavelengths $\lambda = 1/k$. This is avoided by smoothing $\delta(t,\mathbf{x})$ with a unit normalized window function $W(\mathbf{x}-\mathbf{y},R)$ at a smoothing scale R,

$$\delta_R(t,\mathbf{x}) = \int \mathrm{d}^3y\, W(\mathbf{x}-\mathbf{y},R)\delta(t,\mathbf{y}). \tag{5.84}$$

Physically, the coarse graining induced by the smoothing means that at every point $\mathbf{x}$, the smoothed overdensity $\delta_R(t,\mathbf{x})$ represents the average of $\delta(t,\mathbf{x})$ over a spherical region of radius R centered at $\mathbf{x}$, i.e. the substructures in the overdensity $\delta(t,\mathbf{x})$ below the resolution scale R are smoothed out in $\delta_R(t,\mathbf{x})$ by the averaging procedure. We choose a modified Gaussian window function W_G in (5.84). Following the conventions in [131], the window function in Fourier space reads[5]

$$W_\mathrm{G}(kR) = \exp\left[-\frac{(kR)^2}{4}\right]. \tag{5.85}$$

The window function (5.85) strongly damps out contributions from modes much larger than the "smoothing mode" $k_R = 1/R$. Since we assume that a PBH forms when the modes $\delta_{\mathbf{k}}(t)$ re-enter the horizon at $t = t_\mathrm{f}$, the smoothing mode should be identified with the comoving Hubble radius at formation

$$k_R \equiv a(t_\mathrm{f})H(t_\mathrm{f}). \tag{5.86}$$

The variance (5.83) at t_f, smoothed at the horizon scale, acquires the form

$$\sigma_R^2(t_\mathrm{f}) = \int_0^\infty \mathrm{d}(\ln k)\,\frac{16}{81}\left(\frac{k}{k_R}\right)^4 W^2(k/k_R)\,\mathcal{P}_\mathcal{R}(t_\mathrm{f},k). \tag{5.87}$$

In order to have a sizable mass fraction (5.77), the smoothed variance (5.87) must be sufficiently large. This is naturally realized for the power spectrum which features a strong amplification at $k \approx k_R$.

[4] For a discussion taking into account the effects of the more general non-linear relation between the curvature perturbations and the density contrast see [55, 134].

[5] Note the additional factor of $1/2$ in the argument of the exponential in (5.85). For a comparison of the impact of different window function see [59].

Moreover, the horizon mass $M_{\rm H}(t_{\rm f})$ at the time of formation is related to the peak scale k_p [96] such that

$$M_{\rm PBH}(k_{\rm p}) \approx 6.3 \times 10^{12} M_{\odot} \left(\frac{k_{\rm p}}{\rm Mpc^{-1}}\right)^{-2}, \tag{5.88}$$

where k_p is the scale at which the inflationary power spectrum peaks and $M_{\odot}$ denotes the mass of the sun. For instance, $k_{\rm p} \approx 10^{12}{\rm Mpc}^{-1}$ in Fig. 5.5. If we are interested in generating PBHs within a given mass range, relation (5.88) gives an estimate for the peak location in $\mathcal{P}_{\mathcal{R}}$, which ultimately depends on the free parameters of the model. If we demand that all CDM that we observe today is made of PBHs, only a narrow range for the PBH mass is observationally allowed. The scale $k_{\rm p}$ at which $\mathcal{P}_{\mathcal{R}}$ must be strongly amplified is thus strongly constrained by observations thereby resulting in strong constraints on the free parameters of the model. It is also important to realize via Eqs. (5.87) and (5.88) that both the mass and the abundance of PBHs are determined by the inflationary power spectrum $\mathcal{P}_{\mathcal{R}}$.

5.8.2 Primordial black holes as cold dark matter

In the case when sufficiently large number of PBHs are formed in the radiation dominated era, they could make up a large fraction of the presently observed CDM content in the Universe [73, 33, 20, 29, 28, 61]. Since the mass spectrum of PBHs is already considerably constrained on a broad range of scales, there are only a few PBH mass windows in which this possibility can be realized [27, 28]. The observationally allowed masses for PBHs making up the whole of CDM are

$$10^{-17} M_{\odot} \lesssim M^{I}_{\rm PBH} \lesssim 10^{-16} M_{\odot}, \tag{5.89}$$

$$10^{-13} M_{\odot} \lesssim M^{II}_{\rm PBH} \lesssim 10^{-9} M_{\odot}. \tag{5.90}$$

In addition to $M^{I}_{\rm PBH}$ and $M^{II}_{\rm PBH}$, the detection of binary black hole mergers at LIGO/Virgo has renewed interest in the possibility of a primordial origin of CDM for PBHs in the mass range

$$10 M_{\odot} \lesssim M^{III}_{\rm PBH} \lesssim 10^{2} M_{\odot}. \tag{5.91}$$

Although the possibility of explaining all the observed CDM by PBHs in the mass window $M^{III}_{\rm PBH}$ seems to be ruled out observationally [27, 28, 113], a peak leading to the production of PBHs in the mass range $M^{III}_{\rm PBH}$ would provide an inflationary explanation for the observed merger events. For these reasons, only the parameter combinations which lead to PBHs in these three mass windows are considered in this work, as they are the most observationally relevant ones. The mass intervals (5.89)-(5.91) directly translate into k intervals in which the peak featured in $\mathcal{P}_{\mathcal{R}}$, centered at $k_{\rm p}$, must lie (c.f. Eq. (5.88)):

$$k^{I}_{\rm p} \approx 10^{15}{\rm Mpc}^{-1}, \tag{5.92}$$

$$10^{13}{\rm Mpc}^{-1} \gtrsim k^{II}_{\rm p} \gtrsim 10^{11}{\rm Mpc}^{-1}, \tag{5.93}$$

$$k^{III}_{\rm p} \approx 10^{6}{\rm Mpc}^{-1}. \tag{5.94}$$

In order to quantify the fraction of CDM that is made up of PBHs, the parameter $F_{\rm PBH}$ is defined in terms of the distribution $f(M_{\rm PBH})$

$$F_{\rm PBH} := \int_{-\infty}^{\infty} f(M_{\rm PBH}) \mathrm{d} \ln M_{\rm PBH} \,, \tag{5.95}$$

such that $F_{\rm PBH} = 1$ when the CDM energy density $\rho_{\rm CDM}(t_0)$ as observed today is equal to the energy density due to primordial black holes $\rho_{\rm PBH}(t_0)$, $F_{\rm PBH} < 1$ when $\rho_{\rm PBH}(t_0) < \rho_{\rm CDM}(t_0)$ and $F_{\rm PBH} > 1$ when $\rho_{\rm PBH}(t_0) > \rho_{\rm CDM}(t_0)$. As discussed before, the probability that a PBH forms is related to the amplitude of the power spectrum $\mathcal{P}_{\mathcal{R}}$. Therefore, while the observational constraints (5.89)-(5.91) determine the scale at which the power spectrum must peak, demanding that $F_{\rm PBH} = 1$ determines the amplitude of the peak of the power spectrum on those scales. The distribution $f(M_{\rm PBH})$ typically assumes a log-normal shape given by

$$f(M_{\rm PBH}) = \frac{A_M}{\sqrt{2\pi\Delta_M^2}} \exp\left\{ -\frac{\left[\ln\left(M_{\rm PBH}/M_0\right)\right]^2}{2\Delta_M^2} \right\} , \tag{5.96}$$

and is ultimately determined by the inflationary power spectrum. This is because $f(M_{\rm PBH})$ is related to β (Eq. (5.77)). β in turn depends on $P(\delta)$. $P(\delta)$ depends on σ^2 (Eq. (5.78)) and σ^2 depends on $\mathcal{P}_{\mathcal{R}}$ (Eq. (5.87)). The relationship between $f(M_{\rm PBH})$, which encodes the distribution of the PBH masses, and σ_R^2, which is related to the inflationary power spectrum, is rather involved and is derived in the appendix of publication I [68] (Eq. (A23)). Nevertheless, it is clear that starting from the inflationary power spectrum the mass distribution of the PBHs can be computed. Using the expression derived in publication I [68], this distrubtion is plotted in the figures presented in Sec. 5.9.

In the next section it is shown that there exists a suitable combination of the free parameters (ξ, ζ, λ) that leads to $F_{\rm PBH} = 1$ for the mass windows $M^I_{\rm PBH}$ and $M^{II}_{\rm PBH}$. While the observational constraints rule out the possibility of CDM being made of PBHs lying in the mass window $M^{III}_{\rm PBH}$, we also show for completeness that a suitable parameter combination can still lead to maximally allowed PBH production within this mass window such that $F_{\rm PBH} \lesssim 10^{-2}$-$10^{-3}$ [27, 28, 113].

5.9 Results

5.9.1 Mass windows $M^I_{\rm PBH}$ and $M^{II}_{\rm PBH}$

For appropriate parameter values of the two-field generalization of Starobinsky's model, it is shown in this section that the mass distributions $f(M_{\rm PBH})$ with $F_{\rm PBH} = 1$ can be realized in both mass windows $M^I_{\rm PBH}$ and $M^{II}_{\rm PBH}$. In Fig. 5.6 a sample parameter combination is chosen for which $\mathcal{P}_{\mathcal{R}}$ peaks at $k_{\rm p} \approx 10^{15}\mathrm{Mpc}^{-1}$ and generates a significant amount of CDM in mass window $M^I_{\rm PBH}$. The left plot in Fig. 5.6 shows a mass distribution $f(M_{\rm PBH})$ which leads to $F_{\rm PBH} = 0.69$ for $\xi = 38$. The right plot in Fig. 5.6 illustrates the sensitivity of $f(M_{\rm PBH})$ on ξ. For a ξ larger by only 0.5%, the amplification mechanism is already too strong and leads to the observationally unacceptable large value of $F_{\rm PBH} = 1.4$.
Similarly, Fig. 5.7 shows $f(M_{\rm PBH})$ for two parameter combinations in the mass window $M^{II}_{\rm PBH}$. The left plot in Fig. 5.7 shows an observationally viable scenario with $F_{\rm PBH} = 0.5$, while the right

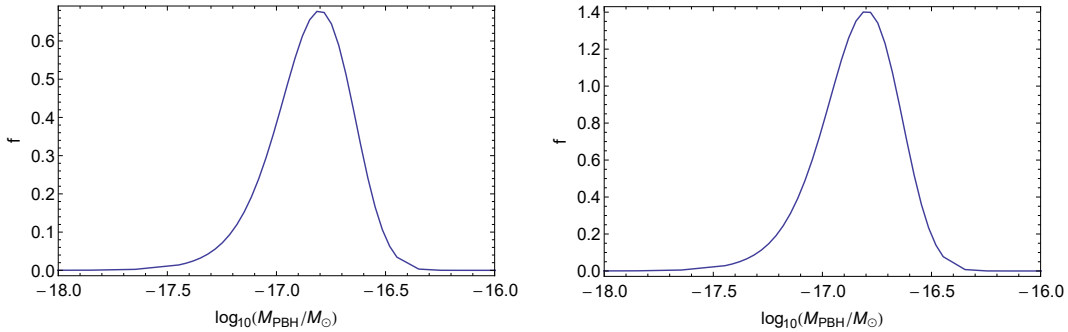

Figure 5.6: Left: $f(M_{\rm PBH})$ for $\lambda = 10^{-5}$, $\xi = 38$, $\zeta = 3.30 \times 10^{-10}$ leading to the log-normal fit with $A_{\rm p} = 0.003835$, $\Delta_{\rm p} = 0.592179$ and $k_{\rm p} = 3.04 \times 10^{15}{\rm Mpc}^{-1}$. Right: $f(M_{\rm PBH})$ for $\lambda = 10^{-5}$, $\xi = 38.2$, $\zeta = 3.31 \times 10^{-10}$ leading to the log-normal fit with $A_{\rm p} = 0.00391$, $\Delta_{\rm p} = 0.5919$ and $k_{\rm p} = 3.03 \times 10^{15}{\rm Mpc}^{-1}$. Both plots are obtained for m_0 as in (5.100).

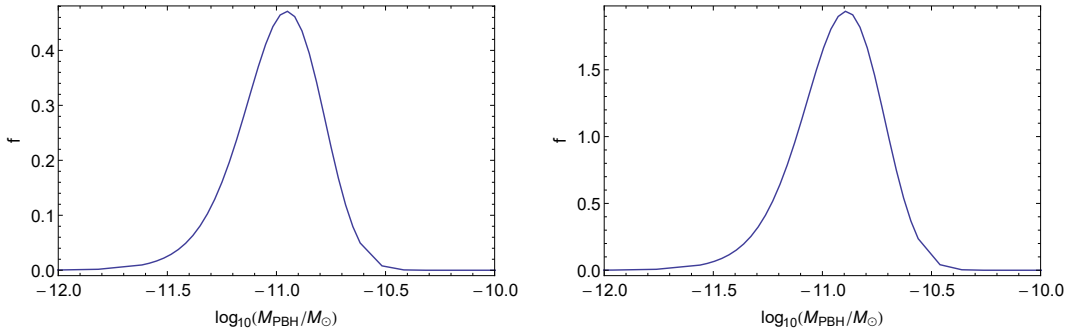

Figure 5.7: Left: $f(M_{\rm PBH})$ for $\lambda = 10^{-5}$, $\xi = 36$, $\zeta = 2.29 \times 10^{-10}$ leading to the log-normal fit with $A_{\rm p} = 0.00485$, $\Delta_{\rm p} = 0.6360$ and $k_{\rm p} = 3.69 \times 10^{12}{\rm Mpc}^{-1}$. Right: $f(M_{\rm PBH})$ for $\lambda = 10^{-5}$, $\xi = 36.5$, $\zeta = 2.31 \times 10^{-10}$ leading to the log-normal fit with $A_{\rm p} = 0.0051$, $\Delta_{\rm p} = 0.6348$ and $k_{\rm p} = 3.46 \times 10^{12}{\rm Mpc}^{-1}$. Both plots are obtained for m_0 as in (5.100).

plot leads to a an unacceptable value $F_{\rm PBH} = 2.1$. This illustrates that the model parameters can be adjusted such that a significant fraction of CDM (including all CDM) is made of PBHs in the two mass windows (5.89)-(5.90).

5.9.2 LIGO mass window $M^{III}_{\rm PBH}$

If the observed LIGO black hole merger events are of inflationary origin, the merger rates may be used to constrain the power spectrum via the PBH mass distribution $f(M_{\rm PBH})$. Observationally, in the LIGO mass window (5.91), the upper bound on the total fraction $F_{\rm PBH}$ is most likely constrained to lie between 10^{-3}-10^{-2}, c.f. [28]. There seems to be some ambiguity concerning the precise upper bound on $F_{\rm PBH}$ for the LIGO mass window $M^{III}_{\rm PBH}$. Some works [34, 107, 60, 43]

suggest that $F_{\rm PBH}$ is closer to 10^{-3} while others indicate that $F_{\rm PBH}$ could attain much higher values [77, 133, 78, 35].

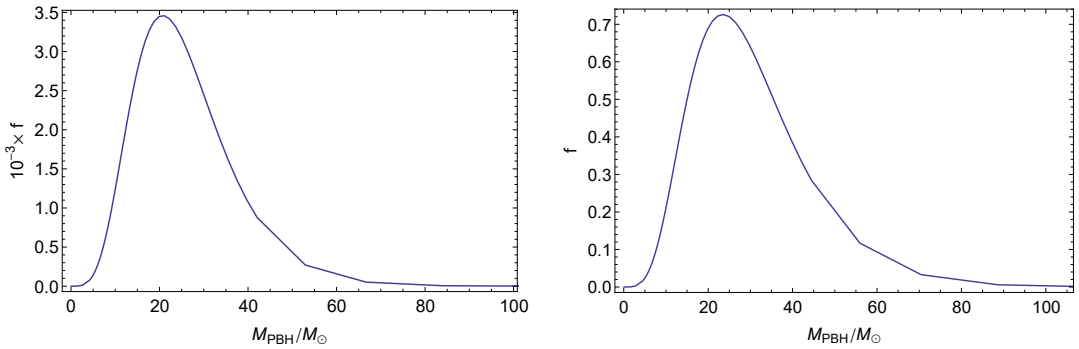

Figure 5.8: Left: $f(M_{\rm PBH})$ obtained for the LIGO mass window $M_{\rm PBH} \approx 10M_\odot$ for parameter values $\lambda = 10^{-5}$, $\xi = 34$ and $\zeta = 1.345 \times 10^{-10}$. Right: $f(M_{\rm PBH})$ in the LIGO mass window $M_{\rm PBH} \approx 10M_\odot$ for parameter values $\lambda = 10^{-5}$, $\xi = 36.70$ and $\zeta = 1.396 \times 10^{-10}$. Both plots are obtained for m_0 as in (5.100).

Fig. 5.8 shows that the chosen model parameters generate a distribution $f(M_{\rm PBH})$ consistent with the observational constraints. The total fraction $F_{\rm PBH}$ is highly sensitive to the model parameters, in particular to ξ, as can be seen by comparing the two plots in Fig 5.8 where $F_{\rm PBH} = 4.1 \times 10^{-3}$ for the left plot and $F_{\rm PBH} = 0.9$ for the right plot. Therefore, by fine tuning the model parameters any numerical value $F_{\rm PBH} \leq 1$ can be obtained.

5.10 Identification with the Higgs field

While in Starobinsky's model inflation is driven by the additional scalar degree of freedom extracted from the R^2 term (Eq. (5.1)), in Higgs inflation, the inflaton is identified with the Standard Model (SM) Higgs boson non-minimally coupled to the Ricci scalar [18]. More explicitly, $f_h(R,\varphi)$ in Eq. (5.2) for Higgs inflation is taken to be

$$f_h(R,\varphi) = \frac{U(\varphi)}{2}R - V(\varphi)\,, \tag{5.97}$$

with $U(\varphi) = M_{\rm P}^2 + \xi\varphi^2$ and $V(\varphi) = \lambda\varphi^4/4$ being the same as in Eqs. (5.15) and (5.17) respectively [6]. The starting action (5.97) is of the same form as Eq. (5.6) with an additional simplification that we only have one scalar field, since the additional scalar field would only appear if one had modified gravity terms in the starting action. As before, we get rid of the non-minimal coupling to the gravity sector by making a conformal transformation $\hat{g}_{\mu\nu} = \Omega(\varphi)g_{\mu\nu}$ such that action reads [18]

$$S_h[\hat{g},\hat{u}] = \int {\rm d}^4x\sqrt{-\hat{g}}\left[\frac{M_{\rm P}^2}{2}\hat{R} - \frac{1}{2}\partial_\mu\hat{u}\partial^\mu\hat{u} - \hat{W}(\hat{u})\right]\,, \tag{5.98}$$

[6] Since $\nu/M_{\rm P} \approx 10^{-16}$, we neglect the constant ν present in the Higgs potential for the inflationary analysis.

where $\Omega(\varphi) := 1 + \xi\varphi^2/M_{\rm P}^2$, $d\hat{u}/d\varphi := \sqrt{(\Omega + 6\xi^2\varphi^2/M_{\rm P}^2)/\Omega^2}$ and $\hat{W} = V(\varphi(\hat{u}))/\Omega^2(\hat{u})$. For large field values $\varphi \gg M_{\rm P}/\sqrt{\xi}$, the effective inflationary potential $\hat{W}(\hat{u})$ can be shown to take the same functional form as the Starobinsky potential (5.11) [18]. Therefore, the model of Higgs inflation in which the scalar field is non-minimally coupled to gravity via the $\xi\varphi^2$ term, and Starobinsky's model, in which inflation is governed by the scalaron extracted from the R^2 term, yield the same predictions for the inflationary observables. The new two-field model (5.12) considered in this work, which leads to the two-field inflationary potential (5.18), can therefore be seen as a combination of the two models with an additional assumption that the R^2 term is also non-minimally coupled to the Higgs field via the coupling constant ζ.

The combination of Higgs inflation and Starobsinksy inflation in which $\zeta = 0$ has already been studied in previous works [48, 129, 74, 69]. It was concluded that also this simple combination of the two models yields the same predictions for the inflationary observables as Higgs inflation and/or Starobinsky inflation. However, with $\zeta = 0$, the amplification of the power spectrum cannot be realized. As we have seen, by paying the price of introducing this additional non-minimal coupling between the R^2 term and the Higgs field, the amplification of the power spectrum can be realized which then offers the possibility to explain the observed CDM content in terms of PBHs.

In the SM, the value of the quartic Higgs coupling $\lambda \approx 10^{-1}$ is determined by the symmetry breaking scale ν and the Higgs mass $M_{\rm h}$. In view of the energy gap between the electroweak energy scale and the inflationary energy scale, the RG flow is needed to determine the value of λ during inflation [17, 44, 8]. An analysis of the full RG system of the extended scalaron-Higgs model would be required for a precise determination of the running λ at the inflationary energy scale which is not done here.

Instead, it is shown that for the likely values of $10^{-2} \lesssim \lambda \lesssim 10^{-6}$ that maybe realized for the Higgs field during inflation [71, 16, 72], the other parameters of the model allow for a sufficient amplification of the power spectrum so as to generate sufficient PBHs within the observationally constrained mass windows $M^{I}_{\rm PBH}$ and $M^{II}_{\rm PBH}$ to account for the observed CDM content.

5.11 Constraining the parameters

Let us assume for the sake of argument that PBHs accounting for CDM have masses ranging within the mass window $M^{II}_{\rm PBH}$. Then the first constraint on the inflationary model is provided by the CMB observations on length scales $2 \times 10^{-4}{\rm Mpc}^{-1} \lesssim k_{\rm CMB} \lesssim 2\,{\rm Mpc}^{-1}$. The second constraint is provided by the fact that the power spectrum must peak at a scale $k^{II}_{\rm PBH}$ to generate PBHs within $M^{II}_{\rm PBH}$. The third constraint is provided by the desire that the amplitude of the power spectrum peak must be just right so that one can account for the whole of dark matter. For a given value of λ that might lie somewhere between $10^{-2} \lesssim \lambda \lesssim 10^{-6}$, these three constraints completely fix the remaining free parameters of the model.

5.11.1 CMB constraint

Since the CMB modes satisfy $k_{\rm CMB} \ll k^{II}_{\rm p}$, they start seeing the inflationary potential much before the inflationary trajectory reaches the critical point. Before reaching the critical point, the inflationary trajectory is along $\varphi = 0$ where the two field potential reduces to the Starobisnky potential. The predictions for the power spectrum $\mathcal{P}_{\mathcal{R}}(k)$ for the CMB modes would then be the same as Starobinsky's model. It was mentioned before that while the predicted value of the spectral index

$n_{\mathcal{R}}$ for Starobinsky's model is independent of the parameter m_0, the amplitude $\mathcal{A}_{\mathcal{R}}$ depends explicitly on this value. An oversimplified way of seeing this is to recall from Eq. (4.50) of chapter (4) that $\mathcal{P}_{\mathcal{R}} \propto H^2$ and within the slow roll approximation $H^2 \propto \hat{W}$. From Eq. (5.11) we see further that $\hat{W} \propto m_0^2$. Thus, the CMB constraints on the scalar power spectrum fix the value of m_0. More precisely, in Starobinsky inflation we have the relations

$$A^*_{\mathcal{R}} \approx \frac{N_*^2}{24\pi^2}\frac{m_0^2}{M_{\rm P}^2}, \quad n^*_{\mathcal{R}} \approx 1 - \frac{2}{N_*}\,, \tag{5.99}$$

where, as mentioned before, N serves as the dimensionless time parameter which counts the number of efolds remaining from the end of inflation. This means that for a given N, the scale factor is smaller by a factor of e^{-N} compared to its value at the end of inflation. N_* is the efolding number at which the mode k_* crosses the horizon (which is to say that it satisfies the condition $k_* = a(N_*)H(N_*)$). *Planck* data [3] constraints $A^*_{\mathcal{R}}$, $n^*_{\mathcal{R}}$ at $k_* = 0.05\ \text{Mpc}^{-1}$ at values already specified in Eq. (5.73).

Taking $N_* = 60$ for $k_* = 0.002\text{Mpc}^{-1}$, the scalaron mass is fixed to be

$$m_0 \approx 1.18 \times 10^{-5}\, M_{\rm P}\,. \tag{5.100}$$

5.11.2 Constraint imposed by the PBH mass

In this section the relationship between the model parameters ζ and ξ and the PBH mass is obtained. Using the definition of the number of efolds $N_* - N = \ln a/a_*$, for modes which cross the horizon at $k = aH$ and $k_* = a_* H$ with constant $H \approx H_*$ respectively, we obtain $N_* - N = \ln k/k_*$. During the phase of effective Starobinsky inflation, there is a simple relation between N and the field value $\hat{\chi}$ given by $N(\hat{\chi}) \approx F(\hat{\chi})$ (with $F(\hat{\chi})$ defined as in Eq. (5.13)). The peak in $\mathcal{P}_{\mathcal{R}}(k)$ is centered around the modes $k \approx k_{\rm p} \pm \Delta k$ which cross the horizon in the vicinity of $\hat{\chi}_{\rm c}$. Hence, we can express $k_{\rm p}$ in terms of $\hat{\chi}_{\rm c}$ defined in (5.49) by the relation

$$k_{\rm p} \approx k_* \exp\left(N_* - 1 - 2\frac{\xi}{\zeta}\frac{m_0^2}{M_{\rm P}^2}\right). \tag{5.101}$$

Since $M_{\rm PBH}$ is related to the peak scale $k_{\rm p}$ via (5.88) we finally obtain $M_{\rm PBH}$ in terms of the model parameters, the pivot scale k_* and the total number of efolds N_*,

$$M_{\rm PBH} \approx M_\odot \left(\frac{4\times 10^{-7}\, k_*}{\text{Mpc}^{-1}}\right)^{-2} e^{-2(N_*-1)+4\frac{\xi}{\zeta}\frac{m_0^2}{M_{\rm P}^2}}. \tag{5.102}$$

For $N_* = 60$, $k_* = 0.002\,\text{Mpc}^{-1}$, and m_0 as in (5.100), we obtain the linear scaling relation between ζ and ξ with a $M_{\rm PBH}$-dependent proportionality coefficient

$$\zeta \approx 5.6 \times 10^{-10}\left[\ln\left(10^{33}\frac{M_{\rm PBH}}{M_\odot}\right)\right]^{-1}\xi. \tag{5.103}$$

Thus, the observational constraint that the PBHs accounting for CDM can either belong to $M^I_{\rm PBH}$ or $M^{II}_{\rm PBH}$, imposes a relationship between the parameters ζ and ξ leaving only one out of the two free. Next, we obtain a relation involving λ and ξ from the requirement that $F_{\rm PBH} = 1$ for a mass distribution $f(M_{\rm PBH})$ centred around a given $M_{\rm PBH}$.

5.11.3 Constraint imposed by the peak amplitude

In view of the complex inflationary dynamics around peak formation, going beyond an order of magnitude estimate based on various simplifying assumptions is rather difficult. Since in any case the results are obtained by a full numerical treatment, the discussion in this section is only meant to provide a rough understanding of how the parameters of the model control the amplification mechanism of the power spectrum.

We begin by noting that $\mathcal{P}_\mathcal{R}(k)$ is related to the perturbation $Q_\sigma(N,\mathbf{x})$ in position space by

$$\int d\ln k \mathcal{P}_\mathcal{R}(k) = \frac{1}{2\varepsilon_\mathrm{H}} \frac{\langle Q_\sigma^2(N,\mathbf{x})\rangle}{M_\mathrm{P}^2}. \tag{5.104}$$

According to Eq. (5.37), Q_σ is related to $\delta\hat{\chi}$ and $\delta\varphi$ via $Q_\sigma = G_{IJ}\hat{\sigma}^I\delta\Phi^J$, with Φ^I and G_{IJ} defined in Eq. (5.20). During most of the inflationary dynamics along φ_0 and the later part of the dynamics in $\varphi_\mathrm{v}^\pm$, the inflaton vector $\hat{\sigma}^I$ points in the $\hat{\chi}$ direction and Q_σ exclusively receives contribution from $\delta\hat{\chi}$. Only during the short peak formation stage in the vicinity of $\hat{\chi}_\mathrm{c}$, where the trajectory turns and $\hat{\sigma}^I$ has a non-zero component in φ-direction, Q_σ also receives contribution from $\delta\varphi$. Here, we assume that during this period $\hat{\sigma}^I$ points in the φ-direction such that $(\hat{\sigma}^\varphi)^2 = F$ (c.f. Eq. (5.26)).[7] For modes $k \approx k_\mathrm{p} \pm \Delta k$, which cross the horizon during this period, (5.104) reduces to

$$\int_{k_\mathrm{p}-\Delta k}^{k_\mathrm{p}+\Delta k} d\ln k \mathcal{P}_\mathcal{R}(k) \approx \frac{1}{2\varepsilon_\mathrm{H} F} \frac{\langle \delta\varphi^2\rangle}{M_\mathrm{P}^2}. \tag{5.105}$$

For a simplified treatment we take the sharp peak limit $\mathcal{P}_\mathcal{R}(k) \approx A_\mathrm{p}\delta(\ln k - \ln k_\mathrm{p})$ such that (5.105) becomes

$$A_\mathrm{p} \approx \frac{1}{2\varepsilon_\mathrm{H} F} \frac{\langle \delta\varphi^2\rangle}{M_\mathrm{P}^2}. \tag{5.106}$$

Although the slow-roll dynamics along $\varphi_\mathrm{v}^\pm$ slightly differs from that of the effective Starobinsky inflation along φ_0, for an order of magnitude estimate we use the background relations of Starobinsky inflation $F(\hat{\chi}) \approx N$ and $\varepsilon_\mathrm{H}(N) \approx 1/N^2$ evaluated at $N_\mathrm{c} := N(\hat{\chi}_\mathrm{c})$, so that (5.106) reduces to[8]

$$A_\mathrm{p} \approx \frac{N_\mathrm{c}}{2} \frac{\langle \delta\varphi^2\rangle}{M_\mathrm{P}^2}. \tag{5.107}$$

As discussed in Sec. 5.5, close to $\hat{\chi}_\mathrm{c}$ quantum diffusive effects dominate and a stochastic treatment is required during which $\varphi(N)$ is identified with $\langle\delta\varphi^2(N,\mathrm{x})\rangle^{1/2}$. But even after the stochastic phase, during the fall from φ_0 to $\varphi_\mathrm{v}^\pm$, both $\delta\varphi$ and φ continue to grow together – $\delta\varphi$ because $\hat{W}_{,\varphi\varphi}$ is still negative, and φ because it moves away from $\varphi = 0$ to larger field values until it reaches $\varphi_\mathrm{v}^\pm$ (inside one of the two adjacent valleys that re-emerge for $\hat{\chi} < \hat{\chi}_\mathrm{c}$). Hence $\sqrt{\langle\delta\varphi^2\rangle}$ is bounded from above by the maximum distance between the hill and one of the two valleys $\varphi_\mathrm{v}^\pm(\hat{\chi}_\mathrm{max}) - \varphi_0 = \varphi_\mathrm{v}^\pm(\hat{\chi}_\mathrm{max})$. This value of $\hat{\chi}_\mathrm{max}$ can be obtained by solving

$$\left.\frac{\partial\varphi_\mathrm{v}^\pm(\hat{\chi})}{\partial\hat{\chi}}\right|_{\hat{\chi}_\mathrm{max}} = 0\,, \text{ such that } \qquad \langle\delta\varphi^2\rangle \leq \left|\varphi_\mathrm{v}^\pm(\hat{\chi}_\mathrm{max})\right|^2\,. \tag{5.108}$$

[7] The exact dynamics is more complicated and involves a short phase in which $\delta\varphi$ and $\delta\hat{\chi}$ simultaneously contribute to Q_σ.

[8] To produce PBHs in the mass windows M_PBH^{III} and M_PBH^{II}, we find $N_\mathrm{c} \approx 40$ and $N_\mathrm{c} \approx 25$, respectively.

A strong amplification of $\mathcal{P}_\mathcal{R}(k)$ requires a large $\delta\varphi$ and hence a large $|\varphi_\mathrm{v}^\pm(\hat{\chi}_\mathrm{max})|$. The inequality in (5.108) can be parametrized by $\langle\delta\varphi^2\rangle \approx \alpha^2|\varphi_\mathrm{v}^\pm(\hat{\chi}_\mathrm{max})|^2$ with $\alpha \in [0.1, 1]$.[9] The analytic expression for $|\varphi_\mathrm{v}^\pm(\hat{\chi}_\mathrm{max})|^2$ is found from (5.44) and the first equation in (5.108) as[10]

$$|\varphi_\mathrm{v}^\pm(\hat{\chi}_\mathrm{max})|^2 = \frac{m_0^2}{\zeta} L(x), \tag{5.109}$$

with x is the same as in Eq. (5.50), and the function $L(x)$ defined by

$$L(x) := \frac{2 - 2\sqrt{1-x} - x}{x}. \tag{5.110}$$

As discussed in Sec. 5.3, the predictions of the model are independent of the point where the inflationary trajectory starts on the two-field potential only if $x < 1$. Taking this to be the case, the function (5.110) takes arguments from $x \in [0, 1)$ which means that (5.110) takes values in the interval $L(x) \in [0, 1)$. For an order of magnitude estimate we approximate $L(x) = x/4 + \mathcal{O}(x^2)$ and obtain

$$\langle\delta\varphi^2\rangle \approx \alpha^2|\varphi_\mathrm{v}^\pm(\hat{\chi}_\mathrm{max})|^2 \approx \frac{\alpha^2 m_0^2}{4\zeta} x. \tag{5.111}$$

Combining (5.107) with (5.111), we obtain the analytic estimate for the peak amplitude

$$A_\mathrm{p} \approx \frac{N_\mathrm{c}}{8\zeta} \frac{m_0^2}{M_\mathrm{P}^2} \alpha^2 x. \tag{5.112}$$

It was argued in Sec. 5.5 that $\Delta N \approx m_0^2/(M_\mathrm{P}^2\zeta)$ corresponds to the duration of the stochastic phase. This phase must be sufficiently short $\Delta N \lesssim 1$ in order to produce a narrow peak in $\mathcal{P}_\mathcal{R}(k)$. If $\Delta N \gg 1$, a larger window of modes would feel the amplification mechanism leading to a broader peak of $\mathcal{P}_\mathcal{R}(k)$ which then risks to produce a broader distribution $f(M_\mathrm{PBH})$ incompatible with the observational constraints. Since $N_\mathrm{c} = \mathcal{O}(10)$, the magnitude of the total prefactor in (5.112) is estimated to be of order $N_\mathrm{c}\,\Delta N\alpha^2/8 \approx 10^{-2}$, leading to the condition

$$A_\mathrm{p} \approx 10^{-2} x. \tag{5.113}$$

Since a significant $F_\mathrm{PBH} \approx 1$ requires a peak amplitude $A_\mathrm{p} \approx 10^{-2}$-$10^{-3}$ [113, 68], it is clear that x cannot be much smaller than one and we finally obtain the estimate

$$x \approx 1. \tag{5.114}$$

This yields the approximate scaling relation

$$\lambda \approx 6 \frac{m_0^2}{M_\mathrm{P}^2} \xi^2. \tag{5.115}$$

[9] Geometrically, the inflection point which lies between φ_0 and $\varphi_\mathrm{v}^\pm$ cannot be too close to $\varphi_0 = 0$. In addition, the inertia of the background dynamics carries the trajectory along φ_0 even after reaching the bifurcation point shown in the left plot of Fig. 5.1, such that the fall into $\varphi_\mathrm{v}^\pm$ happens only after the valleys reach a sufficient separation, justifying the lower bound on α.

[10] The criterion to determine $\hat{\chi}_\mathrm{max}$ in (5.108) only applies to Scenario I. Only in this scenario, the valleys re-emerge at the bifurcation point $\hat{\chi}_\mathrm{c}$ turn and again move towards $\varphi = 0$.

Inserting the scalaron mass m_0 from (5.100), we obtain

$$\lambda \approx 10^{-9}\xi^2. \tag{5.116}$$

The precise value of $F_{\rm PBH}$ for a given power spectrum $\mathcal{P}_\mathcal{R}(k) \approx A_{\rm p}\delta(\ln k - \ln k_{\rm p})$ is exponentially sensitive to the peak amplitude $A_{\rm p}$ [68]. This is the main reason why any attempt to obtain a precise analytical relation for $F_{\rm PBH}$ in terms of the model parameters is hard to realize. Nevertheless, in view of (5.113), the amplification only depends on x such that the same amplification is achieved for different values of ξ and λ as long as they are related by the scaling relation (5.116). In general, the exact numerical factor in the quadratic scaling law (5.116), depends on the values of $F_{\rm PBH}$ and the PBH mass $M_{\rm PBH}$ at which the mass distribution $f(M_{\rm PBH})$ peaks, but the scaling law $\lambda \propto \xi^2$ will be the same for all mass windows and total mass fractions.

Finally, the analytical estimates (5.103) and (5.115) are confirmed by an exact numerical analysis. A systematic parameter scan is performed for different values of λ, ξ and ζ such that a mass distribution $f(M_{\rm PBH})$ in the window $M^{II}_{\rm PBH}$ centered around $M_{\rm PBH} = 10^{-11}M_\odot$ with $F_{\rm PBH} \approx 1$ is realized. The parameters λ, ξ and ζ that permit such realizations, are related to each other by the scaling relations shown in Fig. 5.9, which are remarkably close to the analytical estimates (5.103) and (5.115).

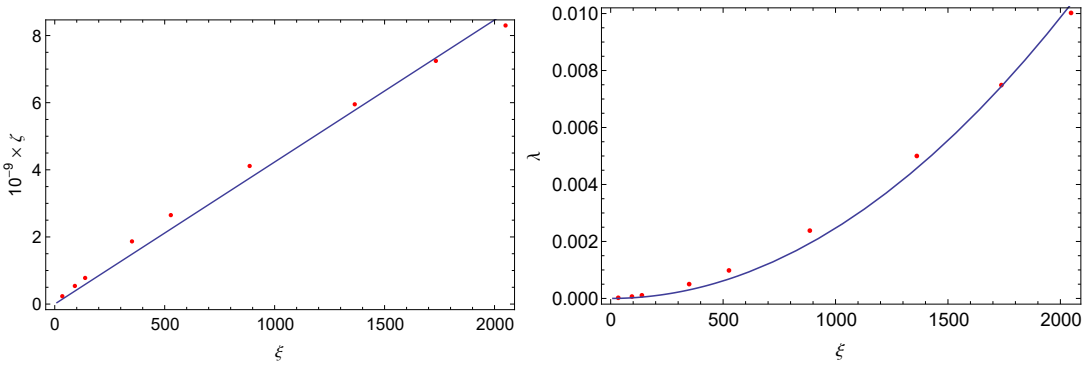

Figure 5.9: Numerically obtained scaling relations for the parameters leading to $F_{\rm PBH} \approx 1$ for $f(M_{\rm PBH})$ centered around $M_{\rm PBH} = 10^{-11}M_\odot$. Left: Linear scaling relation between ζ and ξ. Numerically generated points (red) linear fit (blue). Right: Quadratic scaling relation between λ and ξ. Numerically generated points (red) quadratic fit (blue).

The linear and quadratic fits to the numerically found scaling relations in Fig. 5.9 are given by

$$\zeta = 4.23 \times 10^{-12}\xi, \qquad \lambda = 2.47 \times 10^{-9}\xi^2. \tag{5.117}$$

In addition to the correct functional form of the scaling relations, also the numerical coefficients in (5.117) agree well with those predicted by the analytic estimates (5.103) and (5.116), thereby numerically confirming them.

5.12 Discussion

All parameters of the extended scalaron-Higgs model are fixed. The parameter m_0 is fixed by the CMB constraint (5.100) on the scalar inflationary power spectrum at large wavelengths, independently of the value of λ. In contrast, the non-minimal couplings ζ and ξ are ultimately determined in terms of λ by the scaling relations (5.103) and (5.115). The relations are determined by the requirement that the peak in $\mathcal{P}_{\mathcal{R}}(k)$ leads to a significant $F_{\rm PBH}$ with a PBH mass distribution $f(M_{\rm PBH})$ centered around $M_{\rm PBH}$. It is shown in this work that an analytic relationship between the parameters of the new proposed model can be determined such that the model can offer to account for the whole of dark matter within the observationally viable mass windows while at the same time being compatible with the CMB constraints. Since this relationship holds for a range of values of λ, that might be acquired by the Higgs field at inflationary energy scales, the conclusion is that by considering Starobinsky's model in which both the Ricci scalar and the Starobinsky term are non-minimally coupled to a scalar field, possibly the Higgs field, one can simultaneously account for the CMB observations and the observed CDM content in the universe.

Chapter 6

Inflationary cosmology and its implications for dynamical collapse models

The discussion presented in chapter 5 shows how the various theoretically well motivated models of inflation offer to account for the CMB observations. Even if we cannot yet pinpoint at the nature of the inflaton, cosmological inflation is still widely regarded to be a part of standard cosmology. In particular, the quantum fluctuations of the inflaton field are regarded as the most likely origin for the large-scale structure in the universe. This, however, also raises conceptual questions concerning its quantum-to-classical transition. The subject is still actively debated within the community, where some argue for decoherence as an explanation [4, 105, 82], while others suggest the need for a modification to the standard quantum dynamics [102, 121, 104, 32, 98].

Several works have applied the models of wavefunction collapse to cosmology in a similar context [102, 84, 45, 85, 41, 42, 88, 87]. In this chapter, a plausible generalization of the mass proportional Continuous Spontaneous Localization (CSL) model [101, 58], which is the most studied among the dynamical collapse models, is proposed and its consequences for the evolution of the scalar perturbations during the early universe are investigated.

Under the influence of CSL dynamics, the corrections to the expectation value of any observable can be computed by using standard perturbation theory. This can be done by identifying a suitable stochastic perturbation to the original Hamiltonian, depending upon the choice of the collapse operator. The observable of interest for which the corrections will be computed is the comoving curvature perturbation $\hat{\mathcal{R}}$. Since the modified dynamics a priori does not guarantee even the large wavelength modes of $\hat{\mathcal{R}}$ to remain constant after the end of inflation, the power spectrum $\mathcal{P}_{\mathcal{R}}$ under the modified CSL dynamics is evaluated both during inflation and the radiation dominated era. The discussion presented here concerns publication III [67].

6.1 Mass proportional CSL model

As introduced in chapter 3, dynamical collapse models are phenomenological models which modify the standard Schrödinger evolution through the addition of nonlinear and stochastic terms. The

model is defined through the SDE

$$d|\psi\rangle = \Big[-i\hat{H}dt + \frac{\sqrt{\gamma}}{m_0}\int d\mathbf{x}\left[\hat{M}(\mathbf{x}) - \langle\hat{M}(\mathbf{x})\rangle\right]dW_t(\mathbf{x}) \\ -\frac{\gamma}{2m_0^2}\int d\mathbf{x}d\mathbf{y}\left[\hat{M}(\mathbf{x}) - \langle\hat{M}(\mathbf{x})\rangle\right]G(\mathbf{x}-\mathbf{y})\left[\hat{M}(\mathbf{y}) - \langle\hat{M}(\mathbf{y})\rangle\right]dt\Big]|\psi\rangle\,. \tag{6.1}$$

Here, $\hat{H}$ is the Hamiltonian of the system, γ encodes the strength of the collapse process, $\langle\cdot\rangle$ denotes the expectation value computed with respect to the state $|\psi\rangle$, the noise $W_t(\mathbf{x})$ is defined in terms of the temporal and spatial correlations

$$\mathbb{E}\left[\xi_t(\mathbf{x})\xi_{t'}(\mathbf{y})\right] = G(\mathbf{x}-\mathbf{y})\delta(t-t'), \qquad \text{where} \qquad G(\mathbf{x}-\mathbf{y}) = \frac{1}{(4\pi r_C^2)^{3/2}}e^{-\frac{(\mathbf{x}-\mathbf{y})^2}{4r_C^2}}, \tag{6.2}$$

with $\xi_t(\mathbf{x}) = dW_t(\mathbf{x})/dt$, the symbol $\mathbb{E}[\cdot]$ indicates the stochastic average, r_C denotes the second phenomenological parameter of the model, m_0 is the reference mass scale taken to be the mass of the nucleon and the operator $\hat{M}(\mathbf{x})$ in Eq. (6.1) is the mass density operator which involves the creation and annihilation operators of different types of particles

$$\hat{M}(\mathbf{x}) = \sum_j m_j\hat{a}_j^\dagger(\mathbf{x})\hat{a}_j(\mathbf{x})\,. \tag{6.3}$$

Note that in this chapter we only work with the physical process such that $|\psi\rangle$ denotes the normalized physical statevector and not the one representing the raw process as in chapter 3.

The expectation value $\mathbb{E}[\langle\psi|\hat{O}|\psi\rangle]$ of an arbitrary operator $\hat{O}$ can be calculated in terms of the density operator $\hat{\rho}$ as $\mathbb{E}[\langle\psi|\hat{O}|\psi\rangle] = \mathrm{Tr}[\hat{O}\hat{\rho}]$. As described in chapter 3, under the influence of CSL dynamics, the time evolution of the density matrix corresponding to the statevector (6.1) is the same as the one obtained for the statevector which, instead, satisfies the Schrödinger equation (in the Stratonovich representation) in the presence of an additional stochastic Hamiltonian. For the SDE (6.1) and the CSL noise (6.2), this stochastic Hamiltonian $\hat{H}_{\text{CSL}}$ must be identified with

$$\hat{H}_{\text{CSL}} = \frac{\sqrt{\gamma}}{m_0}\int d\mathbf{x}\hat{M}(\mathbf{x})\xi_t(\mathbf{x})\,. \tag{6.4}$$

6.2 Interaction picture framework

Modifications due to CSL dynamics can be quantified via perturbative approach. The total Hamiltonian $\hat{H}$ can be decomposed as

$$\hat{H} = \hat{H}_0 + \hat{H}_{\text{CSL}}, \tag{6.5}$$

where $\hat{H}_0$ is the Hamiltonian of the system and $\hat{H}_{\text{CSL}}$ is the additional contribution due to dynamical collapse models. The calculations are then performed in the interaction picture where, after identifying $\hat{H}_0$ as the time dependent background Hamiltonian, the operators $\hat{O}^{\text{I}}$ and the states $|\psi^{\text{I}}(t)\rangle$ are given by

$$\hat{O}^{\text{I}}(t) = \hat{U}_0^{-1}(t,t_0)\hat{O}\hat{U}_0(t,t_0)\,, \qquad |\psi^{\text{I}}(t)\rangle = \hat{U}_{\text{CSL}}(t,t_0)|\psi(t_0)\rangle\,, \tag{6.6}$$

with

$$\hat{U}_0(t,t_0) = \mathcal{T}\left\{\exp\left[-i\int_{t_0}^{t} dt' \hat{H}_0(t')\right]\right\}, \qquad \hat{U}_{\rm CSL}(t,t_0) = \mathcal{T}\left\{\exp\left[-i\int_{t_0}^{t} dt' \hat{H}^{\rm I}_{\rm CSL}(t')\right]\right\}. \quad (6.7)$$

Here, $\mathcal{T}$ denotes the time-ordering operator and $\hat{H}^{\rm I}_{\rm CSL}$ the appropriate stochastic Hamiltonian in the interaction picture. The general discussion can be presented without making a specific choice for the collapse operator. Thus, for now, we consider the stochastic Hamiltonian $\hat{H}_{\rm CSL}$ to be given by

$$\hat{H}_{\rm CSL}(t) = \frac{\sqrt{\gamma}}{m_0}\int d\mathbf{x}\, \xi_t(\mathbf{x})\hat{L}_{\rm CSL}(t,\mathbf{x}), \quad (6.8)$$

where $\hat{L}_{\rm CSL}(t,\mathbf{x})$ is an operator yet to be specified but γ, m_0 and $\xi_t(\mathbf{x})$ are the same as in Eq. (6.1). Taking into account the time dependence of both the operator $\hat{O}^{\rm I}(t)$ and the state $|\psi(t)\rangle$, and retaining only the leading order term in γ, we get

$$\begin{aligned}\langle\hat{O}\rangle &= \langle\psi^{\rm I}(t)|\,\hat{O}^{\rm I}(t)\,|\psi^{\rm I}(t)\rangle \\ &\approx \langle\psi(t_0)|\left[\hat{1} + i\int_{t_0}^{t} dt' \hat{H}^{\rm I}_{\rm CSL}(t') - \int_{t_0}^{t}\int_{t_0}^{t'} dt'dt'' \hat{H}^{\rm I}_{\rm CSL}(t'')\hat{H}^{\rm I}_{\rm CSL}(t')\right]\hat{O}^{\rm I}(t)\left[\hat{1} - i\int_{t_0}^{t} dt' \hat{H}^{\rm I}_{\rm CSL}(t')\right. \\ &\quad \left. - \int_{t_0}^{t}\int_{t_0}^{t'} dt'dt'' \hat{H}^{\rm I}_{\rm CSL}(t')\hat{H}^{\rm I}_{\rm CSL}(t'')\right]|\psi(t_0)\rangle \\ &= \langle\psi(t_0)|\left[\hat{O}^{\rm I}(t) - i\int_{t_0}^{t} dt' \left[\hat{O}^{\rm I}(t), \hat{H}^{\rm I}_{\rm CSL}(t')\right] - \int_{t_0}^{t}\int_{t_0}^{t'} dt'dt'' \left[\hat{H}^{\rm I}_{\rm CSL}(t''), \left[\hat{H}^{\rm I}_{\rm CSL}(t'), \hat{O}^{\rm I}(t)\right]\right]\right]|\psi(t_0)\rangle\,. \end{aligned} \quad (6.9)$$

The next step involves taking the stochastic average over all the realizations of the noise such that

$$\begin{aligned}\overline{O} \equiv \mathbb{E}[\langle\hat{O}\rangle] &\approx \langle\psi(t_0)|\,\hat{O}^{\rm I}(t)\,|\psi(t_0)\rangle - \frac{i\sqrt{\gamma}}{m_0}\int_{t_0}^{t} dt' \int d\mathbf{x}' \mathbb{E}[\xi_t(\mathbf{x}')]\,\langle\psi(t_0)|\left[\hat{O}^{\rm I}(t), \hat{L}^{\rm I}_{\rm CSL}(t',\mathbf{x}')\right]|\psi(t_0)\rangle \\ &- \frac{\gamma}{m_0^2}\int_{t_0}^{t}\int_{t_0}^{t'} dt'dt'' \int d\mathbf{x}' \int d\mathbf{x}'' \mathbb{E}\left[\xi_{t''}(\mathbf{x}'')\xi_{t'}(\mathbf{x}')\right]\langle\psi(t_0)|\left[\hat{L}^{\rm I}_{\rm CSL}(t'',\mathbf{x}''), \left[\hat{L}^{\rm I}_{\rm CSL}(t',\mathbf{x}'), \hat{O}^{\rm I}(t)\right]\right]|\psi(t_0)\rangle. \end{aligned} \quad (6.10)$$

Afetr using Eq. (6.2), the expression simplifies further to be

$$\begin{aligned}\overline{O} &\approx \langle\psi(t_0)|\,\hat{O}^{\rm I}(t)\,|\psi(t_0)\rangle \\ &\quad - \frac{\lambda}{2m_0^2}\int_{t_0}^{t} dt' \int d\mathbf{x}' \int d\mathbf{x}'' e^{-\frac{(\mathbf{x}''-\mathbf{x}')^2}{4r_{\rm C}^2}}\langle\psi(t_0)|\left[\hat{L}^{\rm I}_{\rm CSL}(t',\mathbf{x}''), \left[\hat{L}^{\rm I}_{\rm CSL}(t',\mathbf{x}'), \hat{O}^{\rm I}(t)\right]\right]|\psi(t_0)\rangle, \end{aligned} \quad (6.11)$$

where $\lambda := \gamma/(4\pi r_{\rm C}^2)^{3/2}$. The full expectation value $\overline{O}$ can be written as the sum of the original expectation value in the absence of collapse dynamics and the leading order correction that it induces

$$\overline{O} = \langle\hat{O}(t)\rangle_0 + \delta\overline{O}(t)_{\rm CSL}\,. \quad (6.12)$$

Here,

$$\langle \hat{O}(t)\rangle_0 = \langle \psi(t_0)|\, \hat{O}^{\rm I}(t)\, |\psi(t_0)\rangle\,,$$
$$\delta\overline{O}(t)_{\rm CSL} = -\frac{\lambda}{2m_0^2}\int_{t_0}^{t} dt' \int d\mathbf{x}' \int d\mathbf{x}'' e^{-\frac{(\mathbf{x}''-\mathbf{x}')^2}{4r_{\rm C}^2}} \langle \psi(t_0)|\, \big[\hat{\mathcal{H}}^{\rm I}_{\rm CSL}(t',\mathbf{x}''), \big[\hat{\mathcal{H}}^{\rm I}_{\rm CSL}(t',\mathbf{x}'), \hat{O}^{\rm I}(t)\big]\big]\, |\psi(t_0)\rangle\,. \tag{6.13}$$

6.3 Choice of the collapse operator

The FLRW background spacetime offers a simple generalization of the CSL noise (6.2). It is achieved by demanding that, in terms of the physical coordinates $\mathbf{x}_p$ and the cosmic time t, the same correlations for the noise are obtained as in Eq. (6.2). However, since it will be more convenient to work with the conformal time η and the comoving coordinates $\mathbf{x}$, the noise $\xi_\eta(\mathbf{x})$ is expressed in terms of the same, such that the condition mentioned before is satisfied. It is therefore given by

$$\mathbb{E}[\xi_\eta(\mathbf{x})] = 0, \qquad \mathbb{E}[\xi_\eta(\mathbf{x})\xi_{\eta'}(\mathbf{y})] = \frac{\delta(\eta-\eta')}{a(\eta')}G(\mathbf{x}-\mathbf{y}), \qquad G(\mathbf{x}-\mathbf{y}) = \frac{1}{(4\pi r_{\rm C}^2)^{3/2}} e^{-\frac{a^2(\eta)(\mathbf{x}-\mathbf{y})^2}{4r_{\rm C}^2}}. \tag{6.14}$$

In the terms of the same coordinates, the expectation value of the operator $\hat{O}$ can then be expressed as

$$\langle \hat{O}(\eta)\rangle_0 = \langle 0|\, \hat{O}^{\rm I}(\eta)\, |0\rangle\,,$$
$$\delta\overline{O}(\eta)_{\rm CSL} = -\frac{\lambda}{2m_0^2}\int_{\eta_0}^{\eta} \frac{d\eta'}{a(\eta')} \int d\mathbf{x}' \int d\mathbf{x}'' e^{-\frac{a^2(\eta')(\mathbf{x}''-\mathbf{x}')^2}{4r_{\rm C}^2}} \langle 0|\, \big[\hat{\mathcal{H}}^{\rm I}_{\rm CSL}(\eta',\mathbf{x}''), \big[\hat{\mathcal{H}}^{\rm I}_{\rm CSL}(\eta',\mathbf{x}'), \hat{O}^{\rm I}(\eta)\big]\big]\, |0\rangle\,. \tag{6.15}$$

Having proposed a suitable generalization of the CSL noise, we now proceed towards the choice of the collapse operator in a cosmological setting. Working within the framework of cosmological perturbation theory, we remember that only the perturbations of the background quantities are quantized. Therefore, any Hermitian operator $\hat{Q}(\eta,\mathbf{x})$ can be written as $Q(\eta)\mathbb{1} + \delta\hat{Q}(\eta,\mathbf{x})$. Since the collapse operator appears in the form $\hat{M}(\mathbf{x}) - \langle\hat{M}(\mathbf{x})\rangle$ in Eq. (6.1), we see that the background dynamics $Q(\eta)\mathbb{1}$ does not influence the choice of the collapse operator [87]. Since the generalization is confined to this framework, the classicality of the background dynamics makes it sufficient to choose a collapse operator that is a function of the scalar perturbations only.

While different choices for the collapse operator have been previously proposed, most of the choices are either linear or, to leading order, linearized in the field perturbations. In some works, for instance, the collapse operator was taken to be the rescaled variable $\hat{u} = a\delta\hat{\varphi}$ (c.f. Eq. (4.24)) itself [86, 24]. Similarly, in [87], the perturbed matter-energy density $\hat{\delta\rho}$, which is related to the zero-zero component of the stress energy-momentum tensor, was taken to be the collapse operator. These choices differ from the standard CSL model (applied to laboratory situations) in which the collapse operator is quadratic in the creation and annihilation operators and not linear. This trait is important as one would like that the collapse operator couples different Fourier modes as in the standard case [2], which is not possible when the collapse operator is linear in the fields.

In the present work, the collapse operator is taken to be the Hamiltonian density of the scalar cosmological perturbations such that $\hat{L}^{\rm I}_{\rm CSL}(\eta, \mathbf{x}) = \hat{\mathcal{H}}^{\rm I}_0(\eta, \mathbf{x})$. During inflation, following the discussion in chapter 4, it is the Hamiltonian corresponding to the action (4.23). This choice allows one to respect the essentials of both the CSL model and the cosmological perturbation theory, as within its standard framework the Hamiltonian density is already quadratic in the creation and annihilation operators upto leading order in the perturbations. This choice of the collapse operator can also be viewed as making a relativistic generalization of the non-relativistic mass density in the standard laboratory situations.

To proceed towards the goal of computing the CSL modifications to the power spectrum $\mathcal{P}_{\mathcal{R}}$, in Eq. (6.15), the initial state will be taken to be the Bunch-Davies vacuum state $|0\rangle$ and the operator $\hat{O}$ to be $\hat{\mathcal{R}}^2$. The CSL corrections are evaluated over two cosmological epochs. The first one is the phase of cosmological inflation described in Sec. 6.4.1 and the second one is that of the radiation dominated era described in Sec. 6.4.2. These two are separated at $\eta = \eta_e$ by a phase of reheating, with η_e denoting the end of inflation. For a simplified treatment, as in Ref. [87], it will be assumed that the collapse dynamics does not introduce any substantial corrections during this phase connecting the two epochs of interest. In the first epoch, η_0 would correspond to the beginning of inflation and the correction to $\overline{\mathcal{R}^2}$ due to collapse models is computed at the end of inflation. During the radiation dominated epoch, the initial time is taken to be the end of inflation and the correction to $\overline{\mathcal{R}^2}$ is computed at the end of radiation dominated era η_r.

6.4 CSL corrections to the power spectrum

6.4.1 Inflation

Having taken the collapse operator to be $\hat{L}_{\rm CSL} = \hat{\mathcal{H}}_{\rm CSL} = \hat{\mathcal{H}}_0$, from Eqs. (6.6) and (6.8) we get

$$\hat{H}^I_{\rm CSL}(\eta) = \frac{\sqrt{\gamma}}{m_0} \int d\mathbf{x} \xi_\eta(\mathbf{x}) \hat{\mathcal{H}}^I_{\rm CSL}(\eta, \mathbf{x}), \tag{6.16}$$

where $\hat{\mathcal{H}}^I_{\rm CSL} = \hat{U}_0^{-1} \hat{\mathcal{H}}_0(\eta, \mathbf{x}) \hat{U}_0$ represents the Hamiltonian density of the scalar perturbations in the interaction picture. This coincides with the Hamiltonian density of the scalar perturbations in the Heisenberg picture in standard cosmology, where one does not have additional contributions coming from collapse dynamics. During inflation, $\hat{\mathcal{H}}^I_{\rm CSL} = \hat{\mathcal{H}}^{\rm h}_{\rm inf}$. The latter is the standard inflationary Hamiltonian corresponding to the action in Eq. (4.23) given by

$$\hat{\mathcal{H}}^{\rm h}_{\rm inf} = \frac{1}{2} \int d\mathbf{x} \left\{ \hat{u}'^2(\eta, \mathbf{x}) + \delta^{ij} \partial_i \hat{u}(\eta, \mathbf{x}) \partial_j \hat{u}(\eta, \mathbf{x}) - \frac{2}{\eta^2} \hat{u}^2(\eta, \mathbf{x}) \right\}. \tag{6.17}$$

The field operator $\hat{u}(\eta, \mathbf{x})$ in the Fourier space reads (as described before in chapter 4)

$$\hat{u}(\eta, \mathbf{x}) = \int \frac{d\mathbf{k}}{(2\pi)^{3/2}} \exp(i\mathbf{k} \cdot \mathbf{x}) \hat{u}_{\mathbf{k}}(\eta), \tag{6.18}$$

where the Fourier components $\hat{u}_{\mathbf{k}}(\eta)$ are specified in terms of the modes $v_k(\eta)$ and the creation and annilation operators as

$$\hat{u}_{\mathbf{k}}(\eta) = v_k(\eta) \hat{a}_{\mathbf{k}} + v^*_k(\eta) \hat{a}^\dagger_{-\mathbf{k}}. \tag{6.19}$$

Using Eqs. (6.19) and (6.18), the normal ordered Hamiltonian in terms of the creation and annihilation operators is obtained to be

$$\hat{\mathcal{H}}^{I}_{\rm CSL}(\eta,\mathbf{x}) = \int\int d\mathbf{q}d\mathbf{p}\frac{e^{i(\mathbf{p}+\mathbf{q})\cdot\mathbf{x}}}{2(2\pi)^3}\left(b^{\mathbf{p},\mathbf{q}}_{\eta}\hat{a}_{\mathbf{p}}\hat{a}_{\mathbf{q}} + d^{\mathbf{p},\mathbf{q}}_{\eta}\hat{a}^{\dagger}_{-\mathbf{q}}\hat{a}_{\mathbf{p}} + b^{*\mathbf{p},\mathbf{q}}_{\eta}\hat{a}^{\dagger}_{-\mathbf{p}}\hat{a}^{\dagger}_{-\mathbf{q}} + d^{*\mathbf{p},\mathbf{q}}_{\eta}\hat{a}^{\dagger}_{-\mathbf{p}}\hat{a}_{\mathbf{q}}\right). \quad (6.20)$$

Here, the following notations are introduced

$$b^{\mathbf{p},\mathbf{q}}_{\eta} = j^{p,q}_{\eta} - \left(\mathbf{p}\cdot\mathbf{q} + \frac{2}{\eta^2}\right)f^{p,q}_{\eta}, \quad d^{\mathbf{p},\mathbf{q}}_{\eta} = l^{p,q}_{\eta} - \left(\mathbf{p}\cdot\mathbf{q} + \frac{2}{\eta^2}\right)g^{p,q}_{\eta}, \quad (6.21)$$

with

$$f^{p,q}_{\eta} = v_p(\eta)v_q(\eta), \quad g^{p,q}_{\eta} = v_p(\eta)v^{*}_q(\eta), \quad j^{p,q}_{\eta} = \dot{v}_p(\eta)\dot{v}_q(\eta), \quad l^{p,q}_{\eta} = \dot{v}_p(\eta)\dot{v}^{*}_q(\eta). \quad (6.22)$$

We remember further from chapter 4 that in the perfect de Sitter limit, during inflation, the solution for $v_k(\eta)$ reads

$$v_k(\eta) = \frac{e^{-i\eta k}\left(1-\frac{i}{\eta k}\right)}{(2k)^{1/2}}. \quad (6.23)$$

The comoving curvature perturbation $\hat{\mathcal{R}}$ is also related to $\hat{u}$ (and therefore to the modes v_k) as

$$\hat{\mathcal{R}}^2(\eta,\mathbf{x}) = \frac{\hat{u}^2(\eta,\mathbf{x})}{z^2} = \frac{\hat{u}^2(\eta,\mathbf{x})}{2\varepsilon_{\rm inf}M^2_{\rm P}a^2(\eta)}, \quad (6.24)$$

where $\varepsilon_{\rm inf}$ is the slow-roll parameter during inflation (c.f. Eq. (4.11) in which it was denoted by $\varepsilon_{\rm H}$) and $z := aM_{\rm P}\sqrt{2\varepsilon_{\rm inf}}$ (c.f. Eq (4.21)). From Eq. (6.15), we see that the correction induced by the CSL model is encoded in the term

$$\delta\overline{\mathcal{R}^2}(\eta)_{\rm CSL} = -\frac{\lambda}{2m^2_0}\int_{\eta_0}^{\eta}\frac{d\eta'}{a(\eta')}\int d\mathbf{x}'\int d\mathbf{x}''e^{-\frac{a^2(\eta')(\mathbf{x}''-\mathbf{x}')^2}{4r^2_{\rm C}}}\langle 0|\left[\hat{\mathcal{H}}^{I}_{\rm CSL}(\eta',\mathbf{x}''),\left[\hat{\mathcal{H}}^{I}_{\rm CSL}(\eta',\mathbf{x}'),\hat{\mathcal{R}}^2(\eta,\mathbf{x})\right]\right]|0\rangle. \quad (6.25)$$

By expressing the Hamiltonian density $\hat{\mathcal{H}}^{I}_{\rm CSL}(\eta,\mathbf{x})$ and the comoving curvature perturbation $\hat{\mathcal{R}}(\eta,\mathbf{x})$ in terms of the creation and annihilation operators, the correction term becomes

$$\delta\overline{\mathcal{R}^2}(\eta)_{\rm CSL} = -\frac{\lambda r^3_{\rm C}}{8\varepsilon_{\rm inf}M^2_{\rm P}m^2_0a^2(\eta)\pi^{9/2}}\int_{\eta_0}^{\eta}\frac{d\eta'}{a^4(\eta')}\int\int d\mathbf{q}d\mathbf{p}\,e^{-\frac{r^2_{\rm C}}{a^2(\eta')}(\mathbf{q}+\mathbf{p})^2}\mathfrak{Re}\left[b^{\mathbf{q},\mathbf{p}}_{\eta'}\left\{d^{-\mathbf{q},-\mathbf{p}}_{\eta'}(f^{q,-q}_{\eta})^{*} - (b^{-\mathbf{q},-\mathbf{p}}_{\eta'})^{*}g^{q,-q}_{\eta}\right\}\right]. \quad (6.26)$$

Noticing that the exponential is invariant under the interchange of the integration variables $\mathbf{p}$ and $\mathbf{q}$, the properties of the functions $b^{\mathbf{q},\mathbf{p}}_{\eta}$, $d^{\mathbf{q},\mathbf{p}}_{\eta}$, $f^{q,p}_{\eta}$, and $g^{q,p}_{\eta}$ can be used to write the above result as

$$\delta\overline{\mathcal{R}^2}(\eta)_{\rm CSL} = -\frac{\lambda r^3_{\rm C}}{8\varepsilon_{\rm inf}M^2_{\rm P}m^2_0a^2(\eta)\pi^{9/2}}\int_{\eta_0}^{\eta}\frac{d\eta'}{a^4(\eta')}\int\int d\mathbf{q}d\mathbf{p}\,e^{-\frac{r^2_{\rm C}}{a^2(\eta')}(\mathbf{q}+\mathbf{p})^2}\mathcal{F}^{\mathbf{p},\mathbf{q}}_{\eta'}, \quad (6.27)$$

where

$$\mathcal{F}^{\mathbf{p},\mathbf{q}}_{\eta'} = \mathfrak{Re}\left[b^{\mathbf{p},\mathbf{q}}_{\eta'} d^{\mathbf{q},\mathbf{p}}_{\eta'} (f^{q,q}_{\eta})^* - b^{\mathbf{p},\mathbf{q}}_{\eta'} (b^{\mathbf{q},\mathbf{p}}_{\eta'})^* g^{p,p}_{\eta}\right]. \tag{6.28}$$

The goal is to calculate the correction $\delta\mathcal{P}_{\mathcal{R}}$ at the end of inflation when $\eta = \eta_e$. By substituting $v_k(\eta)$ with its solution in Eq. (6.23), the expression for $\mathcal{F}^{\mathbf{p},\mathbf{q}}_{\eta'}$ is obtained to be

$$\begin{aligned}
&\mathcal{F}^{\mathbf{p},\mathbf{q}}_{\eta'} = \\
&\mathfrak{Re}\left[\frac{1}{8\eta'^8 p^3 q^4}\left(1+\frac{i}{\eta_e q}\right)^2 e^{-2iq(\eta'-\eta_e)}\,[\right. \\
&\left(\left(-\eta'^2p^2+i\eta' p+1\right)\left(\eta'^2q^2-i\eta' q-1\right)-(\eta' p-i)(\eta' q-i)\left(\eta'^2(\mathbf{p}\cdot\mathbf{q})+2\right)\right)\times \\
&\times\left(\left(\eta'^2p^2+i\eta' p-1\right)\left(\eta'^2q^2-i\eta' q-1\right)-(\eta' p+i)(\eta' q-i)\left(\eta'^2(\mathbf{p}\cdot\mathbf{q})+2\right)\right)\Big] - \\
&\frac{1}{8\eta'^8 p^4 q^3}\left(1-\frac{i}{\eta_e p}\right)\left(1+\frac{i}{\eta_e p}\right)[\\
&\left(\left(-\eta'^2p^2+i\eta' p+1\right)\left(\eta'^2q^2-i\eta' q-1\right)-(\eta' p-i)(\eta' q-i)\left(\eta'^2(\mathbf{p}\cdot\mathbf{q})+2\right)\right)\times \\
&\left.\times\left(-\left(\eta'^2p^2+i\eta' p-1\right)\left(\eta'^2q^2+i\eta' q-1\right)-(\eta' p+i)(\eta' q+i)\left(\eta'^2(\mathbf{p}\cdot\mathbf{q})+2\right)\right)\Big]\right].
\end{aligned} \tag{6.29}$$

For times close to the end of inflation, the condition $q\eta' \ll 1$ is satisfied by all the modes of cosmological interest since their physical wavelengths $a(\eta)\lambda_q$ become larger than the length scale $1/H_{\rm inf}$ (c.f. discussion below Eq. (4.48)). At earlier times, if this condition is not satisfied, then the exponential appearing in Eq. (6.27) suppresses their contributions. Indeed, during inflation, using the time evolution of the scale factor given by $a(\eta) \approx -1/(\eta H_{\rm inf})$ (c.f. Eq. (4.45)), the exponential function in Eq. (6.27) becomes $\exp\{-r_c^2 {H_{\rm inf}}^2 \eta'^2 (\mathbf{p}+\mathbf{q})^2\}$ where $H_{\rm inf}$ is the value of the Hubble parameter during inflation. To have an estimate of the orders of magnitudes involved, we notice that the value of r_c, which, for the Ghirardi-Rimini-Weber (GRW) model [56], is equal to $r_c \approx 10^{27} M_{\rm P}^{-1}$ ($\approx 10^{-7}$ meters), is much bigger than $1/H_{\rm inf} \approx 10^5 M_{\rm P}^{-1}$ such that $r_c H_{\rm inf} \gg 1$ during inflation. Therefore, we can safely expand Eq. (6.29) in powers of $q\eta'$ (or $p\eta'$), which to leading order gives

$$\mathcal{F}^{\mathbf{p},\mathbf{q}}_{\eta'} = \frac{1}{8p^3q^4\eta'^8}\left(-\frac{2q^4\eta_e^4}{9}+\frac{16q^4\eta_e\eta'^3}{9}-\frac{4p^3q\eta'^6}{\eta_e^2}-\frac{32q^4\eta'^6}{9\eta_e^2}\right). \tag{6.30}$$

Here, the leading order expression presented above contains only the terms that would survive after computing the integral in Eq. (6.27). That is, terms which are symmetrical in $\mathbf{p}$ and $\mathbf{q}$ but appear with opposite signs would not contribute to the integral and therefore do not appear in the effectively leading order expression in Eq. (6.30). Since $|\eta_e| \ll |\eta'|$, the last two terms on the RHS in Eq. (6.30) give the dominant contribution to the corrections with $\mathcal{F}^{\mathbf{p},\mathbf{q}}_{\eta'} \approx -1/(2q^3\eta_e^2\eta'^2) - 4/(9\eta_e^2\eta'^2 p^3)$. Since $\mathbf{p}$ and $\mathbf{q}$ are dummy integration variables, to leading order $\mathcal{F}^{\mathbf{p},\mathbf{q}}_{\eta'}$ effectively depends only on q (or p). After completing the $\mathbf{p}$ integral in Eq. (6.27), which now becomes a standard three dimensional Gaussian integral, we get

$$\delta\overline{\mathcal{R}^2}(\eta_e)_{\rm CSL} \approx -\frac{17}{36}\frac{\lambda {H_{\rm inf}}^3}{\pi^2\varepsilon_{\rm inf} M_{\rm P}^2 m_0^2}\int_{\eta_0}^{\eta_e} d\ln\eta \int d\ln q\,. \tag{6.31}$$

Following the definition of the power spectrum $\mathcal{P}_{\mathcal{R}}$, the correction $\delta\mathcal{P}_{\mathcal{R}}$ to the power spectrum $\mathcal{P}_{\mathcal{R}}$ is identified with $\delta\overline{\mathcal{R}^2}(\eta_e)_{\rm CSL} = \int d\ln q\, \delta\mathcal{P}_{\mathcal{R}}$ leading to the final expression

$$\delta\mathcal{P}_{\mathcal{R}} \approx -\frac{17}{36}\frac{\lambda {H_{\rm inf}}^3}{\pi^2\varepsilon_{\rm inf}M_{\rm P}^2 m_0^2}\ln\left(\frac{\eta_e}{\eta_0}\right). \tag{6.32}$$

To obtain the numerical value of $\delta\mathcal{P}_{\mathcal{R}}$, η_0 is taken to be $\eta_0 \approx -k_*^{-1} \approx -10^{60}M_{\rm P}^{-1}$, where $k_* = 5\times 10^{-60}M_{\rm P}$ is the pivot scale which first crosses the horizon at the efolding number N_* satisfying $a(N_*) = k_*/H(N_*)$. The e-folding number N_* satisfies $50 \leq N_* \leq 60$ [3]. The value $N_* = 60$ is taken for the numerical estimate. The scale factor at the end of inflation $a(\eta_e)$ can then be determined from the relation $a(\eta_e) = a(N_*)\exp(N_*)$. By setting $\varepsilon_{\rm inf} = 0.005$ [87], we find

$$\delta\mathcal{P}_{\mathcal{R}}(k,\eta_e) \sim \lambda/\lambda_{\rm GRW}\times 10^{-34}, \tag{6.33}$$

where $\lambda_{\rm GRW} = 10^{-16}\,{\rm s}^{-1}$ [9]. By comparing $\delta\mathcal{P}_{\mathcal{R}}(k,\eta_e)$ with the observational error of $\mathcal{P}_{\mathcal{R}}$, which is of order $\approx 10^{-11}$ [3], one obtains an upper bound $\lambda \lesssim 10^7\,{\rm s}^{-1}$, which is 17 orders of magnitude weaker than the latest bound $\lambda \lesssim 10^{-10}\,{\rm s}^{-1}$ [128].

6.4.2 Radiation dominated era

At the perturbative level, the action for u during the radiation dominated era reads [87]

$$\delta S^{(2)} = \frac{1}{2}\int d\eta \int d\mathbf{x}\left[\dot{u}^2 - c_s^2\delta^{ij}\partial_i u\partial_j u + \frac{\ddot{z}}{z}u^2\right], \tag{6.34}$$

where c_s is the speed of sound with $c_s = 1$ during inflation and $c_s = 1/\sqrt{3}$ during the radiation dominated era. The general definition of z also depends on the speed of sound with

$$z := aM_{\rm P}\sqrt{2\varepsilon}/c_s\,. \tag{6.35}$$

The parameter ε is still the same as $\varepsilon_{\rm H}$ in Eq. (4.11), the difference being that the time evolution of the Hubble parameter is different after the end of inflation. Note that during inflation when $c_s = 1$, the factor z reduces to its definition during inflation given in Eq. (4.21). As stated before, we neglect in our analysis the reheating stage [87]. By matching the boundary conditions, the scale factor during the radiation dominated era can then be approximated as

$$a(\eta) = \frac{1}{H_{\rm inf}\eta_e^2}\left(\eta - 2\eta_e\right). \tag{6.36}$$

By using this expression of $a(\eta)$ in the definition of ε, one can show that $\varepsilon = 2$ during the radiation dominated era. From this result, as well as the linear dependence of the scale factor on η, the definition of z in Eq. (6.35) leads to $\ddot{z} = 0$. The equation of motion during the radiation dominated thus becomes

$$\ddot{u}_k + \frac{1}{3}k^2 u_k = 0\,. \tag{6.37}$$

In contrast to the dynamics during inflation (4.22), the term proportional to $\ddot{z}$ does not appear. We can decompose u in terms of the modes $v_k(\eta)$ as in Eq. (6.19), where now the modes satisfy

$$\ddot{v}_k(\eta) + \frac{1}{3}k^2 v_k(\eta) = 0. \tag{6.38}$$

As in Ref. [87], the initial conditions required to specify the solution for the modes during the radiation dominated era are determined by matching the curvature perturbation and its derivative at the end of inflation. The full solution of $v_k(\eta)$ then becomes

$$v_k(\eta) = \frac{\sqrt{3}}{2\eta_e^2\sqrt{\varepsilon_{\rm inf}}k^{5/2}} e^{-ik\eta_e} \left\{ \left[(1+\sqrt{3})(k\eta_e)^2 - \sqrt{3} - i(1+\sqrt{3})k\eta_e\right] e^{-ik\frac{\eta-\eta_e}{\sqrt{3}}} \right. \\ \left. + \left[(1-\sqrt{3})(k\eta_e)^2 + \sqrt{3} - i(1-\sqrt{3})k\eta_e\right] e^{ik\frac{\eta-\eta_e}{\sqrt{3}}} \right\}. \tag{6.39}$$

Now, one obtains the Hamiltonian density during the radiation dominated era from Eq. (6.34). It reads

$$\hat{\mathcal{H}}^I_{\rm CSL}(\eta,\mathbf{x}) = \hat{\mathcal{H}}^{\rm h}_{\rm rad}(\eta,\mathbf{x}) = \frac{1}{2}\left(\hat{u}^2(\eta,\mathbf{x}) + \frac{1}{3}\delta^{ij}\partial_i\hat{u}(\eta,\mathbf{x})\partial_j\hat{u}(\eta,\mathbf{x})\right). \tag{6.40}$$

From the expression of the operator $\hat{u}(\eta,\mathbf{x})$ in Eq. (6.18), and its decomposition in terms of the modes $v_k(\eta)$ of Eq. (6.19), straightforward calculations lead to an expression for $\hat{\mathcal{H}}^I_{\rm CSL}(\eta,\mathbf{x})$ that has the structure of Eq. (6.20), but with the functions $b_\eta^{\mathbf{q},\mathbf{p}}$ and $d_\eta^{\mathbf{q},\mathbf{p}}$ defined as

$$b_\eta^{\mathbf{q},\mathbf{p}} = j_\eta^{q,p} - \frac{1}{3}(\mathbf{q}\cdot\mathbf{p})f_\eta^{q,p}, \quad d_\eta^{\mathbf{q},\mathbf{p}} = l_\eta^{q,p} - \frac{1}{3}(\mathbf{q}\cdot\mathbf{p})g_\eta^{q,p}. \tag{6.41}$$

Here, the functions appearing on the RHS of the equalities in Eq. (6.41) are the same as in Eq. (6.22). During the radiation dominated era, the same operator $\hat{O}^I(\eta) = \hat{\mathcal{R}}^2(\eta,\mathbf{x})$ defined in Eq. (6.24) reads

$$\hat{\mathcal{R}}^2(\eta,\mathbf{x}) = \frac{\hat{u}^2(\eta,\mathbf{x})}{12M_{\rm P}^2a^2(\eta)}, \tag{6.42}$$

where the time evolution of the scale factor is instead given by Eq. (6.36) during the radiation dominated era. The fact that $\varepsilon(\eta_e \leq \eta \leq \eta_r) = 2$ and $c_s^2 = 1/3$ during the radiation dominated era (η_r denotes the conformal time at the end of this stage) have also been used in writing Eq. (6.42). The contribution to the modification of the comoving curvature power spectrum during the radiation dominated era is given by Eq. (6.25), where one substitutes η_0 with η_e and η with η_r.

Using Eqs. (6.40), (6.42) and (6.36), and calculating the double commutator explicitly, we obtain

$$\delta\overline{\mathcal{R}^2}(\eta_r)_{\rm CSL} = -\frac{\lambda r_{\rm C}^3}{48M_{\rm P}^2m_0^2a^2(\eta_r)\pi^{9/2}}\int_{\eta_e}^{\eta_r}\frac{d\eta'}{a^4(\eta')}\int\int d\mathbf{q}d\mathbf{p}\, e^{-\frac{r_{\rm C}^2}{a^2(\eta')}(\mathbf{q}+\mathbf{p})^2}\mathcal{F}_{\eta'}^{\mathbf{p},\mathbf{q}}, \tag{6.43}$$

where the function $\mathcal{F}_{\eta'}^{\mathbf{p},\mathbf{q}}$ is given by (c.f. Eqs. (6.22), (6.28) and (6.41))

$$
\begin{aligned}
\mathcal{F}_{\eta'}^{\mathbf{p},\mathbf{q}} = & -\frac{1}{8p^5q^5\varepsilon^3\eta_e^4}9e^{-\frac{2i(p(\eta'-\eta_e)+q(\eta'+\eta_r-2\eta_e))}{\sqrt{3}}}\left(4e^{\frac{2i(p+q)(\eta'-\eta_e)}{\sqrt{3}}}(\mathbf{p}\cdot\mathbf{q})\left(-2q\eta_e\left(q^3\eta_e^3-2q\eta_e+\sqrt{3}i\right)-3\right)p^5\right.\\
&+4e^{\frac{2i(p(\eta'-\eta_e)+q(\eta'+2\eta_r-3\eta_e))}{\sqrt{3}}}(\mathbf{p}\cdot\mathbf{q})\left(2q\eta_e\left(-q^3\eta_e^3+2q\eta_e+\sqrt{3}i\right)-3\right)p^5\\
&+2q^3\left(p^2q^2-(\mathbf{p}\cdot\mathbf{q})^2\right)\left(4p^4\eta_e^4-2p^2\eta_e^2+3\right)\left[e^{\frac{2i(p+2q)(\eta'-\eta_e)}{\sqrt{3}}}+e^{\frac{2i(p\eta'+2q\eta_r-(p+2q)\eta_e)}{\sqrt{3}}}\right]\\
&+4e^{\frac{2i(p(\eta'-\eta_e)+q(\eta'+\eta_r-2\eta_e))}{\sqrt{3}}}\left(4p^4q^3(pq+\mathbf{p}\cdot\mathbf{q})^2\eta_e^4-2p^2q^2\left(2(\mathbf{p}\cdot\mathbf{q})p^3+q^3p^2+q(\mathbf{p}\cdot\mathbf{q})^2\right)\eta_e^2\right.\\
&\left.+3\left(2(\mathbf{p}\cdot\mathbf{q})p^5+q^5p^2+q^3(\mathbf{p}\cdot\mathbf{q})^2\right)\right)+e^{\frac{4i(p\eta'+q\eta_r-(p+q)\eta_e)}{\sqrt{3}}}q^3(-pq+\mathbf{p}\cdot\mathbf{q})^2\left(2p\eta_e\left(p^3\eta_e^3-2p\eta_e-\sqrt{3}i\right)+3\right)\\
&+e^{\frac{4i(p+q)(\eta'-\eta_e)}{\sqrt{3}}}q^3(pq+\mathbf{p}\cdot\mathbf{q})^2\left(2p\eta_e\left(p^3\eta_e^3-2p\eta_e-\sqrt{3}i\right)+3\right)\\
&+2e^{\frac{2i(2p\eta'+q\eta'+q\eta_r-2(p+q)\eta_e)}{\sqrt{3}}}q^3\left(p^2q^2-(\mathbf{p}\cdot\mathbf{q})^2\right)\left(2p\eta_e\left(p^3\eta_e^3-2p\eta_e-\sqrt{3}i\right)+3\right)\\
&+q^3\left(2p\eta_e\left(p^3\eta_e^3-2p\eta_e+\sqrt{3}i\right)+3\right)\left[(-pq+\mathbf{p}\cdot\mathbf{q})^2e^{\frac{4iq(\eta'-\eta_e)}{\sqrt{3}}}+e^{\frac{4iq(\eta_r-\eta_e)}{\sqrt{3}}}q^3(pq+\mathbf{p}\cdot\mathbf{q})^2\right]\\
&\left.+2e^{\frac{2iq(\eta'+\eta_r-2\eta_e)}{\sqrt{3}}}q^3\left(p^2q^2-(\mathbf{p}\cdot\mathbf{q})^2\right)\left(2p\eta_e\left(p^3\eta_e^3-2p\eta_e+\sqrt{3}i\right)+3\right)\right). \qquad (6.44)
\end{aligned}
$$

We now consider, as in the inflationary era, the expansion of $\mathcal{F}_{\eta'}^{\mathbf{p},\mathbf{q}}$ in powers of $q\eta'$, $q\eta_e$ and $q\eta_r$. The leading order term reads

$$
\mathcal{F}_{\eta'}^{\mathbf{p},\mathbf{q}} \approx -\frac{54}{q^3\varepsilon_{\rm inf}^3\eta_e^4}\,, \qquad (6.45)
$$

where the terms that are symmetric in $\mathbf{p}$ and $\mathbf{q}$ but appear with opposite signs have been discarded in the effectively leading order expression of Eq. (6.45) as they would yield a zero contribution to the integral in Eq. (6.43). Using the leading order expansion of Eq. (6.45) in Eq. (6.43), as was the case for the inflationary era, the $\mathbf{p}$ integral becomes a standard three dimensional Gaussian integral. After completing the $\mathbf{p}$ integral first we get

$$
\delta\overline{\mathcal{R}^2}(\eta_r)_{\rm CSL} \approx \frac{9\lambda {H_{\rm inf}}^3\eta_e^2}{2M_{\rm P}^2\varepsilon_{\rm inf}^3(\eta_r-2\eta_e)^2\pi^2m_0^2}\int_{\eta_e}^{\eta_r}d\ln(\eta'-2\eta_e)\int d\ln q. \qquad (6.46)
$$

The correction $\delta\mathcal{P}_{\mathcal{R}}$ to the power spectrum $\mathcal{P}_{\mathcal{R}}$ is given by

$$
\delta\mathcal{P}_{\mathcal{R}} \approx \frac{9\lambda H_{\rm inf}^3\eta_e^2}{2M_{\rm P}^2\varepsilon_{\rm inf}^3(\eta_r-2\eta_e)^2\pi^2m_0^2}\ln\left(\frac{2\eta_e-\eta_r}{\eta_e}\right). \qquad (6.47)
$$

Borrowing the values of the constants from the inflationary dynamics and setting $\eta_r = 3\times10^{60}M_{\rm P}^{-1}$ (which is estimated by using the fact that $a(\eta_r)/a(\eta_e)\approx 3\times10^{26}$ [135]) the correction turns out to be almost zero with

$$
\delta\mathcal{P}_{\mathcal{R}}(k,\eta_r) \sim \lambda/\lambda_{\rm GRW}\times10^{-81}\,. \qquad (6.48)
$$

We must note that strictly speaking, due to the coupling between the modes in Eq. (6.43), the cosmological modes which might be outside the horizon in the outer $\mathbf{p}$ integral can also receive contributions from the subhorizon modes which satisfy $p\eta' \gg 1$, for which the approximation scheme breaks down. This was not a problem during inflation because in that era the scale factor is given by $a = -\frac{1}{H_{\rm inf}\eta'}$. Consequently the exponential function in Eq. (6.27) becomes $\exp\left\{\left(-r_{\rm C}^2 {H_{\rm inf}}^2 {\eta'}^2 (\mathbf{p}+\mathbf{q})^2\right)\right\}$, and as explained before, since typically $r_{\rm C} \gg 1/H_{\rm inf}$, it becomes necessary to have $p^2{\eta'}^2 \ll 1$ (and $q^2{\eta'}^2 \ll 1$) for the integrand to be non-zero. Due to the modified functional dependence of the scale factor during the radiation dominated era given in Eq. (6.36), the exponential function becomes $\exp\left\{\left((\mathbf{p}+\mathbf{q})^2\, \eta_e^2 {H_{\rm inf}}^2 r_{\rm C}^2 \frac{\eta_e^2}{(\eta'-2\eta_e)^2}\right)\right\}$. Clearly, it is no longer necessary to have $p\eta' \ll 1$ in order for the exponent to be non-zero. While the condition $p\eta_e \ll 1$ still remains valid, as all the modes of interest are outside the horizon at the end of inflation, the expansion in $p\eta'$ and $p\eta_r$ needs further justification. In order to see this we notice that the exact expression in Eq. (6.44) depends on η' and η_r only via the terms $p\eta'$ and $p\eta_r$ appearing in the oscillating phases. Thus, when a mode enters the horizon during the radiation dominated era (i.e. the mode p now satisfies $p\eta' \gg 1$ compared to $p\eta_e \ll 1$ at the end of inflation), this phase is expected to oscillate strongly and would not yield any significant contribution to the integrand. Moreover, the a^4 factor in the denominator would also suppress the contribution for a given mode p at a later time, when p enters the horizon and $p\eta' \gg 1$. Therefore, the assumption that $p\eta' \ll 1$ and $p\eta_r \ll 1$ for all modes p and at all times η' is expected to provide an upper bound on the integral.

6.5 Discussion

The results presented here differ from the conclusion reached in [87]. Taking $\delta\hat{\rho}$ to be the collapse operator, for the same values of $\lambda_{\rm GRW}$ and $r_{\rm C}$, in [87], the CSL corrections were found to be too large to be compatible with the CMB constraints. Strictly speaking, the results obtained in [87] were found to depend upon which gauge-invariant construction one uses for the choice of the collapse operator. It was argued that even though there are various possible ways of constructing a guage-invariant version of the energy density contrast $\delta := \delta\rho/\rho$, only if one uses the construction δ_m [87]

$$\delta_m := \delta + (v + B)\frac{\dot{\rho}}{\rho}\,, \tag{6.49}$$

does one end up with a collapse operator that is consistent with the CMB constraints. Here, B is the metric perturbation as in Eq. (4.12) and v the peculiar velocity. On the grounds of this *fine tuning* that is required for the consistency of the collapse operator, it was argued in [87] that CMB rules out the mass proportional CSL model.

We see that even with the existing difficulties in making a relativistic generalization of the collapse models [14, 123, 13, 12, 95, 124], one can come up with a reasonable ansatz that can be applied to a cosmological setting and obtain precise estimates for the observables of interest. However, the work presented here stresses the fact that an eventual validation or discard of the CSL model from cosmological observations depends strongly upon the choice of the collapse operator and cannot be made without addressing the issue of its generalization to the relativistic regime.

Chapter 7

The electromagnetic vacuum as the environment of an electron

Numerous physical phenomena such as the Casimir effect [31, 19, 99], the Unruh effect [125, 53, 122] and the Lamb shift [15, 83, 130, 40] are attributed to the presence of vacuum fluctuations. The possibility of decoherence due to vacuum fluctuations, as being fundamental and unavoidable, has also been discussed in various works [81, 79, 51, 11, 110, 47, 6, 21] without arriving at a general consensus.

The interaction of an electron with the vacuum fluctuations can be studied within the framework of open quantum systems. In this final part of the thesis, this formalism is applied to study two specific phenomena. The first is the motion of an electron under the influence of an external potential and radiation reaction. The second is decoherence due to interactions with vacuum fluctuations.

The quantum mechanical version of the classical Abraham-Lorentz (AL) equation, which describes the recoil force experienced by an accelerated electron due to the emission of radiation [39, 100, 64, 36], has been previously derived, for example, in [40]. Instead of the electron's position, the equation was obtained for the position operator and it was then argued why this operator equation is fundamentally different from the classical one. The implications of the operator equation for the classical AL equation were not understood clearly and the difficulties in making this connection were attributed to the presence of the additional transverse electric field operator of the electromagnetic vacuum, which is zero classically. Similar problem persists concerning the interpretation of the quantum Langevin equation obtained in [6] for an electron interacting with vacuum fluctuations. It is important to mention that even after a quantum mechanical treatment, neither [40] nor [6] found where the solutions to the problems associated with the AL formula could lie.

In this work, the path-integral formalism is used to obtain the explicit expression of the reduced density matrix in the position basis. The main difference between the approach followed in this work compared to the ones followed before, is that instead of the Langevin equation, the master equation is derived which yields the EOM for the expectation value of the position operator which provides a direct correspondence with the classical dynamics. In the presence of an arbitrary potential, it will be shown that the classical EOM is the same as the one obtained from the reduced quantum dynamics. Moreover, the equation that emerges after a quantum mechanical treatment

appears to be free of the problems associated with the AL equation: the existence of the runaway solution which leads to an exponential increase of the electron's acceleration, even in the absence of an external potential [39, 100, 64].

Concerning decoherence, it will be shown that the loss of coherence due to vacuum fluctuations at the level of the reduced density matrix is only apparent and reversible. To this end, by *switching off* the interactions with the EM field, the original coherence is shown to be restored at the level of the electron. Moreover, the expression for the decoherence factor that is obtained differs from the ones obtained in [6, 21] where the authors argue for a finite loss of coherence for momentum superpositions, due to vacuum fluctuations, but with different estimates for the magnitude of decoherence.

The discussion presented in this chapter is based on the preprint [66].

7.1 The Lagrangian and the Hamiltonian formalism

We begin by formulating the Lagrangian and the Hamiltonian relevant for the dynamics of a non-relativistic electron in the presence of an external potential and an external radiation field.

7.1.1 The Lagrangian

In the Coulomb gauge, the standard Lagrangian for the dynamics of a non-relativistic electron in the presence of an external potential and an external radiation field is given by [37]

$$L = \frac{1}{2}m\dot{\mathbf{r}}_e^2 - V_0(\mathbf{r}_e) + \frac{\epsilon_0}{2}\int d^3r \left(\mathbf{E}_\perp^2(\mathbf{r}) - c^2\mathbf{B}^2(\mathbf{r})\right) + \int d^3r \mathbf{j}(\mathbf{r})\cdot\mathbf{A}_\perp(\mathbf{r}) - \int_{1/2} d^3k \frac{|\rho|^2}{\epsilon_0 k^2}\,. \tag{7.1}$$

Here, $\mathbf{r}_e$ denotes the position of the electron, m the bare mass, e the electric charge, $V_0(\mathbf{r}_e)$ an arbitrary bare external potential acting only on the electron, $\mathbf{E}_\perp$ the transverse electric field (obtained by taking the negative partial time derivative of the vector potential $\mathbf{A}_\perp(\mathbf{r},t)$), $\mathbf{B}$ the magnetic field (obtained by taking the curl of $\mathbf{A}_\perp(\mathbf{r},t)$), ϵ_0 the permittivity of free space, c the speed of light, $\rho(\mathbf{r})$ the charge density and $\mathbf{j}(\mathbf{r})$ the corresponding current density.

The last term in Eq. (7.1) describes the Coulomb potential between different particles which is written in Fourier space where the symbol $\int_{1/2}$ means that the integral is taken over half the volume in the reciprocal space. For a single particle, it reduces to the particle's Coulomb self energy E_{Coul}. After the introduction of a suitable cut-off, which is also necessary for the calculations that are to follow, it takes a finite value given by $E_{\text{Coul}} = \alpha\hbar\omega_{\text{max}}/\pi$ [36]. Since this term is a constant, it does not affect the motion of the electron.

Further, within a point particle treatment of the electron, $\rho(\mathbf{r}) = -e\delta(\mathbf{r}-\mathbf{r}_e)$ and the current density is given by $\mathbf{j}(\mathbf{r}) = -e\dot{\mathbf{r}}\delta(\mathbf{r}-\mathbf{r}_e)$. The interaction term thus becomes $-e\dot{\mathbf{r}}_e\mathbf{A}_\perp(\mathbf{r}_e,t)$. For the electron traveling at non-relativistic speeds, the time derivative can be shifted from its position onto the transverse vector potential. This is because in addition to a total derivative term, a term of the form $e\mathbf{r}_e v^i\partial_i\mathbf{A}_\perp(\mathbf{r},t)$ appears (where $v^i := \dot{r}^i$). After the wave expansion of $\mathbf{A}_\perp$, this term is seen to be negligible with respect to $e\mathbf{r}_e\dot{\mathbf{A}}_\perp(\mathbf{r}_e,t) = -e\mathbf{r}_e\mathbf{E}_\perp(\mathbf{r}_e,t)$ as long as $\omega_k \gg vk$ or $v \ll c$. Therefore, for the non-relativistic electron, the Lagrangian relevant for the dynamics reduces to

$$L(t) \approx \frac{1}{2}m\dot{\mathbf{r}}_e^2 - V_0(\mathbf{r}_e) + \frac{\epsilon_0}{2}\int d^3r \left(\mathbf{E}_\perp^2(\mathbf{r}) - c^2\mathbf{B}^2(\mathbf{r})\right) - e\mathbf{r}_e\mathbf{E}_\perp(\mathbf{r}_e)\,. \tag{7.2}$$

In Eq. (7.2) the total derivative $d/dt(\mathbf{r}_e\mathbf{A}_\perp(\mathbf{r}_e))$ and the constant self energy term have been omitted as these do not affect the electron's dynamics.

7.1.2 The Hamiltonian

In terms of the canonical variables $\mathbf{r}_e, \mathbf{p}, \mathbf{A}_\perp$ and $\mathbf{\Pi}$, with $\mathbf{p}$ and $\mathbf{\Pi}$ being the conjugate momentums for the variables $\mathbf{r}_e$ and $\mathbf{A}_\perp$ respectively, the Hamiltonian corresponding to the Lagrangian (7.2) can be written in the form

$$\mathrm{H} = \mathrm{H_S} + \mathrm{H_{EM}} + \mathrm{H_{int}}\,. \tag{7.3}$$

To write its explicit expression, first the quantity $\hat{\mathbf{\Pi}}_\mathrm{E} = -\hat{\mathbf{\Pi}}/\epsilon_0$ is defined since it appears repeatedly in the calculations. The different components of the full Hamiltonian can then be written as $\mathrm{H_{EM}} = \frac{\epsilon_0}{2}\int d^3r(\mathbf{\Pi}_\mathrm{E}^2(\mathbf{r}) + c^2\mathbf{B}^2(\mathbf{r}))$, which is the free field Hamiltonian of the radiation field, $\mathrm{H_{int}} = e\mathbf{r}_e\mathbf{\Pi}_\mathrm{E}(\mathbf{r}_e)$, which is the term that encodes the interaction between the electron and the radiation field and

$$\mathrm{H_S} = \frac{\mathbf{p}^2}{2m} + V_0(\mathbf{r}_e) + \frac{e^2}{2\epsilon_0}\int d^3r r^i \delta^\perp_{im}(\mathbf{r}-\mathbf{r}_e)\delta^\perp_{mj}(\mathbf{r}-\mathbf{r}_e)r^j\,, \tag{7.4}$$

which is the system Hamiltonian. The transverse Dirac delta $\delta^\perp_{ij}(\mathbf{r}-\mathbf{r}_e)$ that appears in the expression for $\mathrm{H_S}$ is defined to be [36]

$$\delta^\perp_{ij}(\mathbf{r}-\mathbf{r}_e) = \frac{1}{(2\pi)^3}\int d^3k\left(\delta_{ij} - \frac{k_ik_j}{k^2}\right)e^{i\mathbf{k}\cdot(\mathbf{r}-\mathbf{r}_e)}\,. \tag{7.5}$$

It appears instead of the Dirac delta due to the coupling of the position of the electron with the transverse electric field in Eq. (7.2). The form of $\mathrm{H_S}$ calls for an identification of the full effective potential $V(\mathbf{r}_e)$ governing the dynamics of the electron such that

$$V(\mathbf{r}_e) := V_0(\mathbf{r}_e) + V_\mathrm{EM}(\mathbf{r}_e)\,, \qquad V_\mathrm{EM}(\mathbf{r}_e) = \frac{e^2}{2\epsilon_0}\int d^3r r^i\delta^\perp_{im}(\mathbf{r}-\mathbf{r}_e)\delta^\perp_{mj}(\mathbf{r}-\mathbf{r}_e)r^j\,. \tag{7.6}$$

It should be emphasized that the extra term $V_\mathrm{EM}(\mathbf{r}_e)$ is not added to the bare potential by hand, but arises due to the $\mathbf{r}_e\mathbf{E}_\perp$ coupling in the Lagrangian (7.2). Although it gives a divergent contribution $\frac{e^2}{2\epsilon_0}\delta^\perp_{ij}(\mathbf{0})r^i_e r^j_e$, after regularizing the transverse delta function on a minimum length scale $r_\mathrm{min} = 1/k_\mathrm{max}$, the contribution coming from this term becomes finite and scales as $\mathcal{O}\left(\frac{e^2}{2\epsilon_0}\mathbf{r}_e^2 k^3_\mathrm{max}\right)$. To be more precise, this convergence is restored by imposing the cut-off consistently throughout the calculations, by introducing the convergence factor e^{-k/k_max} for the integrals in the Fourier space (c.f. Sec. 7.3). Using this procedure, the expression for $\delta^\perp_{ij}(\mathbf{0})$ is obtained to be

$$\delta^\perp_{ij}(\mathbf{0}) = \frac{1}{(2\pi)^3}\int dk k^2 e^{-k/k_\mathrm{max}}\int d\Omega\left(\delta_{ij} - \frac{k_ik_j}{k^2}\right)\,. \tag{7.7}$$

First evaluating the angular integral, which gives a factor $\frac{8\pi}{3}\delta_{ij}$, and then the radial integral, we get

$$V_\mathrm{EM}(\mathbf{r}_e) = \frac{e^2\omega^3_\mathrm{max}}{3\pi^2\epsilon_0 c^3}\mathbf{r}_e^2\,. \tag{7.8}$$

The contribution of $V_{\text{EM}}(\mathbf{r}_e)$ to the electron dynamics is cancelled exactly by another term that appears later in the calculations (upto second order in the interactions), as shown in Sec. 7.5. Therefore, for all practical purposes, $V_{\text{EM}}(\mathbf{r}_e)$ turns out to have no consequences on the dynamics of the electron.

7.2 The master equation

Having obtained the Hamiltonian, we can now study the quantum dynamics. The probability amplitude for a particle to be at the position x_t at some final time t, starting from the position x_i at some initial time t_i, is given by [5]

$$\langle x_t|\,\hat{U}(t;t_i)\,|x_i\rangle = \int_{\substack{x(t)=x_t,\\ x(t_i)=x_i}} D[x,p]e^{-\frac{i}{\hbar}\int_{t_i}^{t}dt'(H_{\text{T}}[x,p]-p\dot{x})} = \int_{\substack{x(t)=x_t,\\ x(t_i)=x_i}} D[x]e^{\frac{i}{\hbar}S_{\text{T}}[x]}\,, \tag{7.9}$$

where H_{T} is the full Hamiltonian and S_{T} is the corresponding action describing some general dynamics. From Eq. (7.9) the expression for the density matrix at time t can be written as [25]

$$\langle x'_t|\,\hat{\rho}(t)\,|x_t\rangle = \int_{\substack{x(t)=x_t,\\ x'(t)=x'_t}} D[x,x']e^{\frac{i}{\hbar}(S_{\text{T}}[x']-S_{\text{T}}[x])}\rho(x'_i,x_i,t_i)\,, \tag{7.10}$$

where the integrals over x_i and x'_i are included within the path integral. The expression analogous to Eq. (7.9) also exists for $\langle p_t|\,\hat{U}(t;t_i)\,|p_i\rangle$ in which the boundary conditions are fixed on $p(t)$ and the phase-space weighing function is instead given by $\exp\{\frac{-i}{\hbar}\int_{t_i}^{t}dt'\,(H_T[x,p]+x\dot{p})\}$ such that

$$\langle p_t|\,\hat{U}(t;t_i)\,|p_i\rangle = \int_{\substack{p(t)=p_t,\\ p(t_i)=p_i}} D[x,p]e^{-\frac{i}{\hbar}\int_{t_i}^{t}dt'(H_{\text{T}}[x,p]+x\dot{p})}\,. \tag{7.11}$$

The case that is of interest here, also involves integrating over the degrees of freedom of the radiation field. For that, with a slight abuse of notation, $\exp\{\frac{i}{\hbar}S_{\text{EM}}\}$ is understood to be simply the appropriate phase-space weighing function appearing inside the path integral with $S_{\text{EM}} := -\int_{t_i}^{t}d^3rdt'(\mathcal{H}_{\text{EM}}-\Pi\dot{\text{A}}_\perp)$ or $S_{\text{EM}} := -\int_{t_i}^{t}d^3rdt'(\mathcal{H}_{\text{EM}}+\text{A}_\perp\dot{\Pi})$ depending upon the basis states between which the transition amplitudes are calculated.

We are interested in the dynamics of the electron, having taken into account its interaction with the radiation field environment. With this distinction, the total phase-space function can be written as $S_{\text{T}} = S_{\text{S}}[x] + S_{\text{EM}}[\mu] + S_{\text{int}}[x,\Pi_{\text{E}}]$, where S_{S} denotes the system action, $S_{\text{EM}}[\mu] := S_{\text{EM}}[\text{A}_\perp,\Pi_{\text{E}}]$ the phase-space function governing the time evolution of the free radiation field in which μ denotes its phase-space degrees of freedom and $S_{\text{int}}[x,\Pi_{\text{E}}] := -e\int_{t_i}^{t}dt'\,x\Pi_{\text{E}}$ encodes the interaction between the two. The expression for the system-environment density matrix can then be written as

$$\begin{aligned}\left\langle x'_t;\Pi_{\text{E}}^{f'}\right|\hat{\rho}(t)\left|x_t;\Pi_{\text{E}}^{f}\right\rangle = &\int_{\substack{x(t)=x_t,\\ x'(t)=x'_t}} D[x,x']e^{\frac{i}{\hbar}(S_{\text{S}}[x']-S_{\text{S}}[x])}\rho_{\text{S}}(x'_i,x_i,t_i)\times\\ &\times\int_{\substack{\Pi_{\text{E}}(t)=\Pi_{\text{E}}^{f},\\ \Pi'_{\text{E}}(t)=\Pi_{\text{E}}^{f'}}} D[\mu,\mu']e^{\frac{i}{\hbar}(S_{\text{EM}}[\mu']+S_{\text{int}}[x',\Pi'_{\text{E}}]-S_{\text{EM}}[\mu]-S_{\text{int}}[x,\Pi_{\text{E}}])}\rho_{\text{EM}}(\Pi'_{\text{E}}(t_i),\Pi_{\text{E}}(t_i),t_i)\,,\end{aligned} \tag{7.12}$$

where $\left|\Pi_{\rm E}^{f}\right\rangle$ denotes the basis state of the environment [1]. In writing Eq. (7.12) we have also assumed the full density matrix $\hat{\rho}(t_i)$ to be in the product state $\hat{\rho}(t_i) = \hat{\rho}_{\rm S}(t_i) \otimes \hat{\rho}_{\rm EM}(t_i)$ at the initial time t_i. We notice that $S_{\rm EM}[\mu]$ is quadratic in the environmental degrees of freedom while $S_{\rm int}[x, \Pi_{\rm E}]$ is linear in both x and $\Pi_{\rm E}$. After tracing over the environment, that is integrating over $\Pi_{\rm E}(t) = \Pi'_{\rm E}(t)$, the term in the second line of Eq. (7.12) yields a Gaussian in x such that [25]

$$\int_{\Pi_{\rm E}(t)=\Pi'_{\rm E}(t)} d\Pi_{\rm E}(t) D[\mu,\mu'] e^{\frac{i}{\hbar}(S_{\rm EM}[\mu']+S_{\rm int}[x',\Pi'_{\rm E}]-S_{\rm EM}[\mu]-S_{\rm int}[x,\Pi_{\rm E}])}\rho^{i}_{\rm EM} = e^{\frac{i}{2\hbar}\iint dt_1 dt_2 M_{ab}(t_1;t_2)x^a(t_1)x^b(t_2)}\,, \tag{7.13}$$

where $\rho^{i}_{\rm EM} := \rho_{\rm EM}(\Pi'_{\rm E}(t_i), \Pi_{\rm E}(t_i), t_i)$. The vector notation with the convention $x^a = x$ for $a = 1$, $x^a = x'$ for $a = 2$ and $x_a = \eta_{ab}x^b$ with $\eta_{ab} = \mathrm{diag}(-1, 1)$, has also been introduced. It is the matrix elements M_{ab} which determine the effective action of the system and contain the information about its interaction with the environment. They can be obtained by acting with $\frac{\hbar}{i}\frac{\delta}{\delta x^a}\frac{\delta}{\delta x^b}|_{x^a=x^b=0}$ (where x^a and x^b are set to zero after taking the derivatives) on Eq. (7.13) such that

$$M^{ab}(t_1;t_2) = \frac{ie^2}{\hbar}\int_{\Pi_{\rm E}(t)=\Pi'_{\rm E}(t)} d\Pi_{\rm E}(t) D[\mu,\mu'] \Pi^{a}_{\rm E}(t_1)\,\Pi^{b}_{\rm E}(t_2)\, e^{\frac{i}{\hbar}(S_{\rm EM}[\mu']-S_{\rm EM}[\mu])}\rho^{i}_{\rm EM}\,. \tag{7.14}$$

Here, in the light of the standard non-relativistic dipole approximation, the spatial dependence of the canonical fields has been neglected (c.f. Sec. 7.3). Depending upon the value of the indices a and b, the matrix elements correspond to the expectation values of the time-ordered, anti-time ordered, path-ordered or anti-path ordered correlations in the Heisenberg picture [25]. For the dynamics of the non-relativistic electron that is being considered here, the expression for M_{ab} reads

$$M_{ab}(t_1;t_2) = \frac{ie^2}{\hbar}\begin{bmatrix} \left\langle \tilde{\mathcal{T}}\{\hat{\Pi}_{\rm E}(t_1)\hat{\Pi}_{\rm E}(t_2)\}\right\rangle_0 & -\left\langle \hat{\Pi}_{\rm E}(t_1)\hat{\Pi}_{\rm E}(t_2)\right\rangle_0 \\ -\left\langle \hat{\Pi}_{\rm E}(t_2)\hat{\Pi}_{\rm E}(t_1)\right\rangle_0 & \left\langle \mathcal{T}\{\hat{\Pi}_{\rm E}(t_1)\hat{\Pi}_{\rm E}(t_2)\}\right\rangle_0 \end{bmatrix}. \tag{7.15}$$

The zero in the subscript denotes that the expectation values are calculated by disregarding the interaction with the system, while $\mathcal{T}$ and $\tilde{\mathcal{T}}$ denote the time-ordered and the anti-time ordered products respectively. It is also understood that since the electron's motion is considered to be along the x-axis, only the x-component of the canonical field operator enters the expression for M_{ab}. In terms of the creation and annihilation operators, and the x-component of the unit polarization vector $\varepsilon^{x}_{\mathbf{k}}$, it is given by [38]

$$\hat{\Pi}_{\rm E}(\mathbf{r},t) = i\left(\frac{\hbar c}{2\epsilon_0(2\pi)^3}\right)^{\frac{1}{2}}\int d^3k\sqrt{k}\sum_{\varepsilon}\hat{a}_{\varepsilon}(\mathbf{k})e^{i(\mathbf{k}\cdot\mathbf{r}-\omega t)}\varepsilon^{x}_{\mathbf{k}} + \mathrm{c.c}\,. \tag{7.16}$$

Since the initial state of the environment is taken to be the vacuum state $|0\rangle$ of the radiation field, $\langle\cdot\rangle_0 = \langle 0|\cdot|0\rangle$. After tracing over the environment, the reduced density matrix of the electron is obtained from Eq. (7.12) to be

$$\left\langle x'_{\rm f}\right|\hat{\rho}_r(t)\left|x_i\right\rangle = \int_{\substack{x(t)=x_{\rm f},\\ x'(t)=x'_{\rm f}}} D[x,x']e^{\frac{i}{\hbar}(S_{\rm S}[x']-S_{\rm S}[x]+S_{\rm IF}[x,x'])}\rho_r(x'_i,x_i,t_i)\,, \tag{7.17}$$

[1] Note that the precise choice of the basis states is unimportant since the reduced density matrix is obtained after tracing over the environment

where the so-called influence functional S_{IF} [50] is given by

$$S_{\text{IF}}[x,x'] = \frac{ie^2}{2\hbar}\int_{t_i}^{t} dt_1 dt_2 \left[\left\langle \tilde{\mathcal{T}}\{\hat{\Pi}_{\text{E}}(t_1)\hat{\Pi}_{\text{E}}(t_2)\}\right\rangle_0 x(t_1)x(t_2) - \left\langle \hat{\Pi}_{\text{E}}(t_1)\hat{\Pi}_{\text{E}}(t_2)\right\rangle_0 x(t_1)x'(t_2) \right.$$
$$\left. - \left\langle \hat{\Pi}_{\text{E}}(t_2)\hat{\Pi}_{\text{E}}(t_1)\right\rangle_0 x'(t_1)x(t_2) + \left\langle \mathcal{T}\{\hat{\Pi}_{\text{E}}(t_1)\hat{\Pi}_{\text{E}}(t_2)\}\right\rangle_0 x'(t_1)x'(t_2)\right] . \tag{7.18}$$

The integral $\int_{t_i}^{t}$ stands for both the t_1 and the t_2 integrals which run from t_i to t. Alternatively, the influence functional S_{IF} can be written in the matrix notation as

$$S_{\text{IF}}[x,x'] = \frac{1}{2}\int_{t_i}^{t} dt_1 dt_2 \begin{bmatrix} x(t_1) & x'(t_1)\end{bmatrix} \cdot \begin{bmatrix} M_{11} & M_{12} \\ M_{21} & M_{22}\end{bmatrix} \cdot \begin{bmatrix} x(t_2) \\ x'(t_2)\end{bmatrix} . \tag{7.19}$$

As it is more convenient, we make a change of basis to $(X\,,u)$ defined by

$$X(t) := (x'(t)+x(t))/2\,, \quad u(t) = x'(t) - x(t)\,, \tag{7.20}$$

in which the influence functional transforms as

$$S_{\text{IF}}[X,u] = \frac{1}{2}\int_{t_i}^{t} dt_1 dt_2 \begin{bmatrix} X(t_1) & u(t_1)\end{bmatrix} \cdot \begin{bmatrix} \tilde{M}_{11} & \tilde{M}_{12} \\ \tilde{M}_{21} & \tilde{M}_{22}\end{bmatrix} \cdot \begin{bmatrix} X(t_2) \\ u(t_2)\end{bmatrix} , \tag{7.21}$$

where

$$\begin{bmatrix} \tilde{M}_{11} & \tilde{M}_{12} \\ \tilde{M}_{21} & \tilde{M}_{22}\end{bmatrix} = \begin{bmatrix} M_{11}+M_{12}+M_{21}+M_{22} & \frac{1}{2}\left((M_{12}-M_{21})+(M_{22}-M_{11})\right) \\ \frac{1}{2}\left(-(M_{12}-M_{21})+(M_{22}-M_{11})\right) & \frac{1}{4}((M_{11}+M_{22})-(M_{12}+M_{21}))\end{bmatrix} . \tag{7.22}$$

Further, from Eq. (7.15), we have the following relations

$$M_{11}+M_{22} = -(M_{12}+M_{21}) = \frac{ie^2}{\hbar}\left\langle\{\hat{\Pi}_{\text{E}}(t_1),\hat{\Pi}_{\text{E}}(t_2)\}\right\rangle_0 , \tag{7.23}$$

$$M_{12}-M_{21} = \frac{ie^2}{\hbar}\left\langle\left[\hat{\Pi}_{\text{E}}(t_2),\hat{\Pi}_{\text{E}}(t_1)\right]\right\rangle_0 , \tag{7.24}$$

$$M_{22}-M_{11} = \frac{ie^2}{\hbar}\left\langle\left[\hat{\Pi}_{\text{E}}(t_1),\hat{\Pi}_{\text{E}}(t_2)\right]\right\rangle_0 \operatorname{sgn}(t_1-t_2)\,. \tag{7.25}$$

Using these relations, $\tilde{M}$ takes the simplified form

$$\begin{bmatrix} \tilde{M}_{11} & \tilde{M}_{12} \\ \tilde{M}_{21} & \tilde{M}_{22}\end{bmatrix} = \frac{ie^2}{\hbar}\begin{bmatrix} 0 & \left\langle\left[\hat{\Pi}_{\text{E}}(t_2),\hat{\Pi}_{\text{E}}(t_1)\right]\right\rangle_0 \theta(t_2-t_1) \\ \left\langle\left[\hat{\Pi}_{\text{E}}(t_1),\hat{\Pi}_{\text{E}}(t_2)\right]\right\rangle_0 \theta(t_1-t_2) & \frac{1}{2}\left\langle\{\hat{\Pi}_{\text{E}}(t_1),\hat{\Pi}_{\text{E}}(t_2)\}\right\rangle_0\end{bmatrix} , \tag{7.26}$$

where $\theta(t)$ is the Heaviside step function. Thus, in the (X,u) basis, the influence functional in Eq. (7.18) takes the compact form

$$S_{\text{IF}}[X,u](t) = \int_{t_i}^{t} dt_1 dt_2 \left[i\frac{u(t_1)\mathcal{N}(t_1;t_2)u(t_2)}{2} + u(t_1)\mathcal{D}(t_1;t_2)X(t_2)\right] , \tag{7.27}$$

where the noise kernel $\mathcal{N}$ and the dissipation kernel $\mathcal{D}$ are defined as

$$\begin{aligned}\mathcal{N}(t_1;t_2) :=& \frac{e^2}{2\hbar}\left\langle\{\hat{\Pi}_{\rm E}(t_1),\hat{\Pi}_{\rm E}(t_2)\}\right\rangle_0 ,\\ \mathcal{D}(t_1;t_2) :=& \frac{ie^2}{\hbar}\left\langle\left[\hat{\Pi}_{\rm E}(t_1),\hat{\Pi}_{\rm E}(t_2)\right]\right\rangle_0\theta(t_1-t_2) .\end{aligned} \tag{7.28}$$

Having determined the full effective action for the electron in terms of the influence functional, the master equation can now be derived. From Eq. (7.17), it can be seen that the time derivative of the reduced density matrix will have, in addition to the standard Liouville-von Neuman term, the contribution coming from the influence functional. In order to compute that, the rate of change of $S_{\rm IF}$ needs to be evaluated. It is given by

$$\delta_t S_{\rm IF}[X,u] = u(t)\int_{t_i}^{t} dt_1\left(i\mathcal{N}(t;t_1)u(t_1)+\mathcal{D}(t;t_1)X(t_1)\right) . \tag{7.29}$$

In terms of the original (x,x') basis, the master equation can now be written as

$$\begin{aligned}\partial_t\rho_r(x'_{\rm f},x_{\rm f},t) =& -\frac{i}{\hbar}\left\langle x'_{\rm f}\right|\left[\hat{\rm H}_{\rm s},\hat{\rho}_r\right]\left|x_{\rm f}\right\rangle + \frac{i}{\hbar}\int_{\substack{x(t)=x_{\rm f},\\ x'(t)=x'_{\rm f}}} D[x,x']\delta_t S_{\rm IF}[x',x]e^{\frac{i}{\hbar}(S_{\rm S}[x']-S_{\rm S}[x]+S_{\rm IF}[x,x'])}\rho_r(x'_i,x_i,t_i)\\ \approx& -\frac{i}{\hbar}\left\langle x'_{\rm f}\right|\left[\hat{\rm H}_{\rm s},\hat{\rho}_r\right]\left|x_{\rm f}\right\rangle + \frac{i}{\hbar}\int_{\substack{x(t)=x_{\rm f},\\ x'(t)=x'_{\rm f}}} D[x,x']\delta_t S_{\rm IF}[x',x]e^{\frac{i}{\hbar}(S_{\rm S}[x']-S_{\rm S}[x])}\rho_r(x'_i,x_i,t_i)\\ \approx& -\frac{i}{\hbar}\left\langle x'_{\rm f}\right|\left[\hat{\rm H}_{\rm s},\hat{\rho}_r\right]\left|x_{\rm f}\right\rangle\\ &-\frac{1}{\hbar}(x'_{\rm f}-x_{\rm f})\int_{t_i}^{t}dt_1\mathcal{N}(t;t_1)\int_{\substack{x(t)=x_{\rm f},\\ x'(t)=x'_{\rm f}}} D[x,x'](x'(t_1)-x(t_1))e^{\frac{i}{\hbar}(S_{\rm S}[x']-S_{\rm S}[x])}\rho_r(x'_i,x_i,t_i)\\ &+\frac{i}{2\hbar}(x'_{\rm f}-x_{\rm f})\int_{t_i}^{t}dt_1\mathcal{D}(t;t_1)\int_{\substack{x(t)=x_{\rm f},\\ x'(t)=x'_{\rm f}}} D[x,x'](x'(t_1)+x(t_1))e^{\frac{i}{\hbar}(S_{\rm S}[x']-S_{\rm S}[x])}\rho_r(x'_i,x_i,t_i) .\end{aligned} \tag{7.30}$$

For the second term on the right hand side in the second line of Eq. (7.30), $S_{\rm IF}$ has been omitted in the exponential. This is because $S_{\rm IF}$ is second order in the coupling constant and is already present adjacent to the exponential. Since the calculations are limited to second order in the interactions, $S_{\rm IF}$ can be neglected inside the exponential.

To simplify the master equation further, we note that the last two lines of Eq. (7.30) can be written much more compactly. This is due to the following identity [25]

$$\begin{aligned}&\int_{\substack{x(t)=x_{\rm f},\\ x'(t)=x'_{\rm f}}} D[x,x']x'(t_1)e^{\frac{i}{\hbar}(S_{\rm S}[x']-S_{\rm S}[x])}\rho_r(x'_i,x_i,t_i) =\\ &= \int dx'(t_1)\left\langle x'_{\rm f}\right|\hat{U}_s(t;t_1)\left|x'(t_1)\right\rangle x'(t_1)\left\langle x'(t_1)\right|\hat{U}_s(t_1;t_i)\hat{\rho}_r(t_i)\hat{U}_s^{-1}(t;t_i)\left|x_{\rm f}\right\rangle\\ &= \left\langle x'_{\rm f}\right|\hat{U}_s(t;t_1)\hat{x}\hat{U}_s(t_1;t_i)\hat{\rho}_r(t_i)\hat{U}_s^{-1}(t;t_i)\left|x_{\rm f}\right\rangle\\ &= \left\langle x'_{\rm f}\right|\hat{U}_s(t;t_1)\hat{x}\hat{U}_s(t_1;t_i)\hat{U}_s^{-1}(t;t_i)\hat{U}_s(t;t_i)\hat{\rho}_r(t_i)\hat{U}_s^{-1}(t;t_i)\left|x_{\rm f}\right\rangle\\ &= \left\langle x'_{\rm f}\right|\hat{U}_s(t;t_1)\hat{x}\hat{U}_s^{-1}(t;t_1)\hat{\rho}_r(t)\left|x_{\rm f}\right\rangle = \left\langle x'_{\rm f}\right|\hat{x}_{\rm H_s}(-\tau)\hat{\rho}_r(t)\left|x_{\rm f}\right\rangle ,\end{aligned} \tag{7.31}$$

where

$$\hat{x}_{\mathrm{H_s}}(-\tau) := \hat{U}_s^{-1}(t-\tau;t)\hat{x}\hat{U}_s(t-\tau;t)\,, \qquad \tau := t - t_1\,. \tag{7.32}$$

Here, the operator $\hat{U}_s(t-\tau;t)$ is the unitary operator that evolves the statevector of the system from time t to $t-\tau$ via the system Hamiltonian $\hat{\mathrm{H}}_s$ only and the operator $\hat{x}$ without the subscript is the usual Schrödinger operator such that

$$\hat{x}_{\mathrm{H_s}}(0) = \hat{x}\,, \tag{7.33}$$

Similarly, we also have the analogous relation

$$\int_{\substack{x(t)=x_f,\\ x'(t)=x'_f}} D[x,x']x(t_1)e^{\frac{i}{\hbar}(\mathrm{S_S}[x']-\mathrm{S_S}[x])}\rho_r(x'_i,x_i,t_i) = \left\langle x'_f\right|\hat{\rho}_r(t)\hat{x}_{\mathrm{H_s}}(-\tau)\left|x_f\right\rangle\,. \tag{7.34}$$

Using these relations, and replacing the t_1 integral with the τ integral ($t_1 = t-\tau$), the master equation takes the compact form

$$\begin{aligned}\partial_t\rho_r(x'_f,x_f,t) =& -\frac{i}{\hbar}\left\langle x'_f\right|\left[\hat{\mathrm{H}}_s,\hat{\rho}_r(t)\right]\left|x_f\right\rangle \\ &-\frac{1}{\hbar}(x'_f-x_f)\int_0^{t-t_i}d\tau\mathcal{N}(t;t-\tau)\left\langle x'_f\right|\left[\hat{x}_{\mathrm{H_s}}(-\tau),\hat{\rho}_r(t)\right]\left|x_f\right\rangle \\ &+\frac{i}{2\hbar}(x'_f-x_f)\int_0^{t-t_i}d\tau\mathcal{D}(t;t-\tau)\left\langle x'_f\right|\left\{\hat{x}_{\mathrm{H_s}}(-\tau),\hat{\rho}_r(t)\right\}\left|x_f\right\rangle\,.\end{aligned} \tag{7.35}$$

The eigenvalues outside of the integrals in Eq. (7.35) can be obtained by acting with the position operator $\hat{x}$ such that

$$\begin{aligned}\left\langle x'_f\right|\partial_t\hat{\rho}_r\left|x_f\right\rangle =& -\frac{i}{\hbar}\left\langle x'_f\right|\left[\hat{\mathrm{H}}_s,\hat{\rho}_r(t)\right]\left|x_f\right\rangle \\ &-\frac{1}{\hbar}\int_0^{t-t_i}d\tau\mathcal{N}(t;t-\tau)\left\langle x'_f\right|\left[\hat{x},\left[\hat{x}_{\mathrm{H_s}}(-\tau),\hat{\rho}_r(t)\right]\right]\left|x_f\right\rangle \\ &+\frac{i}{2\hbar}\int_0^{t-t_i}d\tau\mathcal{D}(t;t-\tau)\left\langle x'_f\right|\left[\hat{x},\left\{\hat{x}_{\mathrm{H_s}}(-\tau),\hat{\rho}_r(t)\right\}\right]\left|x_f\right\rangle\,.\end{aligned} \tag{7.36}$$

The master equation in the operator form can therefore be written as

$$\begin{aligned}\partial_t\hat{\rho}_r =& -\frac{i}{\hbar}\left[\hat{\mathrm{H}}_s,\hat{\rho}_r\right] \\ &-\frac{1}{\hbar}\int_0^{t-t_i}d\tau\mathcal{N}(t;t-\tau)\left[\hat{x},\left[\hat{x}_{\mathrm{H_s}}(-\tau),\hat{\rho}_r(t)\right]\right] \\ &+\frac{i}{2\hbar}\int_0^{t-t_i}d\tau\mathcal{D}(t;t-\tau)\left[\hat{x},\left\{\hat{x}_{\mathrm{H_s}}(-\tau),\hat{\rho}_r(t)\right\}\right]\,.\end{aligned} \tag{7.37}$$

The first line of the master equation is the usual Liouville-von Neuman evolution and involves only the system Hamiltonian $\hat{\mathrm{H}}_s$, while the second and the third lines encode the system's interaction with the environment.

We remember that due to the coupling between the position of the electron and the transverse electric field in Eq. (7.2), the system Hamiltonian receives an additional contribution such that $\hat{\mathrm{H}}_s = \hat{p}^2/(2m) + \hat{V}_0(x) + \hat{V}_{\mathrm{EM}}(x)$, where, having introduced a cut-off scale in the calculations and considering the motion of the electron along the x-axis only, $\hat{V}_{\mathrm{EM}}(x) = \frac{e^2\omega_{\mathrm{max}}^3}{3\pi^2\epsilon_0 c^3}\hat{x}^2$ (c.f. Sec. 7.1.2). Moreover, since the master equation is valid upto second order in the interactions and since the operator $\hat{x}_{\mathrm{H_s}}(-\tau)$ appears alongside the dissipation and the noise kernels (which are already second order in e), the time evolution governed by $\hat{U}_s(t-\tau;t)$ in Eq. (7.32) is understood to involve only $\hat{V}_0$ and not $\hat{V}_{\mathrm{EM}}$. Therefore, upto second order in the interactions, $\hat{V}_{\mathrm{EM}}$ only contributes via the Liouville-von Neuman term.

7.3 The dissipation and the noise kernels

In order to solve the master equation (7.37), the kernels need to be evaluated explicitly. To achieve that, we begin with the expression for the vacuum expectation value of the correlator

$$\langle 0|\,\hat{\Pi}_{\mathrm{E}}(x(t_1),t_1)\hat{\Pi}_{\mathrm{E}}(x(t_2),t_2)\,|0\rangle = \frac{-i\hbar c}{2\epsilon_0 4\pi^2}\hat{\Box}\left\{\frac{1}{r}\int_0^\infty dk e^{-ikc\tau}\left(e^{ikr}-e^{-ikr}\right)\right\}, \tag{7.38}$$

where

$$r := |x(t_1)-x(t_2)|\,, \qquad \tau := t_1 - t_2\,, \qquad \hat{\Box} := -\frac{1}{c^2}\partial_\tau^2 + \partial_r^2\,. \tag{7.39}$$

Here, the right hand side of Eq. (7.38) is obtained with the help of the expression of the quantized canonical transverse electric field operator in Eq. (7.16). The expression in Eq. (7.38) becomes convergent after resorting to the standard Hadamard finite part prescription [25], in which the convergence factor $e^{-\omega_k/\omega_{\mathrm{max}}}$ is introduced inside the integral (with $\omega_k = kc$). Physically, this prescription cuts off the contribution coming from the modes $\omega_k \gg \omega_{\mathrm{max}}$ and mathematically it is the same as using the $i\epsilon$ prescription where one sends $\tau \to \tau - i\epsilon$, with $\epsilon = 1/\omega_{\mathrm{max}}$. After completing the integral by using this prescription, we get

$$\langle 0|\,\hat{\Pi}_{\mathrm{E}}(1)\hat{\Pi}_{\mathrm{E}}(2)\,|0\rangle = \frac{\hbar c}{4\pi^2\epsilon_0}\hat{\Box}\left\{\frac{1}{r^2-c^2(\tau-i\epsilon)^2}\right\} = \frac{\hbar c}{\pi^2\epsilon_0}\frac{1}{\left(r^2-c^2(\tau-i\epsilon)^2\right)^2}\,. \tag{7.40}$$

For the correlator in Eq. (7.40), we ignore the spatial dependence of the fields in the spirit of the non-relativistic approximation $r \ll c\tau$. In this limit, the correlator becomes

$$\langle 0|\,\hat{\Pi}_{\mathrm{E}}(1)\hat{\Pi}_{\mathrm{E}}(2)\,|0\rangle \approx \frac{\hbar}{\pi^2\epsilon_0 c^3\left(\tau-i\epsilon\right)^4}\,. \tag{7.41}$$

Using Eq. (7.41), the expressions for the noise and the dissipation kernels are obtained to be

$$\mathcal{N}(\tau) = \frac{e^2}{\pi^2\epsilon_0 c^3}\frac{\left(\epsilon^4 - 6\epsilon^2\tau^2+\tau^4\right)}{\left(\epsilon^2+\tau^2\right)^4}\,, \tag{7.42}$$

$$\mathcal{D}(\tau) = \frac{8e^2}{\pi^2\epsilon_0 c^3}\frac{\epsilon\tau(\epsilon^2-\tau^2)}{(\epsilon^2+\tau^2)^4}\theta(\tau)\,. \tag{7.43}$$

Further, with some algebraic manipulation, the dissipation kernel can be expressed more compactly as

$$\mathcal{D}(\tau) = \frac{e^2}{3\pi^2\epsilon_0 c^3}\theta(\tau)\frac{d^3}{d\tau^3}\left(\frac{\epsilon}{\tau^2+\epsilon^2}\right). \tag{7.44}$$

Noticing that

$$\frac{\epsilon}{\tau^2+\epsilon^2} = \frac{d}{d\tau}\tan^{-1}(\tau/\epsilon) = \pi\delta_\epsilon(\tau), \tag{7.45}$$

we arrive at the expression

$$\mathcal{D}(\tau) = \frac{e^2}{3\pi\epsilon_0 c^3}\theta(\tau)\frac{d^3}{d\tau^3}\delta_\epsilon(\tau). \tag{7.46}$$

The last equality in Eq. (7.45) can be understood in the limit $\epsilon \to 0$ when the function $\tan^{-1}(\tau/\epsilon)$ takes the shape of a step function. Such an expression for $\mathcal{D}$ would yield infinite results. For that, we keep in mind that these functions are always well behaved for a finite ϵ and that δ_ϵ only behaves like a Dirac delta for $\tau \gg \epsilon$.

7.4 Integrals involving the dissipation kernel

In this section we derive an identity involving the integrals of the form $\int d\tau\mathcal{D}(\tau)f(\tau)$. To proceed, we keep in mind the situation where ϵ is small but finite so that all the derivatives of the *smoothed* Dirac delta are large but finite. However, for times $\tau \gg \epsilon$, we have $\delta_\epsilon(\tau) = \delta'_\epsilon(\tau) = \delta''_\epsilon(\tau) = 0$. In addition, since the derivative of the Dirac delta is an odd function of τ, we also have $\delta'_\epsilon(0) = 0$. In computing the integral of $\mathcal{D}(\tau)$ multiplying an arbitrary function $f(\tau)$, we shift the derivatives acting on δ_ϵ one by one onto $f(\tau)$ by integrating by parts. Since the calculations of interest involve integrating $\int_0^t d\tau\mathcal{D}(\tau)f(\tau)$, where τ takes only non-negative values from 0 to t, the step function $\theta(\tau)$ can be omitted inside the integral.

The first integration by parts gives (the constant pre-factors appearing in Eq. (7.46) will be plugged in at the end)

$$\int_0^t d\tau\delta'''_\epsilon(\tau)f(\tau) = -\int_0^t d\tau\delta''_\epsilon(\tau)f'(\tau) + \delta''_\epsilon(\tau)f(\tau)\big|_0^t. \tag{7.47}$$

Since $\delta''_\epsilon(t) = 0$, only the boundary term $-\delta''_\epsilon(0)f(0)$ survives. Further,

$$-\int_0^t d\tau\delta''_\epsilon(\tau)f'(\tau) = \int_0^t d\tau\delta'_\epsilon(\tau)f''(\tau) - \delta'_\epsilon(\tau)\ f'(\tau)\big|_0^t. \tag{7.48}$$

Since $\delta'_\epsilon(t) = \delta'_\epsilon(0) = 0$ ($\delta'_\epsilon(\tau)$ being an odd function of τ), both the boundary terms vanish. Proceeding further we get

$$\int_0^t d\tau\delta'_\epsilon(\tau)f''(\tau) = -\int_0^t d\tau\delta_\epsilon(\tau)f'''(\tau) + \delta_\epsilon(\tau)\ f''(\tau)\big|_0^t. \tag{7.49}$$

As before, the boundary term at $\tau = t$ is zero and only the term $-\delta_\epsilon(0)f''(0)$ survives. Finally, since $\delta_\epsilon(\tau)$ goes to zero much faster than a generic function $f(\tau)$ for a small ϵ, it can be treated like a Dirac delta such that

$$-\int_0^t d\tau \delta_\epsilon(\tau) f'''(\tau) = -\frac{f'''(0)}{2}\,. \tag{7.50}$$

The factor of half comes because the integral is performed from 0 to t. Collecting the two boundary terms we get the result

$$\int_0^t d\tau \delta_\epsilon'''(\tau) f(\tau) = -\frac{f'''(0)}{2} - \delta_\epsilon(0) f''(0) - \delta_\epsilon''(0) f(0)\,. \tag{7.51}$$

From Eq. (7.45) we have $\delta_\epsilon(0) = 1/(\pi\epsilon) = \omega_{\text{max}}/\pi$ and $\delta_\epsilon''(0) = -2\omega_{\text{max}}^3/\pi$ such that

$$\int_0^t d\tau \mathcal{D}(\tau) f(\tau) = -\frac{2\alpha\hbar}{3c^2} f'''(0) - \frac{4\alpha\hbar\omega_{\text{max}}}{3\pi c^2} f''(0) + \frac{2e^2\omega_{\text{max}}^3}{3\pi^2\epsilon_0 c^3} f(0)\,. \tag{7.52}$$

Here, the constant prefactor appearing in Eq. (7.46) has now been plugged back.

7.5 The Abraham-Lorentz equation as a classical limit

The rate of change of the expectation values can be obtained with the help of the master equation (7.37). For the position operator it is given by

$$\begin{aligned}\frac{d}{dt}\langle\hat{x}\rangle = \text{Tr}\left(\hat{x}\partial_t\hat{\rho}_r\right) = &-\frac{i}{\hbar}\text{Tr}\left(\hat{x}\cdot\left[\hat{\text{H}}_s,\hat{\rho}_r\right]\right) + \frac{i}{2\hbar}\int_0^{t-t_i} d\tau \mathcal{D}(t;t-\tau)\text{Tr}\left(\hat{x}\cdot\left[\hat{x},\{\hat{x}_{\text{H}_s}(-\tau),\hat{\rho}_r(t)\}\right]\right)\\ &-\frac{1}{\hbar}\int_0^{t-t_i} d\tau \mathcal{N}(t;t-\tau)\text{Tr}\left(\hat{x}\cdot\left[\hat{x},\left[\hat{x}_{\text{H}_s}(-\tau),\hat{\rho}_r(t)\right]\right]\right)\,.\end{aligned} \tag{7.53}$$

Due to the identity

$$\text{Tr}\left(\hat{A}\cdot\left[\hat{B},\hat{C}\right]\right) = \text{Tr}\left(\left[\hat{A},\hat{B}\right]\cdot\hat{C}\right)\,, \tag{7.54}$$

the terms involving the dissipation and the noise kernels vanish and we get

$$\frac{d}{dt}\langle\hat{x}\rangle = -\frac{i}{\hbar}\text{Tr}\left(\hat{\rho}_r\cdot\left[\hat{x},\hat{\text{H}}_s\right]\right) = \frac{\langle\hat{p}\rangle}{m}\,. \tag{7.55}$$

Here, we remember that the system Hamiltonian $\hat{\text{H}}_s$ receives a contribution from $\hat{V}_{\text{EM}}$ in addition to the bare potential $\hat{V}_0$ such that (c.f. the discussion between Eqs. (7.4) and (7.8))

$$\hat{\text{H}}_s(t) = \frac{\hat{p}^2}{2m} + \hat{V}_0(x,t) + \frac{e^2\omega_{\text{max}}^3}{3\pi^2\epsilon_0 c^3}\hat{x}^2\,. \tag{7.56}$$

Similarly, for the momentum operator the following relation is obtained

$$\begin{aligned}\frac{d}{dt}\langle\hat{p}\rangle = \text{Tr}\left(\hat{p}\partial_t\hat{\rho}_r\right) = &-\frac{i}{\hbar}\text{Tr}\left(\left[\hat{p},\hat{\text{H}}_s\right]\cdot\hat{\rho}_r\right) + \frac{i}{2\hbar}\int_0^{t-t_i} d\tau \mathcal{D}(t;t-\tau)\text{Tr}\left(\left[\hat{p},\hat{x}\right]\cdot\{\hat{x}_{\text{H}_s}(-\tau),\hat{\rho}_r(t)\}\right)\\ &-\frac{1}{\hbar}\int_0^{t-t_i} d\tau \mathcal{N}(t;t-\tau)\text{Tr}\left(\left[\hat{p},\hat{x}\right]\cdot\left[\hat{x}_{\text{H}_s}(-\tau),\hat{\rho}_r(t)\right]\right)\,.\end{aligned} \tag{7.57}$$

Since $[\hat{x}, \hat{p}] = i\hbar\mathbb{1}$, the term involving the noise kernel vanishes and Eq. (7.57) simplifies to

$$\frac{d}{dt}\langle\hat{p}\rangle = -\langle\hat{V}_{0,x}\rangle - \frac{2e^2\omega_{\rm max}^3}{3\pi^2\epsilon_0 c^3}\langle\hat{x}\rangle + \mathrm{Tr}\left(\hat{\rho}_r(t)\int_0^{t-t_i} d\tau\mathcal{D}(\tau)\hat{x}_{\rm H_s}(-\tau)\right) . \tag{7.58}$$

Evaluating the integral using Eq. (7.52), we see that the last term in the integral gives the contribution $\frac{2e^2\omega_{\rm max}^3}{3\pi^2\epsilon_0 c^3}\langle\hat{x}\rangle$ to $\frac{d}{dt}\langle\hat{p}\rangle$ in Eq. (7.58) and cancels the contribution coming from $\hat{V}_{\rm EM}$. The EOM therefore reduces to

$$\frac{d}{dt}\langle\hat{p}\rangle = -\langle\hat{V}_0(x)_{,x}\rangle - \frac{2\alpha\hbar}{3c^2}\mathrm{Tr}\left(\hat{\rho}_r(t)\,\frac{d^3}{d\tau^3}\hat{x}_{\rm H_s}(-\tau)\Big|_{\tau=0}\right) - \frac{4\alpha\hbar\omega_{\rm max}}{3\pi c^2}\mathrm{Tr}\left(\hat{\rho}_r(t)\,\frac{d^2}{d\tau^2}\hat{x}_{\rm H_s}(-\tau)\Big|_{\tau=0}\right) . \tag{7.59}$$

It is interesting to compare the quantum mechanical EOM with the one derived classically. Within classical electrodynamics, a charged spherical shell of radius R which is accelerated by an external force $\mathrm{F_{ext}}$, experiences an extra recoil force (radiation reaction) due to the emission of radiation. By taking the limit $\mathrm{R} \to 0$ in the equation describing its dynamics, one obtains the Abraham-Lorentz formula

$$m_{\rm R}\ddot{x} = \mathrm{F_{ext}} + \frac{2\hbar\alpha}{3c^2}\dddot{x} , \tag{7.60}$$

where $m_{\rm R}$ denotes the observed renormalized mass. See for example [100, 65] and the references therein for the derivation of the AL formula. The triple derivative term appearing in Eq. (7.60) can be interpreted as the friction term that leads to energy loss due to radiation emission. For instance, when the external potential is taken to be $V_0(x) = (1/2)m\omega_0^2x^2$, one has $\dddot{x} \approx -\omega_0^2\dot{x}$ [36]. However, the issue with Eq. (7.60) is that the same triple derivative term persists even when the external potential is switched off, leading to an exponentially increase of the particle's acceleration.

Defining $\tau_0 := \frac{2\hbar\alpha}{3m_{\rm R}c^2}$, we get (in the absence of any external force) for the acceleration $a(t)$ of the charged particle

$$a(t) = a(t_0)\exp\{(t-t_0)/\tau_0\} . \tag{7.61}$$

One may try to circumvent the problem by simply assuming $a(t_0) = 0$. This, however, does not work. To see why, we consider an external force such that

$$\mathrm{F_{ext}} = \begin{cases} 0 , & \text{for } t \le 0 \\ f(t) , & \text{for } 0 < t \le t_1 \\ 0 & \text{for } t > t_1 . \end{cases} \tag{7.62}$$

It can be shown that in the presence of the triple time derivative term $\dddot{x}$ as in Eq. (7.60), the acceleration $a(t)$ changes continuously even if $F_{\rm ext}$ does not. If we set the initial conditions such that $a = 0$ for $t \le 0$, we get

$$a(t) = \begin{cases} 0 , & \text{for } t \le 0 \\ a_{\rm f}(t) , & \text{for } 0 < t \le t_1 \\ a_{\rm f}(t_1)\exp\{(t-t_1)/\tau_0\} & \text{for } t > t_1 . \end{cases} \tag{7.63}$$

We see that the run-away solution for $t > t_1$ persists since $a_t(t)$ is non-zero in the presence of a generic F_{ext}. We may set the initial conditions such that $a(t_1) = 0$ (and therefore $a(t) = 0$ for $t \geq t_1$) to avoid the run-away solution. However, since $a(t)$ changes continuously due to the presence of $\dddot{x}$ in the differential equation, by matching the boundary conditions we see that if $a(t_1) = 0$, $a(0) \neq 0$, implying that the particle started accelerating before the external force was even switched on. This behaviour is clearly acausal and also unacceptable. Thus, the choice of the initial value of the acceleration only allows us to trade between acausality and the run-away solution, both of which are physically unacceptable. A more elaborate discussion of the AL formula and the problems associated with it can be found in [39, 100, 64, 65] and the references therein.

To see if these problems persist at a quantum mechanical for Eq. (7.59), first we consider the situation when the external potential is switched off. To proceed, we note that the time derivatives of $\hat{x}_{H_s}$ in Eq. (7.59) can be easily computed, since from Eq. (7.32) we have the relation (upto leading order in the interactions)

$$\frac{d}{d\tau}\hat{x}_{H_s}(-\tau) = -\frac{i}{\hbar}\left[\hat{V}_0(x) + \frac{\hat{p}^2}{2m}, \hat{x}_{H_s}(-\tau)\right] . \tag{7.64}$$

Taking another time derivative of $\hat{x}_{H_s}$, with $\hat{V}_0(x) = 0$, we get

$$\frac{d^2}{d\tau^2}\hat{x}_{H_s}(-\tau)\Big|_{\tau=0} = \left(\frac{-i}{\hbar}\right)^2 \left[\frac{\hat{p}^2}{2m}, \left[\frac{\hat{p}^2}{2m}, \hat{x}\right]\right] = 0 , \tag{7.65}$$

where, in Eq. (7.65), the relation $\hat{x}_{H_s}(0) = \hat{x}$ has also been used. Similarly, the third derivative term appearing in Eq. (7.59) also vanishes. Therefore, when $\hat{V}_0(x) = 0$, Eq. (7.59) simply reduces to

$$\frac{d}{dt}\langle\hat{p}\rangle = 0 . \tag{7.66}$$

Unlike the AL formula (7.60), we see that upto second order in the interactions there are no solutions which allow for an exponential increase of the particle's acceleration in the absence of an external potential.

Next we consider the case when the external potential is switched on. When the potential does not depend explicitly on time, the double and triple derivative terms in Eq. (7.59) yield double and triple commutators with respect to the system Hamiltonian respectively (discarding $\hat{V}_{EM}$ upto second order). Eq. (7.59) can then be written as

$$\frac{d}{dt}\langle\hat{p}\rangle = F_{ext} + \frac{4\alpha\hbar\omega_{max}}{3\pi c^2}\mathrm{Tr}\left(\frac{1}{\hbar^2}\hat{\rho}_r(t)\left[\hat{H}_s, \left[\hat{H}_s, \hat{x}\right]\right]\right) - \frac{2\alpha\hbar}{3c^2}\mathrm{Tr}\left(\frac{i}{\hbar^3}\hat{\rho}_r(t)\left[\hat{H}_s, \left[\hat{H}_s, \left[\hat{H}_s, \hat{x}\right]\right]\right]\right) . \tag{7.67}$$

Here, the external force is defined to be $F_{ext} := -\langle\hat{V}_0(x)_{,x}\rangle$. Due to the presence of $\hat{V}_0(x)$, the commutators of $\hat{H}_s$ with $\hat{x}$ no longer vanish. To simplify the equation further, we shift the commutators onto the density matrix using the cyclic property such that

$$\mathrm{Tr}\left(\hat{\rho}_r\left[\hat{H}_s, \left[\hat{H}_s, \hat{x}\right]\right]\right) = \mathrm{Tr}\left(\hat{x}\left[\hat{H}_s, \left[\hat{H}_s, \hat{\rho}_r\right]\right]\right) . \tag{7.68}$$

The same relationship is also obtained for the triple commutator term, with an additional minus sign. Remembering that the master equation is only valid upto second order in the interaction, it is

sufficient to evaluate the trace in Eq. (7.67) at 0^{th} order. This implies that within the trace, the time dependence of the density matrix can be evaluated only by retaining the Liouville-von Neuman term in Eq. (7.37). The right hand side of Eq. (7.68) thus becomes proportional to $\mathrm{Tr}(\hat{x}\ddot{\hat{\rho}}_r)$. With these simplifications, Eq. (7.67) can be written as

$$m_{\text{R}}\frac{d^2}{dt^2}\langle\hat{x}\rangle = F_{\text{ext}} + \frac{2\alpha\hbar}{3c^2}\frac{d^3}{dt^3}\langle\hat{x}\rangle\,. \tag{7.69}$$

After identifying the observed electron mass with the re-normalized mass $m_{\text{R}} := m + \frac{4\alpha\hbar\omega_{\text{max}}}{3\pi c^2}$, Eq. (7.69) reduces to the Abraham-Lorentz formula (7.60). The same result also holds true for the case in which the bare potential $\hat{V}_0(x,t)$ depends explicitly on time (c.f. Appendix E of the preprint [66]). It must be remarked that the equation of motion derived quantum mechanically only reduces to Eq. (7.60) in the presence of an external potential. When the external potential is switched off, the EOM reduces to Eq. (7.66) and is therefore free of the runaway solution.

7.6 Decoherence

In this final section, having already obtained the master equation, we are interested in assessing if the spatial superposition of a charged particle at rest can be suppressed via its interaction with the vacuum fluctuations alone. We begin by writing the position space representation of the master equation (7.37) relevant for decoherence

$$\partial_t\rho_r = \left[-\frac{(x'-x)^2\mathcal{N}_1(t)}{\hbar}\right]\rho_r\,, \tag{7.70}$$

where $\mathcal{N}_1(\tau)$ is defined to be

$$\mathcal{N}_1(\tau) := \int_0^\tau d\tau'\mathcal{N}(\tau') = -\frac{4\alpha\hbar}{3\pi c^2}\frac{(\tau^3-3\tau\epsilon^2)}{(\tau^2+\epsilon^2)^3}\,. \tag{7.71}$$

Here, the initial time has been set to $t_i = 0$ and only the second term involving the noise kernel in Eq. (7.37) has been retained. This is because the other terms typically give subdominant contributions when the question of interest is to evaluate the rate of decay of the off-diagonal elements of the density matrix at late times [114, 25]. We have also used the expression of the noise kernel in Eq. (7.42) inside the integral to obtain the expression for $\mathcal{N}_1$. Integrating Eq. (7.70) we get

$$\rho_r(x',x,t) = \exp\left(-\frac{(x'-x)^2}{\hbar}\mathcal{N}_2(t)\right)\rho_r(x',x,0)\,, \tag{7.72}$$

where $\mathcal{N}_2(t) := \int_0^t d\tau\mathcal{N}_1(\tau)$. The function $\mathcal{N}_2(t)$ is inversely proportional to the coherence length $l_x(t)$ defined by $l_x(t) := (\hbar/\mathcal{N}_2(t))^{\frac{1}{2}}$. After performing the integral over $\mathcal{N}_1$ the expression for the coherence length is obtained to be

$$l_x(t) = \sqrt{\frac{3\pi c^2}{2\alpha\omega_{\text{max}}^2}\cdot\frac{(t^2+\epsilon^2)^2}{t^4+3t^2\epsilon^2}} \overset{t\gg\epsilon}{=} \sqrt{\frac{3\pi}{2\alpha}}\frac{1}{k_{\text{max}}}\,. \tag{7.73}$$

We see that the coherence length approaches a constant value on time scales much larger than $\epsilon = 1/\omega_{\rm max}$ and that its value scales inversely with the UV cut-off. Taken literally, if one sets $k_{\rm max} = 1/\lambda_{db}$, where λ_{db} is the de Broglie wavelength of the electron, one would arrive at the conclusion that vacuum fluctuations lead to decoherence with the coherence length of the charged particle asymptotically reducing to $l_x \approx 25\lambda_{db}$ within the time scales $t \approx \lambda_{db}/c$.

False Decoherence. It is clearly unsatisfactory to have an observable effect scale explicitly with the UV cut-off, since the precise numerical value of the cut-off is strictly speaking arbitrary. A similar situation was encountered in [126] in a different context of a harmonic oscillator coupled to a massive scalar field. However, it was argued in [126] that the reduced density matrix of the harmonic oscillator described false decoherence. In such a situation, the off-diagonal elements of the density matrix are suppressed simply because the state of the environment goes into different configurations depending upon the spatial location of the system. However, these changes in the environmental states remain locally around the system and are reversible. For the electron interacting with vacuum fluctuations, we therefore take the point of view that if the reduced density matrix describes false decoherence, then after adiabatically switching off the interactions with the environment (after having adiabatically switched it on initially), the original coherence must be fully restored at the level of the system.

To formulate the argument we consider a time dependent coupling $q(t) = -ef(t)$ such that $f(t) = 1$ for most of the dynamics between the initial time $t = 0$ and the final time $t = T$, while $f(0) = f(T) = 0$. The quantity relevant for decoherence is the noise kernel which, under the time-dependent coupling, transforms as

$$\mathcal{N} \to \tilde{\mathcal{N}} = f(t_1)f(t_2)\mathcal{N}(t_1;t_2) = f(t_1)f(t_2)\mathcal{N}(t_1 - t_2)\,. \tag{7.74}$$

The decoherence factor in the double commutator in Eq. (7.37) involves replacing t_2 with $t_1 - \tau$ and then integrating over τ. Therefore, the function $\mathcal{N}_1$ transforms as $\mathcal{N}_1 \to \tilde{\mathcal{N}}_1$, with $\tilde{\mathcal{N}}_1$ given by

$$\tilde{\mathcal{N}}_1(t_1) = f(t_1)\int_0^{t_1} d\tau f(t_1 - \tau)\mathcal{N}(\tau)\,. \tag{7.75}$$

From the definitions of $\mathcal{N}_1$ and $\mathcal{N}_2$ we have $\mathcal{N} = (d/d\tau)\mathcal{N}_1$, $\mathcal{N}_1 = (d/d\tau)\mathcal{N}_2$ and $\mathcal{N}_1(0) = \mathcal{N}_2(0) = 0$. Using these relations and integrating by parts, Eq. (7.75) becomes

$$\tilde{\mathcal{N}}_1(t_1) = f(t_1)\mathcal{N}_1(t_1)f(0) + f(t_1)\mathcal{N}_2(t_1)\dot{f}(0) + f(t_1)\int_0^{t_1} d\tau \mathcal{N}_2(\tau)\frac{d^2}{d\tau^2}f(t_1 - \tau)\,. \tag{7.76}$$

In the limit $\epsilon \to 0$ (taking the UV cut-off to infinity), we see from Eq. (7.73) that $\mathcal{N}_2$ looses any time dependence. We can therefore bring $\mathcal{N}_2$ outside the integral such that

$$\tilde{\mathcal{N}}_1(t_1) = f(t_1)\mathcal{N}_1(t_1)f(0) + f(t_1)\mathcal{N}_2\dot{f}(0) - f(t_1)\mathcal{N}_2(\dot{f}(0) - \dot{f}(t_1)) \tag{7.77}$$

The terms involving $\dot{f}(0)$ cancel out and we get

$$\tilde{\mathcal{N}}_1(t_1) = f(t_1)\mathcal{N}_1(t_1)f(0) + f(t_1)\mathcal{N}_2\dot{f}(t_1)\,. \tag{7.78}$$

After integrating by parts Eq. (7.78), in order to obtain $\tilde{\mathcal{N}}_2(T) = \int_0^T dt_1\tilde{\mathcal{N}}_1(t_1)$, we get

$$\tilde{\mathcal{N}}_2(T) = f(0)\left(f(T)\mathcal{N}_2(T) - f(0)\mathcal{N}_2(0)\right) - f(0)\mathcal{N}_2\int_0^T dt_1\dot{f} + \frac{\mathcal{N}_2}{2}\int_0^T dt_1\frac{d}{dt_1}f^2\,. \tag{7.79}$$

In the limit $\epsilon \to 0$, as we noted earlier, $\mathcal{N}_2(t)$ takes a constant value for any time $t > 0$ but is zero at $t = 0$ from the way it is defined. After completing the remaining integrals we get

$$\tilde{\mathcal{N}}_2(T) = \frac{\mathcal{N}_2}{2}\left(f^2(0) + f^2(T)\right) . \tag{7.80}$$

Since we assume that the interactions are switched off in the very beginning and at the very end, we see that $\tilde{\mathcal{N}}_2(T) = 0$ such that Eq. (7.72) becomes $\tilde{\rho}_r(x', x, T) = \rho_r(x', x, 0)$. Therefore, by adiabatically switching off the interactions we recover the original coherence within the system.

This is different from standard collisional decoherence where, for example, one originally has [114]

$$\partial_t \rho_r(x', x, t) = -\Lambda(x' - x)^2 \rho_r(x', x, t) . \tag{7.81}$$

When in this case we send $\Lambda \to \tilde{\Lambda} = f(t)\Lambda$, we get

$$\tilde{\rho}_r(x', x, t) = \exp\left\{-\Lambda(x' - x)^2 \int_0^t dt' f(t')\right\} \rho_r(x', x, 0) \tag{7.82}$$

The density matrix depends on the integral of $f(t)$ rather than its end points and we see that coherence is indeed lost irreversibly.

7.7 Discussion

In this work, the interaction of a non-relativistic electron with the radiation field is formulated within the framework of open quantum systems and the explicit expression for the master equation of the reduced electron dynamics in the position basis is obtained. It is shown that the classical limit of the quantum dynamics is free of the problems associated with the purely classical derivation of the Abraham-Lorentz formula. With respect to possible decoherence induced by vacuum fluctuations alone, the apparent decoherence at the level of the reduced density matrix is shown to be reversible and an artifact of the formalism used. In mathematically tracing over the environment, one traces over the degrees of freedom that physically surround the system being observed. These degrees of freedom must be regarded as the part of the system being observed (possibly as its dressed states [47, 126]), rather than the environment. This interpretation stems from the fact that one restores full initial coherence back into the system after switching off the interactions with the environment adiabatically.

Chapter 8

Summary and outlook

There has been a rising interest in adding the dark matter problem to the list of cosmological puzzles already solved by inflation. While the general mechanism leading to the formation of primordial black holes triggered by inflationary perturbations has already been fairly well established and discussed extensively in the literature, the search for specific theoretically well motivated models of inflation that lead to the formation of PBHs is not yet over. In the first part of the thesis, one such model is constructed which is a simple combination of Starobinsky's model and the model of non-minimal Higgs inflation. It inherits the compatibility of the two models with the CMB observations and also offers the possibility to account for the observed CDM content in the universe.

For a given value of the quartic self-coupling λ, it is shown that the remaining free parameters of the model, the scalaron mass m_0 and the non-minimal coupling parameters ξ and ζ, must all attain a specific value such that the model is consistent with CMB observations and generates sufficiently many PBHs, in an observationally viable mass window, in order to simultaneously account for the observed CDM content in the universe. The model leads to some specific predictions that can be falsified by future observations. For instance, the predictions of the model on wavelengths probed by the CMB are identical to that of Starobinsky's model. Thus, a measurement of the tensor-to-scalar ratio higher than that predicted by Starobinsky's model would rule this model out. While the value of the free parameters of the model can account for any fraction of dark matter that might be attributed to PBHs by future observations, it can only produce a single peak in the adiabatic power spectrum, such that the mass of the PBHs can only lie within a narrow interval. Therefore, the model could also be tested against the possibility of detecting PBHs with very different masses. It would also be interesting to see if the detection of gravitational waves, that might accompany the formation of PBHs [113], puts additional constraints on the model.

As mentioned in the introduction to the thesis, if one believes in the validity of the standard linear quantum dynamics for any system under consideration, one is logically led towards the Everett's interpretation. If, instead, we require the observed measurement record in an experiment to be the only one around which the universal wavefunction localizes, one may instead arrive at the dynamical collapse models which achieve this localization continuously and asymptotically in time. The task then becomes to see if the collapse models are indeed consistent with observations and to constrain the free parameters of the modified, non-linear and stochastic quantum dynamics that they postulate.

In generalizing to a cosmological setting, while the authors in [87] claim that the mass proportional CSL model is incompatible with the CMB observations (for most of the gauge-invariant constructions of their choice of the collapse operator), the work presented in the second part of the thesis shows and emphasizes that this conclusion strongly depends upon how the model is generalized and applied during inflation. Instead of considering the perturbed matter-energy density as the collapse operator (as in [87]), the Hamiltonian density of the scalar perturbations is assumed to play the role of the collapse operator during inflation and the radiation dominated era. At the level of first order cosmological perturbations, this generalization is shown to give negligible corrections to the power spectrum of the comoving curvature perturbation. The constraints imposed by the inflationary dynamics on the free parameters of the CSL model are further found to be insignificant compared to those already imposed by the state of the art laboratory experiments. Thus, the work presented here not only shows that the CSL model can be generalized in a manner that is consistent with CMB observations, but also that we first need to arrive at a general consensus on how the various collapse models should be generalized to a relativistic regime before arriving at a final conclusion concerning their compatibility with the CMB observations.

In the third and final part of the thesis, the dynamics of a non-relativistic electron is studied in the presence of vacuum fluctuations. The subject again relates to the foundational aspects of quantum mechanics where the question of interest is whether or not the environment of vacuum fluctuations of the radiation field, which is fundamental and unavoidable, behaves somewhat like an ordinary environment, such as that comprising of thermal photons, and if it leads to decoherence effects for an electron in a superposition of two spatial locations.

To address this question, standard quantum electrodynamics techniques are applied within the framework of open quantum systems to derive the master equation for the reduced density matrix of the electron in the position basis. From the master equation, it is deduced that the environment of vacuum fluctuations does not behave like an ordinary one and does not lead to decoherence of an electron in a spatial superposition. It is shown that although the off-diagonal elements of the reduced density matrix are suppressed, it does not imply that the vacuum fluctuations lead to irreversible loss of coherence for an electron (at rest) in a superposition of two different spatial locations. This is because full coherence is restored at the level of the electron simply by switching-off its interaction with the radiation field at late times. This would not have been the case had the loss of coherence been genuine and irreversible. Furthermore, the same mathematical formalism is also applied in addressing the well-known and long-standing problems associated with the Abraham-Lorentz formula. It is shown in this thesis that the equation of motion obtained for the expectation value of the position operator, obtained after averaging over the radiation field, is free of the instability problems associated with the Abraham-Lorentz formula that one faces in a purely classical derivation. While there has been a general expectation that these problems might not persist at a quantum mechanical level, it might be for the first time that this is demonstrated clearly.

Bibliography

[1] Stephen L Adler and Angelo Bassi. Collapse models with non-white noises. *Journal of Physics A: Mathematical and Theoretical*, 40(50):15083, nov 2007.

[2] Stephen L. Adler, Angelo Bassi, Matteo Carlesso, and Andrea Vinante. Testing continuous spontaneous localization with fermi liquids. *Phys. Rev. D*, 99:103001, 2019.

[3] Y. Akrami et al. Planck 2018 results. x. constraints on inflation. *Astronomy & Astrophysics*, 641:A10, 2020.

[4] Andreas Albrecht, Pedro Ferreira, Michael Joyce, and Tomislav Prokopec. Inflation and squeezed quantum states. *Phys. Rev. D*, 50:4807, 1994.

[5] Alexander Altland and Ben D. Simons. *Condensed Matter Field Theory*. Cambridge University Press, 2 edition, 2010.

[6] P. M. V. B. Barone and A. O. Caldeira. Quantum mechanics of radiation damping. *Phys. Rev. A*, 43:57–63, Jan 1991.

[7] N. Bartolo, E. Komatsu, Sabino Matarrese, and A. Riotto. Non-Gaussianity from inflation: Theory and observations. *Phys. Rept.*, 402:103–266, 2004.

[8] A. O. Barvinsky, A. Yu. Kamenshchik, C. Kiefer, A. A. Starobinsky, and C. F. Steinwachs. Asymptotic freedom in inflationary cosmology with a non-minimally coupled Higgs field. *J. Cosmol. Astropart. Phys.*, 12:003, 2009.

[9] Angelo Bassi and GianCarlo Ghirardi. Dynamical reduction models. *Physics Reports*, 379(5):257–426, 2003.

[10] Daniel Baumann. Inflation. In *Theoretical Advanced Study Institute in Elementary Particle Physics: Physics of the Large and the Small*, pages 523–686, 2011.

[11] Gordon Baym and Tomoki Ozawa. Two-slit diffraction with highly charged particles: Niels bohr's consistency argument that the electromagnetic field must be quantized. *Proceedings of the National Academy of Sciences*, 106(9):3035–3040, 2009.

[12] Daniel Bedingham. Relativistic state reduction model. *J. Phys.: Conf. Ser.*, 306:012034, 2011.

[13] Daniel J. Bedingham. Relativistic state reduction dynamics. *Found. Phys.*, 41:686–704, 2011.

[14] Gabriel R. Bengochea, Gabriel León, Philip Pearle, and Daniel Sudarsky. Discussions about the landscape of possibilities for treatments of cosmic inflation involving continuous spontaneous localization models. *Eur. Phys. J. C*, 80:1021, 2020.

[15] H. A. Bethe. The electromagnetic shift of energy levels. *Phys. Rev.*, 72:339–341, Aug 1947.

[16] Fedor Bezrukov and Mikhail Shaposhnikov. Higgs inflation at the critical point. *Phys. Lett.*, B734:249–254, 2014.

[17] Fedor L. Bezrukov, Amaury Magnin, and Mikhail Shaposhnikov. Standard Model Higgs boson mass from inflation. *Phys. Lett. B*, 675:88–92, 2009.

[18] Fedor L. Bezrukov and Mikhail Shaposhnikov. The Standard Model Higgs boson as the inflaton. *Phys. Lett. B*, 659:703–706, 2008.

[19] N. D. Birrell and P. C. W. Davies. *Quantum Fields in Curved Space*. Cambridge Monographs on Mathematical Physics. Cambridge Univ. Press, Cambridge, UK, 2 1984.

[20] David Blais, Claus Kiefer, and David Polarski. Can primordial black holes be a significant part of dark matter? *Phys. Lett. B*, 535:11–16, 2002.

[21] Heinz-Peter Breuer and Francesco Petruccione. Radiation damping and decoherence in quantum electrodynamics. In Heinz-Peter Breuer and Francesco Petruccione, editors, *Relativistic Quantum Measurement and Decoherence*, pages 31–65, Berlin, Heidelberg, 2000. Springer Berlin Heidelberg.

[22] Torsten Bringmann, Claus Kiefer, and David Polarski. Primordial black holes from inflationary models with and without broken scale invariance. *Phys. Rev. D*, 65:024008, 2002.

[23] Christian T. Byrnes, Edmund J. Copeland, and Anne M. Green. Primordial black holes as a tool for constraining non-Gaussianity. *Phys. Rev. D*, 86:043512, 2012.

[24] Pedro Cañate, Philip Pearle, and Daniel Sudarsky. Continuous spontaneous localization wave function collapse model as a mechanism for the emergence of cosmological asymmetries in inflation. *Phys. Rev. D*, 87(10):104024, 2013.

[25] Esteban A. Calzetta and Bei-Lok B. Hu. *Nonequilibrium Quantum Field Theory*. Cambridge Monographs on Mathematical Physics. Cambridge University Press, 2008.

[26] Matteo Carlesso, Sandro Donadi, Luca Ferialdi, Mauro Paternostro, Hendrik Ulbricht, and Angelo Bassi. Present status and future challenges of non-interferometric tests of collapse models. *Nature Phys.*, 18(3):243–250, 2022.

[27] Bernard Carr, Kazunori Kohri, Yuuiti Sendouda, and Jun'ichi Yokoyama. Constraints on primordial black holes. *Rept. Prog. Phys.*, 84(11):116902, 2021.

[28] Bernard Carr and Florian Kuhnel. Primordial Black Holes as Dark Matter: Recent Developments. *Ann. Rev. Nucl. Part. Sci.*, 70:355–394, 2020.

[29] Bernard Carr, Florian Kuhnel, and Marit Sandstad. Primordial Black Holes as Dark Matter. *Phys. Rev. D*, 94(8):083504, 2016.

[30] Bernard J. Carr. Primordial black holes as a probe of cosmology and high energy physics. *Lect. Notes Phys.*, 631:301–321, 2003.

[31] H. B. G. Casimir. On the Attraction Between Two Perfectly Conducting Plates. *Indag. Math.*, 10:261–263, 1948.

[32] Mario Castagnino, Sebastian Fortin, Roberto Laura, and Daniel Sudarsky. Interpretations of Quantum Theory in the Light of Modern Cosmology. *Found. Phys.*, 47(11):1387–1422, 2017.

[33] George F. Chapline. Cosmological effects of primordial black holes. *Nature*, 253(5489):251–252, 1975.

[34] Zu-Cheng Chen and Qing-Guo Huang. Merger Rate Distribution of Primordial-Black-Hole Binaries. *Astrophys. J.*, 864(1):61, 2018.

[35] Sebastien Clesse and Juan Garcia-Bellido. GW190425, GW190521 and GW190814: Three candidate mergers of primordial black holes from the QCD epoch. *Phys. Dark Univ.*, 38:101111, 2022.

[36] C. Cohen-Tannoudji, J. Dupont-Roc, and G. Grynberg. *Classical Electrodynamics: The Fundamental Equations and the Dynamical Variables*, chapter 1, pages 5–77. John Wiley and Sons, Ltd, 1997.

[37] C. Cohen-Tannoudji, J. Dupont-Roc, and G. Grynberg. *Lagrangian and Hamiltonian Approach to Electrodynamics, The Standard Lagrangian and the Coulomb Gauge*, chapter 2, pages 79–168. John Wiley & Sons, Ltd, 1997.

[38] C. Cohen-Tannoudji, J. Dupont-Roc, and G. Grynberg. *Quantum Electrodynamics in the Coulomb Gauge*, chapter 3, pages 169–252. John Wiley & Sons, Ltd, 1997.

[39] Sidney Coleman. Classical electron theory from a modern standpoint. In Doris Teplitz, editor, *Electromagnetism: Paths to Research*, pages 183–210. Springer US, Boston, MA, 1982.

[40] J Dalibard, J. Dupont-Roc, and C. Cohen-Tannoudji. Vacuum fluctuations and radiation reaction : identification of their respective contributions. *Journal de Physique*, 43(11):1617–1638, 1982.

[41] Suratna Das, Kinjalk Lochan, Satyabrata Sahu, and T. P. Singh. Quantum to classical transition of inflationary perturbations: Continuous spontaneous localization as a possible mechanism. *Phys. Rev. D*, 88:085020, 2013.

[42] Suratna Das, Kinjalk Lochan, Satyabrata Sahu, and T. P. Singh. Erratum: Quantum to classical transition of inflationary perturbations: Continuous spontaneous localization as a possible mechanism [phys. rev. d 88, 085020 (2013)]. *Phys. Rev. D*, 89:109902, 2014.

[43] V. De Luca, G. Franciolini, P. Pani, and A. Riotto. Primordial Black Holes Confront LIGO/Virgo data: Current situation. *JCAP*, 06:044, 2020.

[44] Andrea De Simone, Mark P. Hertzberg, and Frank Wilczek. Running Inflation in the Standard Model. *Phys. Lett. B*, 678:1–8, 2009.

[45] Alberto Diez-Tejedor and Daniel Sudarsky. Towards a formal description of the collapse approach to the inflationary origin of the seeds of cosmic structure. *J. Cosmol. Astropart. Phys.*, 2012:045, 2012.

[46] L. Diósi. Models for universal reduction of macroscopic quantum fluctuations. *Phys. Rev. A*, 40:1165–1174, Aug 1989.

[47] Lajos Diósi. Comments on "objectification of classical properties induced by quantum vacuum fluctuations". *Physics Letters A*, 197(2):183–184, 1995.

[48] Yohei Ema. Higgs Scalaron Mixed Inflation. *Phys. Lett.*, B770:403–411, 2017.

[49] Albert Escrivà, Cristiano Germani, and Ravi K. Sheth. Universal threshold for primordial black hole formation. *Phys. Rev. D*, 101(4):044022, 2020.

[50] R.P Feynman and F.L Vernon. The theory of a general quantum system interacting with a linear dissipative system. *Annals of Physics*, 24:118–173, 1963.

[51] L. H. Ford. Electromagnetic vacuum fluctuations and electron coherence. *Phys. Rev. D*, 47:5571–5580, Jun 1993.

[52] G. Franciolini, A. Kehagias, S. Matarrese, and A. Riotto. Primordial Black Holes from Inflation and non-Gaussianity. *JCAP*, 03:016, 2018.

[53] Stephen A. Fulling. Nonuniqueness of canonical field quantization in riemannian spacetime. *Phys. Rev. D*, 7:2850–2862, May 1973.

[54] C.W. Gardiner. *Handbook of Stochastic Methods for Physics, Chemistry, and the Natural Sciences*. Proceedings in Life Sciences. Springer-Verlag, 1985.

[55] Cristiano Germani and Ravi K. Sheth. Nonlinear statistics of primordial black holes from Gaussian curvature perturbations. *Phys. Rev. D*, 101(6):063520, 2020.

[56] G. C. Ghirardi, A. Rimini, and T. Weber. Unified dynamics for microscopic and macroscopic systems. *Phys. Rev. D.*, 34:470–491, 1986.

[57] Gian Carlo Ghirardi, Renata Grassi, and Fabio Benatti. Describing the macroscopic world: closing the circle within the dynamical reduction program. *Foundations of Physics*, 25(1):5–38, 1995.

[58] Gian Carlo Ghirardi, Philip Pearle, and Alberto Rimini. Markov processes in hilbert space and continuous spontaneous localization of systems of identical particles. *Phys. Rev. A*, 42:78–89, Jul 1990.

[59] Andrew D. Gow, Christian T. Byrnes, Philippa S. Cole, and Sam Young. The power spectrum on small scales: Robust constraints and comparing PBH methodologies. *JCAP*, 02:002, 2021.

[60] Andrew D. Gow, Christian T. Byrnes, Alex Hall, and John A. Peacock. Primordial black hole merger rates: distributions for multiple LIGO observables. *JCAP*, 01:031, 2020.

[61] Anne M. Green and Bradley J. Kavanagh. Primordial Black Holes as a dark matter candidate. *J. Phys. G*, 48(4):043001, 2021.

[62] Anne M. Green and Andrew R. Liddle. Constraints on the density perturbation spectrum from primordial black holes. *Phys. Rev. D*, 56:6166–6174, 1997.

[63] Ross N. Greenwood, David I. Kaiser, and Evangelos I. Sfakianakis. Multifield Dynamics of Higgs Inflation. *Phys. Rev. D*, 87:064021, 2013.

[64] David J. Griffiths. *Introduction to Electrodynamics*. Cambridge University Press, 4 edition, 2017.

[65] David J Griffiths, Thomas C Proctor, and Darrell F Schroeter. Abraham–lorentz versus landau–lifshitz. *American Journal of Physics*, 78(4):391–402, 2010.

[66] Anirudh Gundhi and Angelo Bassi. On the motion of an electron through vacuum fluctuations. *arXiv:2301.11946*.

[67] Anirudh Gundhi, José Luis Gaona-Reyes, Matteo Carlesso, and Angelo Bassi. Impact of Dynamical Collapse Models on Inflationary Cosmology. *Phys. Rev. Lett.*, 127(9):091302, 2021.

[68] Anirudh Gundhi, Sergei V. Ketov, and Christian F. Steinwachs. Primordial black hole dark matter in dilaton-extended two-field Starobinsky inflation. *Phys. Rev. D*, 103(8):083518, 2021.

[69] Anirudh Gundhi and Christian F. Steinwachs. Scalaron-Higgs inflation. *Nucl. Phys. B*, 954:114989, 2020.

[70] Anirudh Gundhi and Christian F. Steinwachs. Scalaron–Higgs inflation reloaded: Higgs-dependent scalaron mass and primordial black hole dark matter. *Eur. Phys. J. C*, 81(5):460, 2021.

[71] Yuta Hamada, Hikaru Kawai, Kin-ya Oda, and Seong Chan Park. Higgs Inflation is Still Alive after the Results from BICEP2. *Phys. Rev. Lett.*, 112(24):241301, 2014.

[72] Yuta Hamada, Hikaru Kawai, Kin-ya Oda, and Seong Chan Park. Higgs inflation from Standard Model criticality. *Phys. Rev.*, D91:053008, 2015.

[73] Stephen Hawking. Gravitationally collapsed objects of very low mass. *Mon. Not. Roy. Astron. Soc.*, 152:75, 1971.

[74] Minxi He, Alexei A. Starobinsky, and Jun'ichi Yokoyama. Inflation in the mixed Higgs-R^2 model. *JCAP*, 05:064, 2018.

[75] P. Ivanov, P. Naselsky, and I. Novikov. Inflation and primordial black holes as dark matter. *Phys. Rev. D*, 50:7173–7178, 1994.

[76] K. Jedamzik and Jens C. Niemeyer. Primordial black hole formation during first order phase transitions. *Phys. Rev. D*, 59:124014, 1999.

[77] Karsten Jedamzik. Primordial Black Hole Dark Matter and the LIGO/Virgo observations. *JCAP*, 09:022, 2020.

[78] Karsten Jedamzik. Consistency of Primordial Black Hole Dark Matter with LIGO/Virgo Merger Rates. *Phys. Rev. Lett.*, 126(5):051302, 2021.

[79] E. Joos, H.D. Zeh, D.J.W. Giulini, C. Kiefer, J. Kupsch, and I.O. Stamatescu. *Decoherence and the Appearance of a Classical World in Quantum Theory*. Physics and astronomy online library. Springer, 2003.

[80] M. Khlopov, B.A. Malomed, and Ia.B. Zeldovich. Gravitational instability of scalar fields and formation of primordial black holes. *Mon. Not. Roy. Astron. Soc.*, 215:575–589, 1985.

[81] C. Kiefer. Decoherence in quantum electrodynamics and quantum gravity. *Phys. Rev. D*, 46:1658–1670, 1992.

[82] Claus Kiefer and David Polarski. Why do cosmological perturbations look classical to us? *Adv. Sci. Lett.*, 2:164–173, 2009.

[83] Willis E. Lamb and Robert C. Retherford. Fine structure of the hydrogen atom by a microwave method. *Phys. Rev.*, 72:241–243, Aug 1947.

[84] S. J. Landau, C. G. Scóccola, and D. Sudarsky. Cosmological constraints on nonstandard inflationary quantum collapse models. *Phys. Rev. D*, 85:123001, 2012.

[85] Susana Landau, Gabriel León, and Daniel Sudarsky. Quantum origin of the primordial fluctuation spectrum and its statistics. *Phys. Rev. D*, 88:023526, 2013.

[86] Gabriel León and María Pía Piccirilli. Generation of inflationary perturbations in the continuous spontaneous localization model: The second order power spectrum. *Phys. Rev. D*, 102:043515, 2020.

[87] Jérôme Martin and Vincent Vennin. Cosmic microwave background constraints cast a shadow on continuous spontaneous localization models. *Phys. Rev. Lett.*, 124:080402, 2020.

[88] Jerome Martin, Vincent Vennin, and Patrick Peter. Cosmological Inflation and the Quantum Measurement Problem. *Phys. Rev. D*, 86:103524, 2012.

[89] J. C. Mather et al. Measurement of the Cosmic Microwave Background Spectrum by the COBE FIRAS Instrument. *Astrophys. J.*, 420:439, January 1994.

[90] J. C. Mather et al. Calibrator Design for the COBE Far-Infrared Absolute Spectrophotometer (FIRAS). *Astrophys. J.*, 512(2):511–520, February 1999.

[91] V. Mukhanov. *Physical Foundations of Cosmology*. Cambridge University Press, 2005.

[92] V.F. Mukhanov, H.A. Feldman, and R.H. Brandenberger. Theory of cosmological perturbations. *Physics Reports*, 215(5):203 – 333, 1992.

[93] Viatcheslav F. Mukhanov. Quantum Theory of Gauge Invariant Cosmological Perturbations. *Sov. Phys. JETP*, 67:1297–1302, 1988.

[94] Ilia Musco, John C. Miller, and Luciano Rezzolla. Computations of primordial black hole formation. *Class. Quant. Grav.*, 22:1405–1424, 2005.

[95] Wayne C. Myrvold. Relativistic markovian dynamical collapse theories must employ nonstandard degrees of freedom. *Phys. Rev. A*, 96:062116, 2017.

[96] Tomohiro Nakama, Joseph Silk, and Marc Kamionkowski. Stochastic gravitational waves associated with the formation of primordial black holes. *Phys. Rev. D*, 95(4):043511, 2017.

[97] Takahiro T. Nakamura and Ewan D. Stewart. The spectrum of cosmological perturbations produced by a multi-component inflaton to second order in the slow-roll approximation. *Physics Letters B*, 381(4):413–419, 1996.

[98] Elias Okon and Daniel Sudarsky. Less Decoherence and More Coherence in Quantum Gravity, Inflationary Cosmology and Elsewhere. *Found. Phys.*, 46(7):852–879, 2016.

[99] Leonard Parker and David Toms. *Quantum Field Theory in Curved Spacetime: Quantized Fields and Gravity*. Cambridge Monographs on Mathematical Physics. Cambridge University Press, 2009.

[100] Philip Pearle. Classical electron models. In Doris Teplitz, editor, *Electromagnetism: Paths to Research*, pages 211–295. Springer US, Boston, MA, 1982.

[101] Philip Pearle. Combining stochastic dynamical state-vector reduction with spontaneous localization. *Phys. Rev. A*, 39:2277–2289, 1989.

[102] Alejandro Perez, Hanno Sahlmann, and Daniel Sudarsky. On the quantum origin of the seeds of cosmic structure. *Class. Quantum Grav.*, 23:2317, 2006.

[103] Patrick Peter and Jean-Philippe Uzan. *Primordial Cosmology*. Oxford Graduate Texts. Oxford University Press, 2 2013.

[104] Nelson Pinto-Neto, Grasiele Santos, and Ward Struyve. Quantum-to-classical transition of primordial cosmological perturbations in de Broglie–Bohm quantum theory. *Phys. Rev. D*, 85:083506, 2012.

[105] David Polarski and Alexei A. Starobinsky. Semiclassicality and decoherence of cosmological perturbations. *Class. Quantum Grav.*, 13:377, 1996.

[106] William H. Press and Paul Schechter. Formation of galaxies and clusters of galaxies by selfsimilar gravitational condensation. *Astrophys. J.*, 187:425–438, 1974.

[107] Martti Raidal, Christian Spethmann, Ville Vaskonen, and Hardi Veermäe. Formation and Evolution of Primordial Black Hole Binaries in the Early Universe. *JCAP*, 02:018, 2019.

[108] Lisa Randall, Marin Soljacic, and Alan H. Guth. Supernatural inflation: Inflation from supersymmetry with no (very) small parameters. *Nucl. Phys. B*, 472:377–408, 1996.

[109] Antonio Riotto. Inflation and the theory of cosmological perturbations. *ICTP Lect. Notes Ser.*, 14:317–413, 2003.

[110] Emilio Santos. Objectification of classical properties induced by quantum vacuum fluctuations. *Physics Letters A*, 188(3):198–204, 1994.

[111] Misao Sasaki. Large scale quantum fluctuations in the inflationary universe. *Prog. Theor. Phys.*, 76(5):1036–1046, 1986.

[112] Misao Sasaki and Ewan D. Stewart. A General analytic formula for the spectral index of the density perturbations produced during inflation. *Prog. Theor. Phys.*, 95:71–78, 1996.

[113] Misao Sasaki, Teruaki Suyama, Takahiro Tanaka, and Shuichiro Yokoyama. Primordial black holes—perspectives in gravitational wave astronomy. *Class. Quant. Grav.*, 35(6):063001, 2018.

[114] Maximilian A. Schlosshauer. *Decoherence and the Quantum-To-Classical Transition*. Springer-Verlag Berlin Heidelberg, 2007.

[115] Masaru Shibata and Misao Sasaki. Black hole formation in the Friedmann universe: Formulation and computation in numerical relativity. *Phys. Rev. D*, 60:084002, 1999.

[116] Joseph Silk and Michael S. Turner. Double Inflation. *Phys. Rev. D*, 35:419, 1987.

[117] G. F. Smoot et al. Structure in the COBE Differential Microwave Radiometer First-Year Maps. *Astrophys. J. Lett.*, 396:L1, September 1992.

[118] Alexei A. Starobinsky. A new type of isotropic cosmological models without singularity. *Phys. Lett. B*, 91:99–102, 1980.

[119] Alexei A. Starobinsky. STOCHASTIC DE SITTER (INFLATIONARY) STAGE IN THE EARLY UNIVERSE. *Lect. Notes Phys.*, 246:107–126, 1986.

[120] K. S. Stelle. Classical gravity with higher derivatives. *Gen. Relativ. Gravit.*, 9:353–371, 1978.

[121] Daniel Sudarsky. Shortcomings in the Understanding of Why Cosmological Perturbations Look Classical. *Int. J. Mod. Phys. D*, 20:509–552, 2011.

[122] Shin Takagi. Vacuum Noise and Stress Induced by Uniform Acceleration: Hawking-Unruh Effect in Rindler Manifold of Arbitrary Dimension. *Prog. Theor. Phys. Suppl.*, 88:1–142, 1986.

[123] Roderich Tumulka. A relativistic version of the ghirardi–rimini–weber model. *J. Stat. Phys.*, 125:821–840, 2006.

[124] Roderich Tumulka. A relativistic grw flash process with interaction. In Valia Allori, Angelo Bassi, Detlef Dürr, and Nino Zanghi, editors, *Do Wave Functions Jump?: Perspectives of the Work of GianCarlo Ghirardi*, pages 321–347. Springer International Publishing, Cham, 2021.

[125] W. G. Unruh. Notes on black-hole evaporation. *Phys. Rev. D*, 14:870–892, Aug 1976.

[126] William G. Unruh. False loss of coherence. In Heinz-Peter Breuer and Francesco Petruccione, editors, *Relativistic Quantum Measurement and Decoherence*, pages 125–140, Berlin, Heidelberg, 2000. Springer Berlin Heidelberg.

[127] Vincent Vennin. *Stochastic inflation and primordial black holes*. PhD thesis, U. Paris-Saclay, 6 2020.

[128] A. Vinante, M. Carlesso, A. Bassi, A. Chiasera, S. Varas, P. Falferi, B. Margesin, R. Mezzena, and H. Ulbricht. Narrowing the parameter space of collapse models with ultracold layered force sensors. *Phys. Rev. Lett.*, 125:100404, Sep 2020.

[129] Yun-Chao Wang and Tower Wang. Primordial perturbations generated by Higgs field and R^2 operator. *Phys. Rev.*, D96(12):123506, 2017.

[130] Theodore A. Welton. Some observable effects of the quantum-mechanical fluctuations of the electromagnetic field. *Phys. Rev.*, 74:1157–1167, Nov 1948.

[131] Sam Young. The primordial black hole formation criterion re-examined: Parametrisation, timing and the choice of window function. *Int. J. Mod. Phys. D*, 29(02):2030002, 2019.

[132] Sam Young and Christian T. Byrnes. Primordial black holes in non-Gaussian regimes. *JCAP*, 08:052, 2013.

[133] Sam Young and Adrian S. Hamers. The impact on distant fly-bys on the rate of binary primordial black hole mergers. *JCAP*, 10:036, 2020.

[134] Sam Young, Ilia Musco, and Christian T. Byrnes. Primordial black hole formation and abundance: contribution from the non-linear relation between the density and curvature perturbation. *JCAP*, 11:012, 2019.

[135] Y. Zhang, W. Zhao, T. Y. Xia, X. Z. Er, and H. X. Miao. Relic gravitational waves and cmb polarization in the accelerating universe. *Int. J. Mod. Phys. D*, 17:1105–1123, 2008.